Introduction to NMR Product Operators

C. Griesinger

Max Planck Institute for Biophysical Chemistry

Am Faßberg 11

D-37077 Göttingen

Germany

cigr@nmr.mpibpc.mpg.de

http://goenmr.de

EMBO Course

Heidelberg

Sept. 2003

1.1. Basics

Approximately 100 nuclear isotopes possess a nuclear spin. The spin I is proportional to a magnetic moment μ according to $\mu = \gamma(h/2\pi)\mathbf{I}$. The magnetic moment of a spin orients itself either parallel or antiparallel to an external magnetic field B_0. We assume by convention that B_0 is along the z-axis. The parallel orientation of the spin is energetically most, the antiparallel orientation is least favourable. A spin with spin moment I has altogether 2I+1 different states which differ in their quantum number I_z. I_z ranges from –I, –(I–1), ..., (I–1), I. The energy of the states is given by: $E = -\gamma(h/2\pi)B_0I_z$.

1.1.1. Most important nuclear spins: I = 1/2

Isotope: X	^{3}H	^{1}H	^{15}N	^{31}P	^{13}C	^{19}F	^{29}Si	^{57}Fe	^{77}Se	^{111}Cd	^{113}Cd
nat. Ab	0	1	0.377	1	0.01	1	4.7%	2.19%	7.58%	12,75%	12.26%
γ_X/γ_H	1.06	1	0.1	0.4	0.25	0.94	0.2	0.032	0.19	0.21	0.22

Some important nuclear spins: I ≠ 1/2

	I = 1			I = 3/2		I = /2
Isotop	^{2}D	^{14}N	^{6}Li	^{7}Li	^{23}Na	^{17}O
nat. Ab.	$1.5\ 10^{-2}$%	99.63%	7.42%	92.58%	1	$3.7\ 10^{-2}$%
γ_X/γ_H	0.15	0.07	0.15	0.39	0.26	0.136

The energy level scheme for a ^{1}H and a D are shown in Fig. 1.

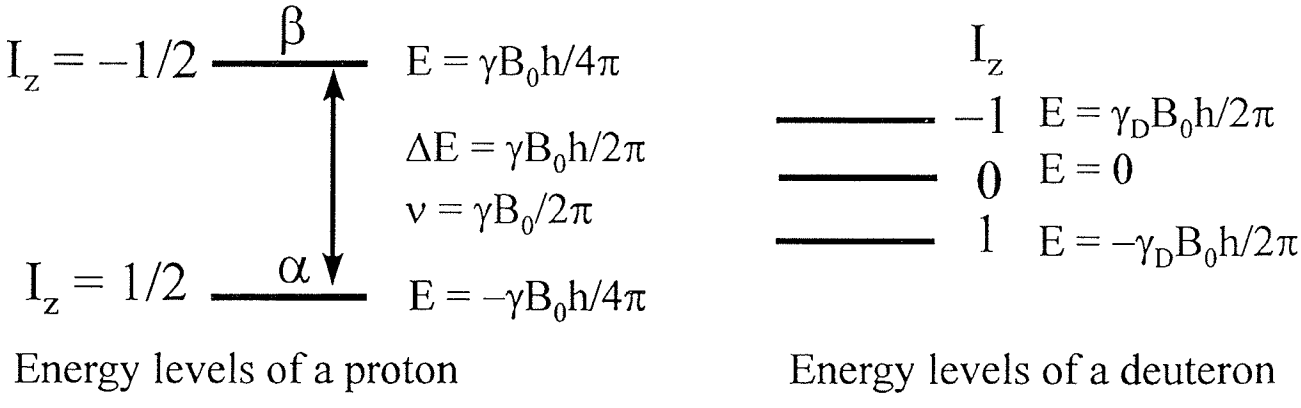

Energy levels of a proton Energy levels of a deuteron

1.1.2. Boltzmann distribution:

Due to the laws of statistical thermodynamics the population of the spin levels by an ensemble of identical spins is given by the Boltzmann distribution. For a spin ½ we find for the population of the β state: $p_\beta = \dfrac{e^{-(\gamma B_0 \hbar/2kT)}}{2\cosh(\gamma B_0 \hbar / 2kT)}$

and for the population of the α state: $p_\alpha = \frac{e^{(\gamma B_0 \hbar / 2kT)}}{2\cosh(\gamma B_0 \hbar / 2kT)}$

The factor $2\cosh(\gamma B_0 \hbar / 2kT)$ makes sure that the normalization $p_\alpha + p_\beta = 1$ is fulfilled. It is also related to the partition function of a spin ½ system. The z-magnetization observed for the Boltzmann equilibrium is given by $(\mu_\alpha p_\alpha + \mu_\beta p_\beta)$ where μ_α represents the magnetic moment of the spin in the α state: ½ γh and μ_β represents the magnetization of the β state: -½ γh. Thus the equilibrium magnetization is given by:

$$(\mu_\alpha p_\alpha + \mu_\beta p_\beta) = \frac{1}{2}\gamma\hbar(p_\alpha - p_\beta) = \frac{1}{2}\gamma\hbar\frac{\sinh(\gamma B_0\hbar / 2kT)}{\cosh(\gamma B_0\hbar / 2kT)} \approx \frac{1}{4}\gamma\hbar(\gamma B_0\hbar / kT) = \frac{1}{4}\gamma\hbar 10^{-4}$$

for ^1H and $\gamma B_0/2\pi$ = 600 MHz and room temperature.

Therefore only every 10.000th molecule can be observed at room temperature and NMR is therefore a very insensitive spectroscopic technique. The sensitivity can be increased by increasing the B_0 field or by choosing nuclei with the highest gyromagnetic ratio.

1.2e. Principles of measurement of nuclear magnetic resonance:

In principle magnetic resonance can be measured by the application of an electromagnetic field that is absorbed whenever it meets the resonance condition: $\Delta E = h\nu$ (cf. Fig.1). We want to introduce now the vector formalism of macroscopic magnetizations which takes the fact into account that a whole ensemble of spins contributes to the magnetization of the sample. We have come across the equilibrium magnetization M_0 already which is given by $M_0 = \gamma^2 h^2 B_0/(8\pi kT)$. It is oriented along the z-axis. In the following we want to use the equation of motion for the magnetization:

$$\frac{d\vec{M}}{dt} = \gamma\vec{M} \times \vec{B} - \Gamma(\vec{M} - M_0\vec{e}_z) \qquad [1]$$

This so called Bloch equation expresses the fact that the change in time of the magnetization is equal to the vector product of the magnetization itself and the external field. Due to the nature of the vector product, the change in time of the magnetization is orthogonal to both the magnetic field and the magnetization. The second term describes the relaxation of the magnetization back to the equilibrium state: $\vec{M}_0 = M_0\vec{e}_z$

1.2.1 Rotating coordinate system:

For the description of NMR experiments the rotating frame proves to be essential. For transverse magnetization we find the following equations for the three vector components M_x, M_y, and M_z under the assumptions: $\vec{B} = B_0\vec{e}_z$, $\gamma B_0 = \omega_0 = 2\pi\nu_0$ for the Bloch equation:

$$\frac{dM_x}{dt} = \gamma(\vec{M} \times \vec{B}_0\vec{e}_z)_x = \gamma B_0 M_y$$

$$\frac{dM_y}{dt} = \gamma(\vec{M} \times \vec{B}_0\vec{e}_z)_y = -\gamma B_0 M_x$$

$$\frac{dM_z}{dt} = \gamma(\vec{M} \times \vec{B}_0\vec{e}_z)_z = 0$$

Additional differentiation of the two equations for the transverse components of the magnetization yields:

$$\frac{d^2M_x}{dt^2} = -(\gamma B_0)^2 M_x \text{ and}$$

$$\frac{d^2M_y}{dt^2} = -(\gamma B_0)^2 M_y$$

These two equations are the classical oscillator equations. Their solutions are:

$M_x(t) = M_x(0)\cos(\omega_0 t) - M_y(0)\sin(\omega_0 t)$

$M_y(t) = M_x(0)\sin(\omega_0 t) + M_y(0)\cos(\omega_0 t)$

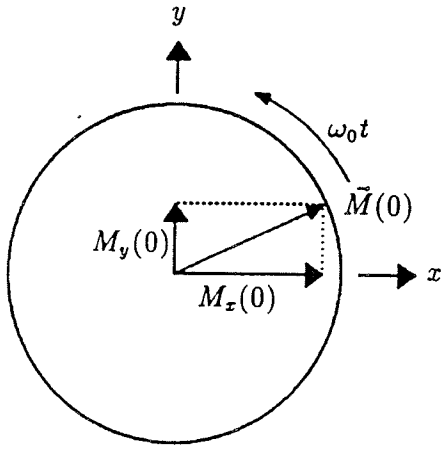

Suppose that the initial magnetization is exclusively along the x-direction with the length M_0 we have: $M_x(0) = M_0$ and $M_y(0) = 0$. This leaves us with the equation:

$M_x(t) = M_0\cos(\omega_0 t)$

$M_y(t) = M_0\sin(\omega_0 t)$

These equations give us the value for the magnetization components $M_x(t)$ and $M_y(t)$. These components form a vector and it is common to write down this vector:

$\vec{M}(t) = M_0\cos(\omega_0 t)\vec{e}_x + M_0\sin(\omega_0 t)\vec{e}_y$

It is common to rewrite this equation with the convention: $\vec{M}_x = M_0\vec{e}_x; \vec{M}_y = M_0\vec{e}_y$ in the following form which is rather an expression for a "chemical reaction" than for an equation:

$M_x \rightarrow M_x\cos(\omega_0 t) + M_y\sin(\omega_0 t)$. [2]

The transverse magnetization precesses around the static magnetic field B_0 with the frequency: $\omega_0 = \gamma B_0$. This precession applies to all nuclei with a given γ. The frequency differences due to the different chemical environment of nuclei in a compound is for most nuclei only in the 10^{-6} region (ppm). This is taken into account by the following formula: $\omega = \gamma B_0(1-\sigma)$ where σ expresses the

chemical shift. However, these small chemical shift differences are the most interesting information to be recovered from the spectrum. Therefore the huge frequency contribution due to $\omega_0 = \gamma B_0$ is subtracted from the frequency ω yielding the frequency $\Omega = \omega - \omega_0$. This is done by the transformation into a coordinate system that precesses with the frequency ω_0 around the z-axis (Fig. 3).

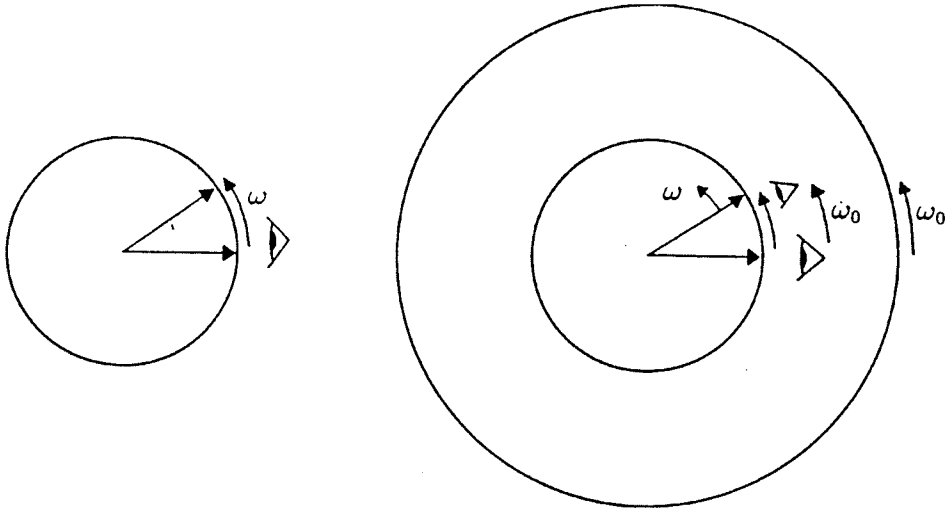

Laboratory system rotating frame

In the rotating frame the nuclei rotate now with their characteristic larmor frequency ω diminuished by the frequency ω_0 yielding a frequency of rotation: $\Omega = \omega - \omega_0$. The Bloch equation in the rotating frame now reads:

$$\frac{d\bar{M}}{dt} = \gamma\bar{M} \times (\bar{B} - \frac{\omega_0}{\gamma}\vec{e}_z) - \Gamma(\bar{M} - M_0\vec{e}_z)$$

Precession in the rotating frame of a magnetization with chemical shift then boils down to:

$M_x \rightarrow M_x \cos(\Omega t) + M_y \sin(\Omega t)$. [3]

and

$M_y \rightarrow M_y \cos(\Omega t) - M_x \sin(\Omega t)$. [4]

1.2.2 CW irradiation in the rotating frame:

During an NMR experiment, radio frequency (rf) with the frequency ω_0 of the rotating frame is irradiated. The field strenght is normally abbreviated with B_1. We suppose that we irradiate a field of the form: $\vec{B}_1(t) = 2B_1\vec{e}_x \cos(\omega_0 t)$. This linearly polarized field can be split into two components of circularly polarized rf given by:

$\vec{B}_1(t) = B_1(\vec{e}_x \cos(\omega_0 t) + \vec{e}_y \sin(\omega_0 t)) + B_1(\vec{e}_x \cos(\omega_0 t) - \vec{e}_y \sin(\omega_0 t))$ (Fig. 4)

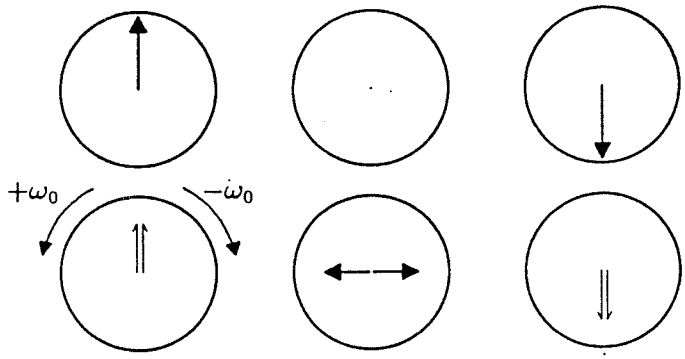

linearly polarized
B field

two circularly polarized
B fields

The first component rotates clockwise with the frequency ω_0, the other counterclockwise with the frequency $-\omega_0$.

Transformation into the rotating frame yields:

$\vec{B}_1(t) = B_1\vec{e}_x + B_1(\vec{e}_x \cos(2\omega_0 t) - \vec{e}_y \sin(2\omega_0 t))$

The clockwise component is a constant field along the x axis whereas the counterclockwise component rotates with the frequency $-2\omega_0$. It can be neglected for our further considerations.

1.2.3 Transient solutions of the Bloch equations:

The Bloch equation for a nucleus with chemical shift Ω under the action of an rf field with strength $\gamma B_1 = \omega_1$ disregarding relaxation is therefore given by:

$$\frac{d\vec{M}}{dt} = \vec{M} \times \Omega\vec{e}_z + \vec{M} \times \omega_1\vec{e}_x$$

The solution to this equation can be derived in the same way as before for the precession around the z-axis. However, there are special cases:

When $\Omega = 0$ we have an on-resonance spin. The equation of motion then boils down to a rotation of the magnetization around the x axis with the frequency ω_1. We find for example for an initial z-magnetization:

$$M_z \xrightarrow{\omega_1\vec{e}_x} M_z \cos(\omega_1 t) - M_y \sin(\omega_1 t) \qquad [5]$$

and

$$M_z \xrightarrow{\omega_1\vec{e}_x} M_z \cos(\omega_1 t) + M_x \sin(\omega_1 t) \qquad [6]$$

It is easy to see that after a duration $t = \pi/(2\omega_1)$ the z-magnetization has turned to $-M_y$ which amounts to an 90° rotation. The corresponding pulse is therefore called a 90° pulse. For $t = \pi/(\omega_1)$ we find that the magnetization is inverted and aligns itself along $-M_z$. The corresponding pulse is a 180° pulse.

When the spin is off-resonance ($\Omega \neq 0$) the magnetization rotates about the effective field $\vec{B}_{eff} / \gamma = \Omega\vec{e}_z + \omega_1\vec{e}_x = \Omega_{eff}\vec{e}'_z$ with $\Omega_{eff} = \sqrt{\Omega^2 + \omega_1^2}$ and $\vec{e}'_z = \cos\theta\vec{e}_z + \sin\theta\vec{e}_x$; $\text{arctg}(\theta) = \frac{\omega_1}{\Omega}$. (Fig. 5)

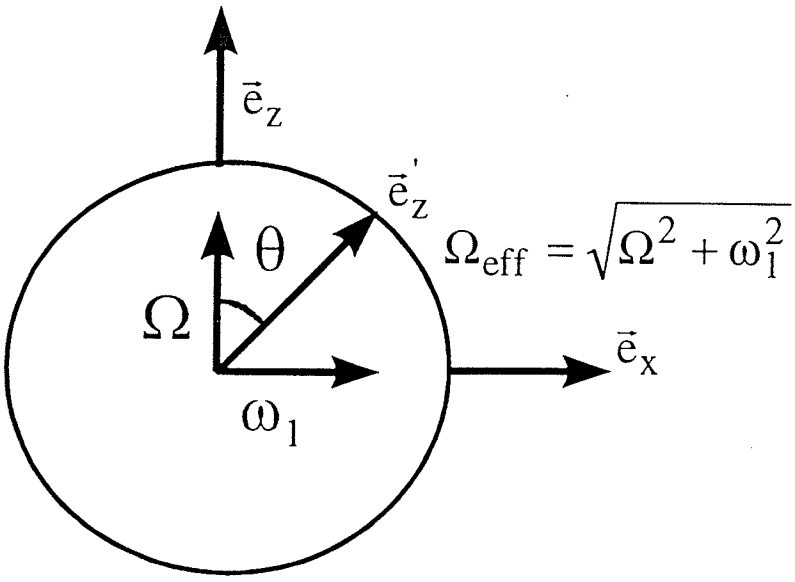

Fig. 5.

Effective field for an off-resonance pulse

1.2.4 Stationary solutions of the Bloch equations:

The stationary solutions to the Bloch equation are important to understand saturation experiments as well as spin-lock experiments. These rely on the extended application of CW irradiation at a certain frequency ω_0. We find for a field $\omega_1 = \gamma B_1$ and the chemical shift Ω the following steady state solutions:

$$M_x = M_0 \gamma B_1 \frac{\Omega}{(1 + \gamma^2 B_1^2 T_1 T_2)/T_2^2 + \Omega^2}$$

$$M_y = M_0 \gamma B_1 \frac{T_2^{-1}}{(1 + \gamma^2 B_1^2 T_1 T_2)/T_2^2 + \Omega^2}$$

$$M_z = M_0 (1 - \gamma B_1 \frac{\gamma B_1 T_1 / T_2}{(1 + \gamma^2 B_1^2 T_1 T_2)/T_2^2 + \Omega^2})$$

We can distinguish between two extremal cases.

Weak irradiation:

This means $\gamma^2 B_1^2 T_1 T_2 << 1$. The transverse components become:

$$M_x = M_0 \gamma B_1 \frac{\Omega T_2^2}{1 + T_2^2 \Omega^2} = M_0 \gamma B_1 D(\Omega)$$

$$M_y = M_0 \gamma B_1 \frac{T_2}{1 + T_2^2 \Omega^2} = M_0 \gamma B_1 A(\Omega)$$

$$M_z = M_0$$

$A(\Omega)$ and $D(\Omega)$ are the absorption and dispersion part of a Lorentzian line and constitute the response of a spin to the "old fashioned" CW NMR experiments. The z-magnetization is not disturbed in essence and the response is weak.

Strong irradiation:

this means $\gamma^2 B_1^2 T_1 T_2 >> 1$. On resonance we obtain:

$$M_x = 0$$

$$M_y = \frac{M_0}{\gamma B_1 T_1}$$

$$M_z = 0$$

Since T_1 normally is larger than T_2 $\gamma B_1 T_1$ is also large and all components of the magnetization vanish. An on-resonance CW irradiation therefore allows to saturate a spin completely.

1.2.5. 1D experiment:

The 1D experiment is then constructed by a strong $90°_y$ pulse followed by a time t during which the magnetization is let evolve freely. The response of the magnetization is therefore called FID (free induction decay).

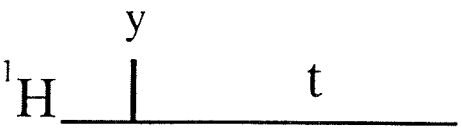

Fig. 6

z-magnetization before the pulse is rotated to M_x during the 90° pulse according to Eq. [6]. After the application of the pulse the magnetization begins to precess about the z-axis according to Eq. [4]. The NMR detector is phase sensitive. Therefore both the M_x and the M_y component in the rotating frame can be recorded. Recording takes place in the laboratory frame for example along the x axis. The rotating transverse magnetization induces according to Faraday's law of induction an oscillating voltage that is proportional to the derivative of the magnetization (Fig. 7).

Phase sensitive detection of the NMR signal by a quadrature detector

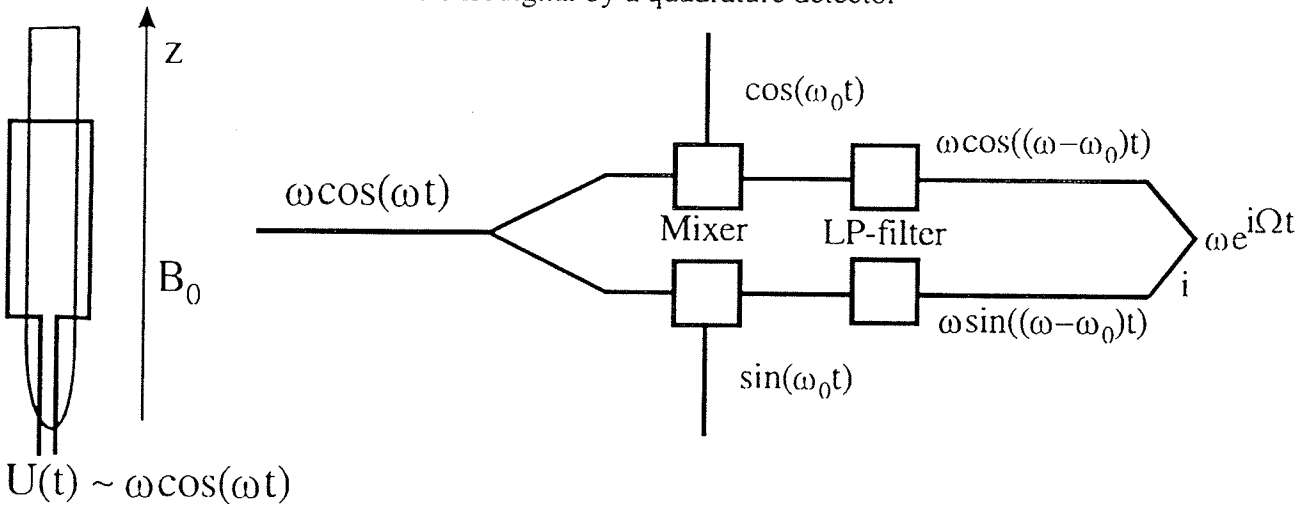

Fig. 7.

The amplitude of the detected signal depends on the γB_0 due to the factor ω. However, for the signal to noise ratio only the square root of this factor is gained $(\gamma B_0)^{1/2}$ due to the fact that also the noise increases with $\sqrt{\omega} = (\gamma B_0)^{1/2}$.

In the detector two signals one modulated with $\cos(\omega-\omega_0)t$ and the other with $\sin(\omega-\omega_0)t$ are recorded. They correspond to detection of x magnetization and y magnetization in the rotating frame, respectively:

M_x: $M_0 \cos(\Omega t)$

M_y: $M_0 \sin(\Omega t)$

Complex addition of the two signals according to $M_x + iM_y$ yields the signal:

$M^+ = M_0 (\cos(\Omega t)+i\sin(\Omega t)) = M_0 e^{i\Omega t}$. [7]

If we take an exponential decay of the transverse magnetization with the constant $1/T_2$ into account, the time domain signal is then given by: $f(t) = e^{i\Omega t} e^{-t/T_2}$

$$F(\omega) = \int_0^\infty e^{-i\omega t} e^{i\Omega t} e^{-t/T_2} dt = \frac{e^{-i\omega t} e^{i\Omega t} e^{-t/T_2}}{-i(\omega-\Omega)-T_2^{-1}} \Big|_0^\infty = \frac{1}{i(\omega-\Omega)+T_2^{-1}} = L(\omega)$$

The real part $A(\omega)$ and the imaginary part $D(\omega)$ are given in the following way. (Fig. 8)

$$\frac{1/T_2}{(\omega-\Omega)^2+(1/T_2)^2} = A(\omega)$$

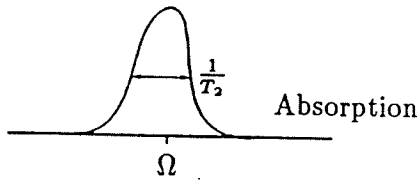

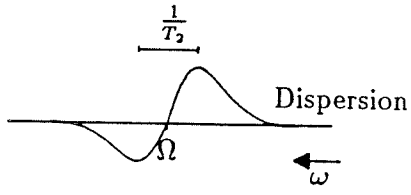

$$\frac{\omega-\Omega}{(\omega-\Omega)^2+(1/T_2)^2} = D(\omega)$$

Both resonances are centered around $\omega = \Omega$. The absorption part assumes its maximum at this position whereas the antisymmetric dispersion part is zero exactly on resonance. The line width at half height of the signal of the absorptive part is $2/T_2$ on an ω scale and $1/(\pi T_2)$ on a ν scale. The absorption part decays to zero with $(\omega-\Omega)^{-2}$ whereas the dispersive part decays only to zero with $(\omega-\Omega)^{-1}$. Therefore the dispersive part of a Lorentzian line is much broader than the absorptive part. Therefore spectra with pure phases in which the absorptive part of the signal can be observed separately are most desirable. This not only applies to 1D spectra but also to multidimensional NMR spectroscopy as well.

1.2.5.1 Phase correction:

Often it is necessary to resolve the linear combination of the absorptive and dispersive Lorentzian line after the Fourier transformation. This procedure is called phase correction. In praxis, we apply a phase correction of zeroth and first order. The zero order phase correction is a constant phase correction applied for the whole spectrum whereas the first order phase correction depends linearly on the frequency Ω.

Zero order phase correction:

In case that the detector for the signal is not aligned with the initial orientation of the magnetization at t=0 we obtain as initial magnetization for example the following situation:

$\vec{M}(0) = M_0 \cos(\phi)\vec{e}_x + M_0 \sin(\phi)\vec{e}_y$

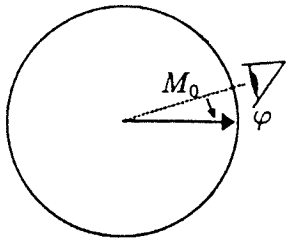

The phase ϕ is the phase of the signal which can be removed by a phase correction of zero order. This can be seen in the following way by considering the signal that is recorded:

$M_x(t) = \cos\phi \cos(\Omega t) - \sin\phi \sin(\Omega t) = \cos(\Omega t + \phi)$

$M_y(t) = \sin\phi \cos(\Omega t) + \sin\phi \cos(\Omega t) = \sin(\Omega t + \phi)$

Linear combination of the two signals according to Eq. [7] yields:

$M^+(t) : f(t) = \cos(\Omega t + \phi) + i \sin(\Omega t + \phi) = e^{i(\Omega t+\phi)}$

Fourier transformation of this signal yields:

$S(\omega) = e^{i\phi} L(\omega) = \cos\phi\ A(\omega) - \sin\phi\ D(\omega) + i(\sin\phi\ A(\omega) + \cos\phi\ D(\omega))$

Real and imaginary part are mixed with cosine and sine of the phase ϕ. Multiplication of the spectrum with $e^{-i\phi}$ eliminates this error in the phase and we are left with:

$e^{-i\phi}S(\omega) = e^{-i\phi}\, e^{i\phi}\, L(\omega) = L(\omega)$.

This phase correction can be applied in the computer mainly by interactive dials.

First order phase correction:

A phase correction of first order often originates from the fact that there is a short delay Δ between the pulse and the detection. This delay normally amounts to only a few µs. Then the vectors for different chemical shifts have acquired a phase $\Omega\Delta$. This phase is linearly dependent on the chemical shift Ω.

Expressed in equations the following orientation of the vectors is obtained:

$M^+(t)$: $f(t) = \cos(\Omega t+\phi) + i \sin(\Omega t+\phi) = e^{i(\Omega t+\phi)}$ with $\phi = \Omega\Delta$.

Fourier transformation yields:

$S(\omega) = FT(f(t)) = e^{i\Omega\Delta} L(\omega) = \cos(\Omega\Delta)\ A(\omega) - \sin(\Omega\Delta)\ D(\omega) + i(\sin(\Omega\Delta)\ A(\omega) + \cos(\Omega\Delta)\ D(\omega))$

This phase error can be approximately removed by a linear phase correction $e^{i\omega\Delta}$. This leads to the correct phase correction on-resonance, however, not slightly off-resonance. For example the phase correction to be applied $1/T_2$ away from the center of the signal should be $\Omega\Delta$ and not $(\Omega-1/T_2)\Delta$. Due to the fact that this is impossible, line shape distortions are effected. The real part of the spectrum yields:

$S(\omega) = \cos[(\Omega-\omega)\Delta]\ A(\omega) - \sin[(\Omega-\omega)\Delta]\ D(\omega)$

This is a combination of an absorption and dispersion signal weighted with the sine and cosine of the deviation of ω from Ω (Fig. 10). Therefore one always tries to keep the linear phase correction as small as possible in order to minimize these effects. When the product of line width and delay Δ is small compared to 1, the effect is negligable.

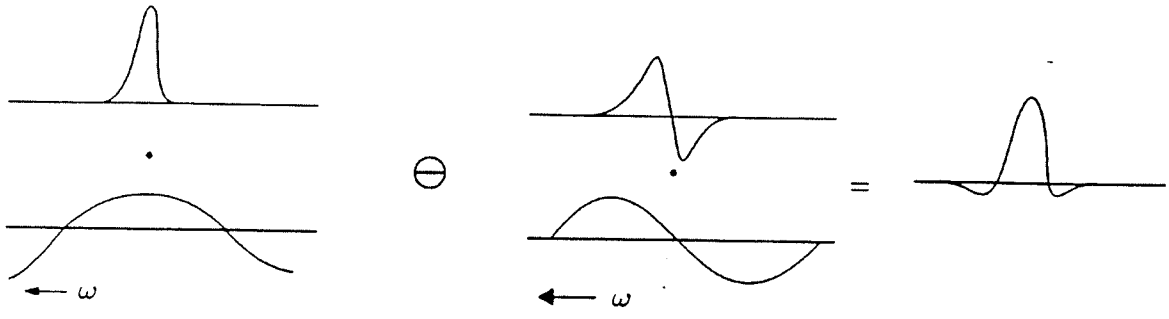

1.2.6. Summary:

The 1D FT sequence rotates with an rf pulse the longitudinal magnetization oriented along the z-axis into the transverse plane. The magnetization then starts to precess about the z-axis with its characteristic chemical shift Ω. The receiver records the x and y component of the magnetization and creates a complex signal that after Fourier transformation yields a lorentzian line at the characteristic position Ω.

1.2.7. Sensitivity

The sensitivity of NMR is inherently low because the energy differences between nuclear spin states are of the order of 10^{-5} of the thermal energy at room temperature. Therefore sensitivity enhancement is one of the major goals in NMR spectroscopy. The sensitivity (signal to noise, S/N) of a one dimensional experiment is proportional to:

$$S/N \sim N (\gamma_{exc} B_0) \gamma_{det} (\gamma_{det} B_0)^{1/2} (NS)^{1/2} T_2/T = N \gamma_{exc} \gamma_{det}^{3/2} B_0^{3/2} (NS)^{1/2} T_2/T$$

N is the number of molecules in the active sample volume. The first factor stems from the Boltzman factor: $(\gamma_{exc} B_0)$. γ_{exc} is the gyromagnetic ratio of the excited spin. γ_{det} stems from the fact that the magnetization is detected which is proportional to the gyromagnetic ratio of the spin being detected. Finally the $(\gamma_{det} B_0)^{1/2}$ factor stems from the fact that the derivative of the magnetization is detected $(\gamma_{det} B_0)$ and the amplitude of the noise is proportional to $(\gamma_{det} B_0)^{1/2}$. B_0 is the static magnetic field, NS is the number of experiments, T_2 is the homogeneous line width, and T is the temperature. This formula immediately shows how to increase the S/N:

a) Increase the number of molecules N by increasing the concentration of the sample at fixed volume, increasing the number of magnetically active molecules at fixed volume by labeling of low natural abundance spins or increasing the volume of the sample at fixed concentration.

b) Increase the static magnetic field B_0.

c) Increase NS, either by increasing the number of experiments (NS) or by decreasing the duration of one experiment that is, decreasing the repetition time, see the section describing BIRD.

d) Increase T_2 by decreasing the viscosity of the sample.

e) Choose the gyromagnetic ratio of the excited and detected nucleus to be as high as possible.

For a given sample and magnetic field strength B_0, item e) especially can be optimized by the selection of the most advantageous pulse scheme.

Signal to noise considerations are especially important for heteronuclear NMR. Table 3-1a lists the relative sensitivity for heteronuclear NMR. The relative measurement times to achieve identical S/N are given in Table 3-1b.

Table 3-1a: Relative Sensitivity S/N

Heteronuclear combination	X exc X det	H exc X det	X exc H det	H exc H det
H/P	1/10	0.25	0.4	1
H/C	1/32	1/8	1/4	1
H/N	1/300	1/30	1/10	1

Table 3-1b: Relative Measurement Time to achieve identical S/N

Heteronuclear combination	X exc X det	H exc X det	X exc H det	H exc H det
H/P	100	16	6.25	1
H/C	1024	64	16	1
H/N	100000	1000	100	1

The gain in sensitivity is the more dramatic the larger the difference in gyromagnetic ratio between the proton and the heterospin. Experiments that start with proton magnetization and detect proton magnetization are in principle the most sensitive.

2.1. The Density matrix:

The density matrix is introduced for the description of an ensemble of quantum mechanical objects. It is based on the eigenfunctions of a quantum mechanical system. The equation of motion is the Schrödinger equation for the functions describing the system. The Schrödinger equation acts in the Hilbert space. We want to derive the equation of motion for the density matrix and introduce handy bases for the density matrix in addition. We will focus our discussion to a spin system with just one spin 1/2. So the eigenfunctions in Hilbert space are: $\alpha = |m_z=1/2\rangle$ and $\beta = |m_z=-1/2\rangle$.
The equation of motion for the functions is:

$$ih\dot{\psi} = H\psi \text{ with } \dot{\psi} = \frac{\partial}{\partial t}\psi \qquad [8]$$

We want to look at the implications of this equation when we consider an ensemble of three spins. The first of them should reside at t=0 in the state ψ_1 (e.g. α), the second and third are assumed to be in the state ψ_2 (e.g. β). In addition we require that every of these functions ψ_1 and ψ_2 can be expanded into an eigenbasis to the Hamilton operator ϕ_i which is always easily possible given the closedness of the Hilbert space. The eigenvalues of the functions ϕ_i are h_{ii}. Then we obtain the time evolution of the functions $\psi_1(t)$ and $\psi_2(t)$ according to the following equation:

$$\psi_1(t) = \Sigma_i\, c_{1i}\, \phi_i \exp(ih_{ii}t) \qquad [9]$$
$$\psi_2(t) = \Sigma_i\, c_{2i}\, \phi_i \exp(ih_{ii}t)$$

The time evolution for our ensemble of three spins is:

$$\psi[1,2,3](t) = \psi_1[1](t)\, \psi_2[2](t)\, \psi_2[3](t) \qquad [10]$$

the value for an observable A, e.g. z-magnetization for this state of our ensemble of three spins is given by:

$$\langle A\rangle = \langle A[1]\rangle + \langle A[2]\rangle + \langle A[3]\rangle \qquad [11]$$

and according to conventional quantum mechanical calculus we obtain:

$$\langle A\rangle = \langle\psi(t)\,|A|\,\psi(t)\rangle =$$
$$\langle\psi_1[1](t)\,|A[1]|\,\psi_1[1](t)\rangle + \langle\psi_2[2](t)\,|A[2]|\,\psi_2[2](t)\rangle + \langle\psi_2[3](t)\,|A[3]|\,\psi_2[3](t)\rangle \qquad [12]$$

Taking Eq. [9] into consideration we obtain:

$$\langle A\rangle = \Sigma_{i,j}\, \langle\phi_i[1]|A[1]|\phi_j[1]\rangle\, c^*_{1i}\, c_{1j} \exp(i(h_{ii}-h_{jj})t) + \qquad [13]$$

$$<\phi_i[2]|A[2]|\phi_j[2]> c^*_{2i} c_{2j} \exp(i(h_{ii}-h_{jj})t) +$$
$$<\phi_i[3]|A[3]|\phi_j[3]> c^*_{2i} c_{2j} \exp(i(h_{ii}-h_{jj})t)$$

The expression $<\phi_i|A|\phi_j> = A_{ij}$ is the matrix representation of A in the ϕ_i basis. Since equivalent spins in different molecules cannot be distinguished, we can leave out the molecule indices and arrive at the following expression:

$$<A> = \Sigma_{i,j} A_{ij} (c^*_{1i} c_{1j} + c^*_{2i} c_{2j} + c^*_{2i} c_{2j}) \exp(i(h_{ii}-h_{jj})t) \qquad [14]$$

We define the j,i element of the density matrix to be: $\rho_{ji} = c^*_{1i} c_{1j} + c^*_{2i} c_{2j} + c^*_{2i} c_{2j}$.

With this definition the expectation value of A is: $<A> = \Sigma_{i,j} A_{ij} \rho_{ij} = Sp (A\rho)$

We will in the following make use of this central equation. We want to construct the density matrix for our ensemble of three spins:
With $\psi[1] = \alpha = \phi_1$, $\psi[2] = \beta = \phi_2$, and $\psi[3] = \beta$ we find: $\rho_{11}=1$, $\rho_{21}=0$, $\rho_{12}=0$, $\rho_{22}=2$.
The density matrix is then given in a matrix description as:

$$\rho = \begin{pmatrix} 1 & 0 \\ 0 & 2 \end{pmatrix}$$

(This density matrix is not normalized. From now on, a normalization constant of 1/N will be applied, when N is the number of molecules in the ensemble.
This density matrix has a simple meaning. The diagonal elements indicate the populations of the spin eigenfunctions: α and β respectively. The level α is populated with just one spin whereas the level β is populated with two spins. In general, the density matrix is diagonal when all the quantum systems setting up the ensemble are in an eigenstate of H. However, the off-diagonal elements of the density matrix reflect the "life" of the spin system. It is obvious that the populations are invariant with time. They do not evolve.

$$\rho_{ii}(t) = \rho_{ii}(0) \exp(i(h_{ii}-h_{ii})t) = \rho_{ii}(0). \qquad [15]$$

2.2 Time evolution of the Density matrix:

The time evolution of the density matrix can be constructed from the Schrödinger equation that describes the evolution for state functions. We choose now the notation: $\phi_k = |k>$. With this notation we can reformulate the Schrödinger equation:

$$ih \dot{\psi} = H \psi = \Sigma_i i h \dot{c}_i \phi_i = \Sigma_i c_i H \phi_i = \Sigma_{ik} c_i h_{ki} |k>$$

Formation of the scalar product with the function: $<\ell| = \int \phi^*_\ell d\tau$ yields:

$$ih\dot{c}_\ell = \Sigma_i c_i h_{\ell i}$$

From the analogous equation for $\dot{c}_\ell^*$ we find:

$$-ih\dot{\psi}^* = (ih\dot{\psi})^* = (H\psi)^* = \Sigma_i\, i h\, (\dot{c}_i)^* (\phi_i)^* = \Sigma_i (c_i H \phi_i)^* = \Sigma_{ik} (c_i h_{ki} |k\rangle)^* = \Sigma_{ik} c_i^* h_{ik} \phi_k^*$$

and after multiplication with <ml we obtain:

$$ih\dot{c}_m^* = -\Sigma_i c_i^* h_{im}$$

These two equations can now be merged together by multiplication of the first with c_m^* and the second with c_ℓ and we obtain:

$$ih[\dot{c}_\ell c_m^* + (\dot{c}_m^*) c_\ell] = ih(c_\ell c_m^*)^\bullet = \Sigma_i (h_{\ell i} c_i c_m^* - c_\ell c_i^* h_{im})$$

With the convention: $\rho_{\ell m} = c_\ell c_m^*$ we find:

$$ih(\rho_{\ell m})^\bullet = \Sigma_i (h_{\ell i} \rho_{im} - \rho_{\ell i} h_{im}) = (H\rho - \rho H)_{\ell m} = [H,\rho]_{\ell m}$$

This is the Liouville von Neuman Equation. It describes the evolution of the density matrix under the action of an Hamiltonian. The general solution to this equation for a time independent Hamiltonian is given by:

$$\rho(t) = e^{-iHt/h} \rho(0) e^{iHt/h}$$

2.3. Bases of the Density matrix:

The density matrix can be represented in various bases. For spin ½ with the functions α and β there are two bases sets in use that can be even mixed for certain applications. The first is constructed from so called single element matrices. This means that every operators being a basis vector of the density matrix contains just one non-vanishing element:

$$I_\alpha = \begin{pmatrix} 1 & 0 \\ 0 & 0 \end{pmatrix}, I_\beta = \begin{pmatrix} 0 & 0 \\ 0 & 1 \end{pmatrix}, I_+ = \begin{pmatrix} 0 & 1 \\ 0 & 0 \end{pmatrix}, I_- = \begin{pmatrix} 0 & 0 \\ 1 & 0 \end{pmatrix}$$

Whereas I_α and I_β represent populations of the α and β state, we have to find out what the operators I_+ and I_- represent.

The second even more commonly used basis set is the set of cartesian operators:

$$I_z = 1/2 \begin{pmatrix} 1 & 0 \\ 0 & -1 \end{pmatrix}, E = \begin{pmatrix} 1 & 0 \\ 0 & 1 \end{pmatrix}, I_x = 1/2 \begin{pmatrix} 0 & 1 \\ 1 & 0 \end{pmatrix}, I_y = i/2 \begin{pmatrix} 0 & -1 \\ 1 & 0 \end{pmatrix}$$

The two basis sets are connected with each other by the following equations:

$I_\alpha = ½ (E + 2I_z)$, $I_\beta = ½ (E - 2I_z)$ $\qquad$ $I_+ = I_x + i\, I_y$; $I_- = I_x - i\, I_y$

For the cartesian operators we find the following equations:

$½\, i\, I_x = I_y\, I_z$ $\qquad$ $½\, i\, I_x = -I_z\, I_y$
$½\, i\, I_y = I_z\, I_x$ $\qquad$ $½\, i\, I_x = -I_x\, I_z$
$½\, i\, I_z = I_x\, I_y$ $\qquad$ $½\, i\, I_z = -I_y\, I_x$
$¼ = I_x\, I_x = I_y\, I_y = I_z\, I_z$

The one element operators fulfil the following equations:

$I_-\, I_+ = I_\beta$ $\qquad$ $I_+\, I_- = I_\alpha$
$I_\alpha\, I_\beta = I_\beta\, I_\alpha = I_+\, I_+ = I_-\, I_- = 0$
$I_\alpha\, I_\alpha = I_\alpha$ $\qquad$ $I_\beta\, I_\beta = I_\beta$
$I_+\, I_\alpha = 0$ $\qquad$ $I_\alpha\, I_+ = I_+$
$I_-\, I_\alpha = I_-$ $\qquad$ $I_\alpha\, I_- = 0$
$I_+\, I_\beta = I_+$ $\qquad$ $I_\beta\, I_+ = 0$
$I_-\, I_\beta = 0$ $\qquad$ $I_\beta\, I_- = I_-$

We are now in a position to calculate some expectation values for some operators A in order to find out by the properties of a certain spin state what this spin state is. E.g. we find that if $\rho = I_z$ then the spin system is in a state containing z-magnetization. $\langle M_z \rangle = Sp(\gamma I_z \rho) = Sp(\gamma I_z I_z) = \gamma\, Sp(1/4) = \gamma/2$. This state does not have any x or y magnetization because $Sp(\gamma I_z I_x) = i\gamma/2\, Sp(I_y) = 0$.
One element operators I_α and I_β on the other hand do not contain any transverse magnetization, however, they do contain z-magnetization:

$\langle M_x \rangle = \gamma Sp(I_\alpha I_x) = 0$ $\qquad$ $\langle M_x \rangle = \gamma Sp(I_\beta I_x) = 0$
$\langle M_y \rangle = \gamma Sp(I_\alpha I_y) = 0$ $\qquad$ $\langle M_y \rangle = \gamma Sp(I_\beta I_y) = 0$
$\langle M_z \rangle = \gamma Sp(I_\alpha I_z) = \gamma/2$ $\qquad$ $\langle M_z \rangle = \gamma Sp(I_\beta\, I_z) = -\gamma/2$

For the transverse single element operators we find:

$\langle M_x \rangle = \gamma Sp(I_- I_x) = \gamma/2$ $\qquad$ $\langle M_x \rangle = \gamma Sp(I_+ I_x) = \gamma/2$

$\langle M_y \rangle = \gamma Sp(I_- I_y) = -i\gamma/2$ $\qquad$ $\langle M_x \rangle = \gamma Sp(I_+ I_y) = i\gamma/2$

$\langle M_z \rangle = \gamma Sp(I_- I_z) = 0$ $\qquad$ $\langle M_z \rangle = \gamma Sp(I_+ I_z) = 0$

Obviously the single element operators I_- and I_+ contain x and y magnetization.

Product operators:

In order to describe spin systems of more than one spin, the density matrix is expanded in products of operators or so called product operators. Consider for example a two spin system. There are four spin states: $\alpha\alpha$, $\alpha\beta$, $\beta\alpha$ and $\beta\beta$. The density matrix is therefore a 4x4 matrix. We can form a complete basis of the 4x4 matrices by forming the Kronecker product between the basis operators for each spin. In this notation, e.g.

$$I_x S_\alpha = \frac{1}{2}\begin{pmatrix} 0 & 1 \\ 1 & 0 \end{pmatrix} \otimes \begin{pmatrix} 1 & 0 \\ 0 & 0 \end{pmatrix} = \frac{1}{2}\begin{pmatrix} 0 & 1 & 0 & 0 \\ 1 & 0 & 0 & 0 \\ 0 & 0 & 0 & 0 \\ 0 & 0 & 0 & 0 \end{pmatrix}$$

by the same token we find for $2I_xS_y$:

$$2I_x S_y = 2\frac{1}{2}\begin{pmatrix} 0 & 1 \\ 1 & 0 \end{pmatrix} \otimes \frac{i}{2}\begin{pmatrix} 0 & -1 \\ 1 & 0 \end{pmatrix} = \frac{i}{2}\begin{pmatrix} 0 & 0 & 0 & -1 \\ 0 & 0 & -1 & 0 \\ 0 & 1 & 0 & 0 \\ 1 & 0 & 0 & 0 \end{pmatrix}$$

It is found that products of operators for different spins can be treated successively. This is one of the extremely nice properties of product operators.

2.5. Hamilton operator:

The hamilton operator for a spin system with different spins in a molecule has to be discussed. From the correspondence between the energy and the Hamiltonian we find:

$$E = -\vec{\mu}\vec{B} = -\hbar\gamma B_0 I_z = -\hbar\omega I_z$$

This is the Zeeman term or chemical shift term. In the rotating frame this reduces to $E = -\hbar\omega I_z$. Often we write the Hamiltonian in frequency units by dividing by $h/(2\pi)$.

Pulses are represented in the rotating frame by an additional constant field along x or y:

$$E = -\vec{\mu}\vec{B}_1 = -\hbar\gamma B_1 I_x = -\hbar\omega_1 I_x$$

Finally the coupling is represented by the following bilinear term:

$$E_J = h\,J\,(I_xS_x + I_yS_y + I_zS_z).$$

In the weak coupling limit, the energy is given by:

$$E_J = h\,J\,I_zS_z$$

We will solve the Liouville equation now for certain commonly encountered situations:

2.5.1. Chemical shift evolution:

The Hamiltonian in frequency units is: ΩI_z. We solve the Liouville von Neuman equation:

$$i\dot{I}_x = [\Omega I_z, I_x] = i\Omega I_y\,; \qquad i\dot{I}_y = [\Omega I_z, I_y] = -i\Omega I_x\,;$$

Comparison of these equations with those in Chap. 1.2.1 immediately yields the following evolution:

$$I_x \;\text{->}\; I_x\cos\Omega t + I_y\sin\Omega t$$
$$I_y \;\text{->}\; I_y\cos\Omega t - I_x\sin\Omega t$$

2.5.2. Evolution of Coupling:

For the evolution of the coupling in the weak coupling approximation we find:

$$i\dot{I}_x = [2\pi J I_zS_z, I_x] = i\pi J 2I_yS_z\,;$$
$$i\dot{2I_yS_z} = [2\pi J I_zS_z, 2I_yS_z] = -i\pi J I_x\,;$$

From these two equations we find in an analogous way:

$$I_x \;\text{->}\; I_x\cos\pi Jt + 2I_y\,S_z\sin\pi Jt$$
$$2I_y\,S_z \;\text{->}\; 2I_y\,S_z\cos\pi Jt - I_x\sin\pi Jt$$

In addition we find for I_y the following transformations:

$$I_y \;\text{->}\; I_y\cos\pi Jt - 2I_x\,S_z\sin\pi Jt$$

$2I_x S_z \quad \rightarrow \quad 2I_x S_z \cos\pi Jt + I_y \sin\pi Jt$

Another handy result is the following: $[I_xS_y, 2\pi JI_zS_z] = 0$. This is a general result and the conclusion ist that a product of transverse operators or two different spins I and S does not evolve the I,S coupling.

2.5.3 Successive Evolution:

Normally chemical shift and couplings or chemical shifts and rf pulses act simultaneously. However, whenever in a Hamiltonian we have commuting parts they can be applied successively. This is easily seen in the following way. The time evolution of the density matrix is given by:

$\rho(t) = e^{-i(H_1+H_2)t}\rho(0)e^{i(H_1+H_2)t} = e^{-iH_1t}e^{-iH_2t}\rho(0)e^{iH_2t}e^{iH_1t}$, provided H_1 and H_2 commute.

During free evolution the chemical shifts: ΩI_z and the couplings $2\pi JI_zS_z$ commute. In addition, chemical shifts commute mutually. However, neither of these operators commutes with pulses. Therefore, free evolution of chemical shift and coupling is interrupted by the action of pulses.

2.5.4. Detection:

The detection operator is given by: I_x and I_y. We find that we can only detect I_x or I_y. This is a result of the following equation:

$\langle I_x \rangle = Sp(I_x\rho)$. The latter product vanishes unless ρ contains I_x. The same is true for I_y.
Therefore we only detect cartesian product operators that contain just one operator either I_x or I_y.
Detection of $M_x+iM_y = \gamma Sp(I_x\rho) + i\,\gamma Sp(I_x\rho) = \gamma Sp(I_+\rho) = 0$ except for $\rho = I_-$. Therefore I_- is detected in the quadrature detector.

2.5.5 Evolution of chemical shift for single element operators:

Evolution of chemical shift for single element operators can be derived in the same form as we did for the cartesian product operators:

$i\dot{I}_+ = [\Omega I_z, I_+] = \Omega I_+$ and $i\dot{I}_- = [\Omega I_z, I_-] = -\Omega I_-$

Integration of these two differential equations yields:

$I_+(t) = e^{-i\Omega t}I_+(0)$; and $I_-(t) = e^{i\Omega t}I_-(0)$

this shows that the single element operators evolve chemical shift with an exponential function. They are also eigenoperators under the evolution of chemical shift which is sometimes of great

advantage. The single element operators also have the unique property that under any rotation about the z-axis they are transformed into themselves:

$\beta_z I_- = e^{i\phi} I_-$; $\beta_z I_+ = e^{-i\phi} I_+$ or in general: $\beta_z I_+ = e^{-ip\phi} I_+$ with p = 1. p is the coherence order which is 1 for I_+.

A product of single element operators has the sum of the coherence orders of the individual operators. E.g. $\beta_z I_+S_+ = e^{-i2\phi} I_+S_+$. Thus p = 2 and we have double quantum coherence.

In addition the evolution of a coherence of the type I_+S_+ can be described very easily. We find for the evolution under chemical shift:

$$I_+S_+ \rightarrow I_+S_+ e^{-i(\Omega_I+\Omega_S)t}$$
$$I_+S_- \rightarrow I_+S_- e^{-i(\Omega_I-\Omega_S)t}$$

It can be seen that the double quantum coherence I_+S_+ evolves the sum of the chemical shifts of the two involved spins, whereas the zero quantum coherence I_+S_- evolves the difference of the two chemical shifts.

2.5.6. Evolution of coupling for single element operators:

We find for the evolution of coupling using the commutation relations:

$$i\dot{I}_+ = [2\pi J I_z S_z, I_+] = \pi J 2I_+S_z;$$
$$i2\dot{I}_+S_z = [2\pi J I_z S_z, 2I_+S_z] = \pi J I_+$$

We derive using the earlier results:

$$I_+ \rightarrow I_+ \cos\pi Jt + 2I_+S_z \sin\pi Jt$$
$$2I_+S_z \rightarrow 2I_+S_z \cos\pi Jt + I_+ \sin\pi Jt$$

Doing the same with the operator I_+S_- under evolution of the coupling to a third spins T we arrive at:

$$i\dot{I}_+S_- = [2\pi J_{IT} T_z I_z + 2\pi J_{ST} S_z T_z, I_+S_-] = \pi(J_{IT} - J_{ST}) 2I_+S_-T_z$$
$$i2\dot{I}_+S_-T_z = [2\pi J_{IT} T_z I_z + 2\pi J_{ST} S_z T_z, 2I_+S_-T_z] = \pi(J_{IT} - J_{ST}) I_+S_-$$

from this set of differential equations we obtain the following evolution:

$I_+S_- \rightarrow I_+S_- \cos[\pi(J_{IT}-J_{ST})t] + 2I_+S_-T_z \sin[\pi(J_{IT}-J_{ST})t]$
$2I_+S_-T_z \rightarrow 2I_+S_- T_z \cos[\pi(J_{IT}-J_{ST})t] + I_+S_- \sin[\pi(J_{IT}-J_{ST})t]$

Multiple quantum coherence obviously evolves the coupling to a third passive spin with the sum of the couplings weighted with the respective coherence orders of the spins involved in the multiple quantum coherence.

3. Hand waving derivation of the Product Operator Formalism

We will use throughout this course the product operator formalism, which is the most appropriate tool for the description of complicated experiments for weakly coupled spin systems. The product operator formalism provides a handy description of the states of the spin system under conditions which can be described by a density matrix. Like any quantum mechanical state, the state of the density matrix has certain observables, such as magnetization, which have to be extracted by mathematical procedures.

We have presented a mathematical introduction in the previous chapter, starting from the Liouville von Neumann equation and introducing the observables as traces of the product of density matrix and the corresponding operator to the observable. This approach can be reread in many references (1-3). Now, we present a more phenomenological introduction based on analogy to the easy-to-grasp vector model. This approach was also used in Ref. (4).

In the vector formalism, the magnetization of a spin is composed of the components M_x, M_y, and M_z. These magnetizations precess around an externally applied magnetic field tracing out the surface of a cone. This external field may either be the static magnetic field along the z-axis or a transverse field which is generated by an rf pulse and is static in the rotating frame. The axis of the cone on whose outer surface the magnetization precesses is given by the orientation of the external field. The precession frequency ω is given by the product of the field strength and the gyromagnetic ratio: $\omega = \gamma B$.

The precession of magnetization in the rotating frame due to its chemical shift is understood as the precession about a static field along z with strength Ω. This is illustrated in Fig. 3-1a for the evolution of x-magnetization. The transformation properties for the other orientations of magnetizations are:

$$M_x \xrightarrow{\Omega t} M_x \cos\Omega t + M_y \sin\Omega t \qquad M_y \xrightarrow{\Omega t} M_y \cos\Omega t - M_x \sin\Omega t$$
$$M_z \xrightarrow{\Omega t} M_z$$

The application of rf pulses can be understood as the application of a magnetic field that is static in the rotating frame and lies in the transverse plane. A pulse about the x-axis originates from a field B_1 along the x-axis in the rotating frame. Any magnetization will then precess about this axis with

the frequency $\omega_1 = \gamma B_1$. Fig. 3-1b gives a graphic representation of this precession for the evolution of z-magnetization. z-magnetization is present, for example, at the beginning of any pulse sequence.

$$\begin{array}{lll} & \omega_1 t & \\ M_y & \rightarrow & M_y \cos\omega_1 t + M_z \sin\omega_1 t = M_y \cos\beta + M_z \sin\beta \\ M_z & \rightarrow & M_z \cos\omega_1 t - M_y \sin\omega_1 t = M_z \cos\beta - M_y \sin\beta \\ M_x & \rightarrow & M_x \end{array}$$

The flip angle β is given by the product of rotation frequency ω_1 and the duration t of the pulse. A special duration is $t = \pi/2\omega_1$ which defines a 90° pulse. A $90_y°$ pulse (which is a transverse field of duration $t = \pi/(2\gamma B_1)$ followed by evolution of chemical shift will lead to the following transformations:

$$\begin{array}{lllll} & 90_y & & \Omega t & \\ M_z & \rightarrow & M_x & \rightarrow & M_x \cos\Omega t + M_y \sin\Omega t \end{array}$$

A phase sensitive detector records M_x and M_y as a function of time and stores them in different memory locations A and B, respectively. A complex signal is reconstructed, of the form:

$$\exp(i\Omega t) = \cos\Omega t + i \sin\Omega t$$

by adding the contents of A and i times the contents of B. Fourier transformation of this complex FID yields a complex Lorentzian line provided the FID decays with a time constant T_2.
The transition to the product operator formalism is achieved by the following correspondence principle. The magnetization M generated by the ensemble of microscopic spins is replaced by operators I which are indexed by the cartesian coordinates. I_x then represents a state of an ensemble of spins I that carries x-magnetization. The transformations and properties indicated above are exactly the same as for the magnetizations:
Thus precession of a state of the ensemble that carries I spin magnetization about a static magnetic field along z with frequency Ω in the rotating frame gives the following transformation:

$$I_x \rightarrow I_x \cos\Omega t + I_y \sin\Omega t \qquad I_y \rightarrow I_y \cos\Omega t - I_x \sin\Omega t$$
$$I_z \rightarrow I_z$$

A transverse B_1 field, e.g. from the x-direction, will lead to a precession about the x-axis with the frequency $\omega_1 = \gamma B_1$:

$$I_y \rightarrow I_y \cos\omega_1 t + I_z \sin\omega_1 t \qquad I_z \rightarrow I_z \cos\omega_1 t - I_y \sin\omega_1 t$$
$$I_x \rightarrow I_x$$

Thus a 90_y^o pulse (which is a transverse field of duration $t = \pi/(2\gamma B_1)$ applied on the equilibrium state of the spin followed by chemical shift precession will lead to the following transformations:

$$I_z \xrightarrow{90_y} I_x \xrightarrow{\Omega t} I_x \cos\Omega t + I_y \sin\Omega t$$

3.1. Coupling:

The advantage of the product operator formalism is that it allows the description of coupled spin systems, where states that do not carry observable magnetization play the central role. The transformation of these non-observable states under pulses cannot be described by the vector formalism. We will introduce those states relying as long as possible on the vector formalism. Suppose we have a spin that is coupled to another spin with a coupling constant J = 10 Hz and therefore appears in the spectrum as a doublet. When transverse magnetization of this spin is excited it disappears at odd multiples of 50 ms and then reappears again. In the vector model this is rationalized by two magnetization vectors that rotate in opposite directions, each with a frequency of 5 Hz. The two vectors are oriented antiparallel (antiphase) after 1/4 of a full revolution, i.e. after 50 ms. The state of the spin system at 50 ms is devoid of any macroscopic magnetization, yet it is very different from the state that is reached after a long irradiation of the spin of interest, which destroys all magnetization. The product operator formalism makes it possible to describe states without observable magnetization. These turn out to be the crucial states of a spin system which make possible most of the heteronuclear transfer experiments we are about to discuss in this Chapter. We come back to our two-spin system again:
A spin I_1 that is coupled to another spin I_2 (spin 1/2) appears as a doublet in the spectrum. The doublet structure of the signal of I_1 arises from two different types of molecules, namely one type of molecule in which I_2 is in the α-state and a second type of molecule in which I_2 is in the β-state. Suppose the chemical shift of the spin I_1 is Ω_1. Then, the frequency of the I_1 line in the $I_{2\alpha}$ spin-isomers is $\Omega_1+\pi J$, and the frequency of the I_1 line in the $I_{2\beta}$ spin-isomers is $\Omega_1-\pi J$. The spectrum of the I_1 spin is the superposition (sum) of the spectra originating from the two spin-isomers (Fig. 3-2). Therefore we can write down the transformations in the following way:

$$I_{1x}I_{2\alpha} \rightarrow I_{1x}I_{2\alpha}\cos(\Omega_1+\pi J)t + I_{1y}I_{2\alpha}\sin(\Omega_1+\pi J)t$$
$$I_{1x}I_{2\beta} \rightarrow I_{1x}I_{2\beta}\cos(\Omega_1-\pi J)t + I_{1y}I_{2\beta}\sin(\Omega_1-\pi J)t$$

We need to introduce two rules:

1) $I_\alpha + I_\beta = 1$

This equation can be rationalized by referring to the previous chapter or by considering I_α and I_β as the probability of finding a spin in these states or the population of these states. Since there are just these two states for a spin 1/2 the sum over these probabilities is 1.

2) $I_\alpha - I_\beta = 2I_z$

This can be rationalized by referring to the previous chapter or by the observation that a population difference between α-state and β-state carries z-magnetization. The factor 2 is just a normalization constant. This rule actually describes a transformation from a single element basis set for the description of longitudinal magnetization (I_α, I_β) to a cartesian basis set ($2I_z$, identity operator) (2). With these two rules for the calculation and some trigonometric transformations we arrive at:

$$I_{1x} \rightarrow \quad I_{1x} \cos\pi t \cos\pi Jt + I_{1y} \sin\pi t \cos\pi Jt$$
$$+2I_{1y}I_{2z} \cos\pi t \sin\pi Jt - 2I_{1x}I_{2z} \sin\pi t \sin\pi Jt$$

The transformation properties of I_y can be obtained by cyclic permutation: x -> y -> -x -> -y.
The state $2I_{1y}I_{2z}$ is a product of two operators. It does not carry magnetization; in fact it is a general rule that only states of the spin system that can be represented by a single operator carry magnetization. The $2I_{1y}I_{2z}$ operator is called an antiphase operator (Fig. 3-3). This becomes plausible if one considers this operator in detail:

$$2I_{1y}I_{2z} = I_{1y} I_{2\alpha} - I_{1y} I_{2\beta}$$

Obviously, $2I_{1y}I_{2z}$ is the difference spectrum of the spin isomers with I_2 in the α and in the β state. This spectrum has two lines at $\Omega_1+\pi J$ and at $\Omega_1-\pi J$, respectively; the two lines have different sign. In the absence of pulses such an antiphase operator evolves as follows:

$$2I_{1y}I_{2z} \rightarrow \quad +2I_{1y}I_{2z} \cos\Omega_1 t \cos\pi Jt - 2I_{1x}I_{2z} \sin\Omega_1 t \cos\pi Jt$$
$$-I_{1x} \cos\Omega_1 t \sin\pi Jt - I_{1y} \sin\Omega_{11} t \sin\pi Jt$$

The transformation properties of product operators under pulses are as follows:

- A pulse is applied to all operators individually.
- Chemical shift evolution and evolution of coupling need not be applied simultaneously in periods of free evolution that may be interrupted by 180° pulses. Often one achieves a simpler description by consecutive application of the interactions to the spin state (*vide infra*).

To conclude this rather cursory introduction to product operators we discuss the polarization transfer process that is essential for all experiments in high resolution NMR that use J coupling for transfer of magnetization from one spin to another spin. Using the product operator formalism (and

assuming for the moment that spin I_1 is on resonance), polarization transfer can be described very simply. An in-phase operator I_{1x} evolves during a delay Δ completely into an antiphase operator $2I_{1y}I_{2z}$, provided $\sin\pi J\Delta = 1$, i.e. $\Delta = 1/(2J)$. Application of a 90_x pulse to I_1 and I_2 transforms this operator into $-2I_{1z}I_{2y}$, which after another delay $\Delta = 1/(2J)$ forms I_{2x}; this state again carries observable magnetization. Thus transverse magnetization of spin I_1 is transferred to transverse magnetization of spin I_2.

3.2. Some handy formulae for product operator calculus:

Transformations of cartesian operators under pulses, chemical shift and coupling provides:

$$I_z \xrightarrow{\beta_y} I_z\cos\beta + \sin\beta I_x \qquad I_x \xrightarrow{\beta_y} I_x\cos\beta - \sin\beta I_z \qquad I_y \xrightarrow{\beta_y} I_y$$

$$I_z \xrightarrow{\beta_x} I_z\cos\beta - \sin\beta I_y \qquad I_x \xrightarrow{\beta_x} I_x \qquad I_y \xrightarrow{\beta_x} I_y\cos\beta + I_z\sin\beta$$

$$I_z \xrightarrow{\beta_z} I_z \qquad I_x \xrightarrow{\beta_z} I_x\cos\beta + I_y\sin\beta \qquad I_y \xrightarrow{\beta_z} I_y\cos\beta - I_x\sin\beta$$

$$I_z \xrightarrow{\Omega t I_z} I_z \qquad I_x \xrightarrow{\Omega t I_z} I_x\cos\Omega t + I_y\sin\Omega t \qquad I_y \xrightarrow{\Omega t I_z} I_y\cos\Omega t - I_x\sin\Omega t$$

$$I_x \xrightarrow{2\pi J t I_z S_z} I_x\cos(\pi J t) + 2I_yS_z\sin(\pi J t) \qquad I_y \xrightarrow{2\pi J t I_z S_z} I_y\cos(\pi J t) - 2I_xS_z\sin(\pi J t)$$

All these transformations have the same structure: If we consider the left hand side to represent an educt of a transformation, then the educt is reproduced on the right side with a cosine. In addition exactly one product is formed with a sine. The argument is β for a flip angle, it is Ωt, and it is πJt for a coupling. Only the evolution under coupling can increase or decrease the number of operators making up a product operator. Only the number of z-operators is changed. It is either increased by 1 with the $\sin(\pi Jt)$ or it is decreased by 1 with the same factor. Creation or annihilation of a z-operator ensues modulation with the sine of the coupling.

Transformations of single element operators under pulses, chemical shifts and couplings provides:

$$I_\alpha \xrightarrow{\beta_\phi} I_\alpha\cos^2(\beta/2) + I_\beta\sin^2(\beta/2) + i/2(I_+e^{-i\phi} - I_-e^{i\phi})\sin\beta$$

$$I_\beta \xrightarrow{\beta_\phi} I_\beta\cos^2(\beta/2) + I_\alpha\sin^2(\beta/2) - i/2(I_+e^{-i\phi} - I_-e^{i\phi})\sin\beta$$

$$I_+ \xrightarrow{\beta_\phi} I_+\cos^2(\beta/2) + I_-\sin^2(\beta/2)e^{i2\phi} - e^{i\phi}\sin\beta(I_\alpha - I_\beta)/2$$

$$I_- \xrightarrow{\beta_\phi} I_-\cos^2(\beta/2) + I_+\sin^2(\beta/2)e^{-i2\phi} + e^{-i\phi}\sin\beta(I_\alpha - I_\beta)/2$$

$$I_+ \xrightarrow{\Omega t I_z} I_+e^{-i\Omega t} \qquad I_- \xrightarrow{\Omega t I_z} I_-e^{i\Omega t}$$

$$I_+I_\alpha \xrightarrow{2\pi J t I_z S_z} I_+I_\alpha e^{-i\pi Jt} \qquad I_-I_\alpha \xrightarrow{2\pi J t I_z S_z} I_-I_\alpha e^{i\pi Jt}$$

$$I_+I_\beta \xrightarrow{2\pi J t I_z S_z} I_+I_\beta e^{i\pi Jt} \qquad I_-I_\beta \xrightarrow{2\pi J t I_z S_z} I_-I_\beta e^{-i\pi Jt}$$

Signal structure

Most of the NMR experiments to be discussed create during evolution times or detection times certain operators that predefine the structure of the signal to be observed later on. Therefore we want to know which traces which operator leaves in the spectrum.

Given a two spin system we find for an initial state at t=0 : I_x the following transformation:

$$I_x \rightarrow \cos(\pi Jt)\,(I_x \cos\Omega t + I_y \sin\Omega t) + 2S_z \sin(\pi Jt)\,(I_y \cos\Omega t - I_x \sin\Omega t)$$

Only the first two terms can be observed and according to the recording of both I_x and I_y in the phase sensitive detector, the signal is $\cos\pi Jt\ e^{i\Omega t}$. Of course we know that the Fourier transformation of this FID yields a doublet at the position Ω with a splitting of $2\pi J$:

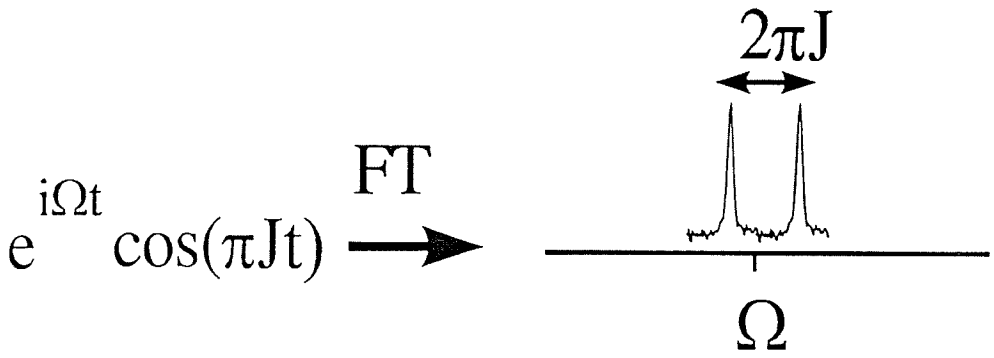

We can obtain this signal also by explicite Fourier transformation:

$$\cos(\pi Jt)e^{i\Omega t} = \frac{1}{2}\left(e^{i(\Omega+\pi J)t} + e^{i(\Omega-\pi J)t}\right)$$

So we expect to lines with equal phase at the positions $\Omega+\pi J$ and $\Omega-\pi J$ as is shown in the Figure. Such a signal is called in-phase absorptive signal.
The next signal type is derived from $2I_xS_z$. According to the evolution under chemical shift and coupling we obtain:

$$2I_xS_z \rightarrow \cos(\pi Jt)\,2S_z\,(I_x \cos\Omega t + I_y \sin\Omega t) + \sin(\pi Jt)\,(I_y \cos\Omega t - I_x \sin\Omega t)$$

We can detect here:

$$\sin(\pi Jt)\,(i\cos\Omega t - \sin\Omega t) = \sin(\pi Jt)ie^{i\Omega t} = \frac{1}{2}\left(e^{i(\Omega+\pi J)t} - e^{i(\Omega-\pi J)t}\right)$$

Obviously, we expect two absorptive signals at $\Omega+\pi J$ and $\Omega-\pi J$, however with opposite relative sign.

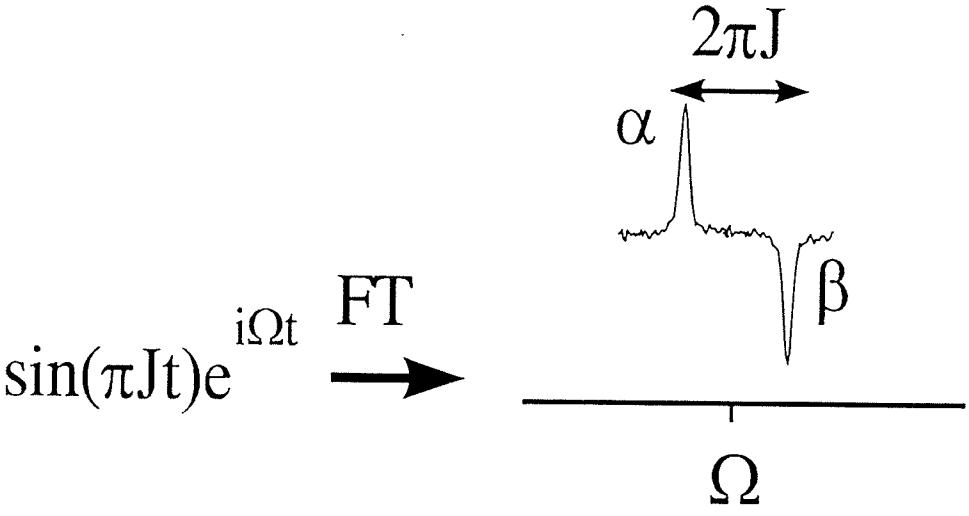

Such a signal is called an antiphase absorptive signal.
Obviously, the operator $2I_xS_z$ yields an absorptive doublet in antiphase in the real part. The corresponding operator is therefore called antiphase coherence. The corresponding operators with I_y instead of I_x would yield dispersive signals. It should be noted that when I_x yields an absorptive signal then all operators of the form $I_xS_z^m$ also yield absorptive signal.
The shape of the signal and the operators are clearly linked with each other. We obtained an in phase signal when no z-operator was created or annihilated because then the coupling evolution yields only cosine modulations. Creation or annihilation of a z-operator introduces a $\sin(\pi Jt)$ which leads to an antiphase splitting.

Also the single element operators give unique spectra: For example we have learned the transformation properties of the operator: I_S_α:

$I\_S_\alpha \rightarrow I\_S_\alpha\, e^{i\pi Jt}e^{i\Omega t} = e^{i(\pi J+\Omega)t}$. Fourier transformation of this signal gives a single line at position: $\pi J+\Omega$.

On the other hand I_S_β yields a line at $\Omega-\pi J$:
$I\_S_\alpha \rightarrow I\_S_\beta\, e^{-i\pi Jt}e^{i\Omega t} = e^{i(\Omega-\pi J)t}$.

The next thing to worry about is now: How does this work out in a n-spin system?

3.4. Signals in multi spin systems:

Let us look at a three spin system: I S T. All spins shall be coupled and we want to discuss evolution of the following operator under chemical shift and couplings. We retain only the detectable part and obtain as signal:

$2I_xS_z$: $\quad e^{i\Omega_I t} i \sin(\pi J_{IS} t) \cos(\pi J_{IT} t)$

The Fourier transformation of this time domain signal can be done by Fourier transforming each factor in the product and then convoluting the result. The Fouriertransformations of each of the products are given in the figure on the next page.

3.5. 2D spectroscopy

2D spectroscopy is the realm of pulse sequences that are constructed in the following way:

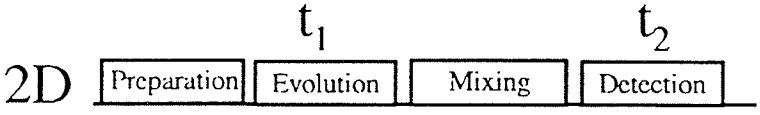

3.5.1 2D COSY

The COSY pulse sequence correlates two spins that are mutually coupled. The pulse sequence is:

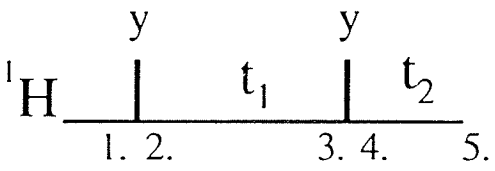

We separate the pulse sequence and start with the Boltzmann magnetization at position 1:

1. $I_{1z} + I_{2z}$
2. $I_{1x} + I_{2x}$

Since we treat a sum we can consider the evolution of each of the contributions separately. We will first look at the I_{1x} term.

2. I_{1x}

Evolution of coupling and chemical shift yields:

3. $I_{1x} \rightarrow \cos(\pi J t_1)\,(I_{1x}\cos\Omega_1 t_1 + I_{1y}\sin\Omega_1 t_1) + 2I_{2z}\sin(\pi J t_1)\,(I_{1y}\cos\Omega_1 t_1 - I_{1x}\sin\Omega_1 t_1)$

They are transformed by the 90_y pulse into the following four terms:

4. $\cos(\pi J t_1)\,(-I_{1z}\cos\Omega_1 t_1 + I_{1y}\sin\Omega_1 t_1) + 2I_{2x}\sin(\pi J t_1)\,(I_{1y}\cos\Omega_1 t_1 + I_{1z}\sin\Omega_1 t_1)$

Now free evolution takes place until the signal is detected. Two of the operators cannot be observed and they do not form operators that are observable: These are: I_{1z} and $2I_{2x}\,I_{1y}$. So we are left with:

4. $\cos(\pi J t_1)\,I_{1y}\sin\Omega_1 t_1 + 2I_{2x}\sin(\pi J t_1)\,I_{1z}\sin\Omega_1 t_1$

Since only I_x and I_y terms can be detected we can reduce the number of signals taken into account. We also know that whenever a term of the form I_x is created, a term I_y is concommitantly created which is shifted in phase by 90°. Therefore we detect during t_2 the following operators:

5. $\cos(\pi J t_1)\sin\Omega_1 t_1\cos(\pi J t_2)\,(I_{1y}\cos\Omega_1 t_2 - I_{1x}\sin\Omega_1 t_2) +$
$\sin(\pi J t_1)\sin\Omega_1 t_1\sin(\pi J t_2)\,(I_{2y}\cos\Omega_2 t_2 - I_{2x}\sin\Omega_2 t_2)$

The detected signal is then given by the usual combination procedure and yields:

5. $\cos(\pi J t_1)\sin(\Omega_1 t_1)\cos(\pi J t_2)\,ie^{i\Omega_1 t_2} + \sin(\pi J t_1)\sin(\Omega_1 t_1)\sin(\pi J t_2)\,ie^{i\Omega_2 t_2}$

The first term leads to the diagonal signal, since the chemical shift evolving during t_1 is the same as the one evolving during t_2. This is not the case for the second term where we have evolution of Ω_1 during t_1 and Ω_2 during t_2.The above given signal depends on two time variables that can be Fourier transformed separately. Fourier transformation along t_2 yields:

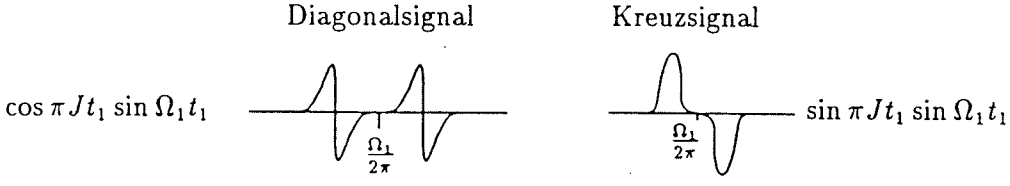

We have arbitrarily corrected the diagonal peak to dispersion the cross peak to absorption.
The remaining modulation along t_1: $\cos(\pi J t_1)\sin(\Omega_1 t_1)$ and $\sin(\pi J t_1)\sin(\Omega_1 t_1)$ is not of the form we would like it to have, namely of the type:

$\cos(\pi J t_1)ie^{i\Omega_1 t_1}$ or $\sin(\pi J t_1)ie^{i\Omega_2 t_1}$

This problem can be remedied by recording a second experiment in which the phase of the first pulse is rotated with respect to the second by 90°. This yields the following second signal:

5. $\cos(\pi Jt_1)\cos(\Omega_1 t_1)\cos(\pi Jt_2)ie^{i\Omega_1 t_2} + \sin(\pi Jt_1)\cos(\Omega_1 t_1)\sin(\pi Jt_2)ie^{i\Omega_2 t_2}$

Combination of the two signal forms yields now a modulation in t_1 according to:

$\cos(\pi Jt_1)ie^{i\Omega_1 t_1}$ 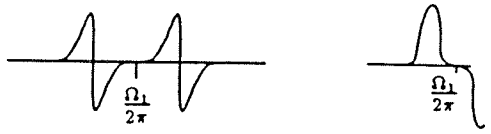 $\sin(\pi Jt_1)ie^{i\Omega_2 t_1}$

Fourier transformation along t_1 provides then the multiplet structure of the diagonal and cross peak. The diagonal peak is in dispersion, the cross peak in absorption in both frequency dimensions. In the cross peak, the active coupling is in antiphase in both dimensions.

doubly dispersive
diagonal peak

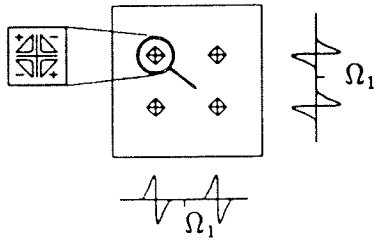

doubly absorptive
cross peak

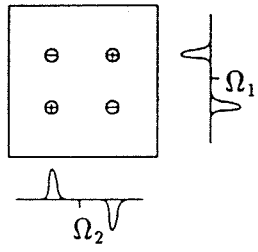

After this long calculation we want to discuss this experiment again from a bird's perspective so that we do not have to discuss all the terms for all experiments. This would be impracticable given the large number of pulses encountered later on. The key pulse in the sequence is the 90° mixing pulse. Suppose it acts at position 3. in the sequence on an operator of the form: $I_{1x}\, I_z^m$ where I_z^m represents a product of m I_z operators, then a $90_y°$ pulse will produce only detectable terms for m=1 at position 4. $2I_{1x}I_{2z} \rightarrow: -2I_{2x}I_{1z}$. This so called coherence transfer is the most frequently used tool in NMR spectroscopy. A 90° pulse transfers antiphase coherence on one spin to antiphase coherence on a second spin.

We can now formulate the transfer that leads to the cross peaks:

$$I_{1z} \xrightarrow{90_y} I_{1x} \xrightarrow{t_1} 2I_{1x}I_{2z} \xrightarrow{90_y} -2I_{1z}I_{2x} \xrightarrow{t_2} I_{2x}$$

The transfer function for the cross peak signal is given by:

$$\sin(\pi J t_1)\sin(\Omega_1 t_1)\sin(\pi J t_2)ie^{i\Omega_2 t_2}$$

There is only one additional operator that passes the $90°_y$ pulse and that is I_{1y}. It leads to the diagonal peak.

$$I_{1z} \xrightarrow{90_y} I_{1x} \xrightarrow{t_1} I_{1y} \xrightarrow{90_y} I_{1y} \xrightarrow{t_2} I_{1x}$$

The transfer function for the diagonal peak is given by:

$$\cos(\pi J t_1)\sin(\Omega_1 t_1)\cos(\pi J t_2)ie^{i\Omega_1 t_2}$$

The transfer function of the cross peak contains two sine functions whereas the diagonal peak contains only one in each time domains t_1 and t_2. Therefore the phases of the peaks are 90° different.

3.5.2.1 COSY of a three spin system:

We want to apply the COSY experiment to three spins I_1, I_2, I_3 and construct the cross peak between I_1 and I_2. The transfer pathway is the same as for two spins since the 90° pulse selects the two spin anti phase operators:

$$I_{1z} \xrightarrow{90_x} I_{1x} \xrightarrow{t_1} 2I_{1x}I_{2z} \xrightarrow{90_y} -2I_{1z}I_{2x} \xrightarrow{t_2} I_{2x}$$

The transfer function can be easily written down:

$$\sin(\pi J_{12} t_1)\cos(\pi J_{13} t_1)\sin(\Omega_1 t_1)\sin(\pi J_{12} t_2)\cos(\pi J_{13} t_2)ie^{i\Omega_2 t_2}$$

The transfer function is different from the two spin COSY spectrum only by the additional $\cos(\pi J_{13} t_1)$ and $\cos(\pi J_{13} t_2)$ terms. We obtain a 16 line multiplet with the active coupling J_{12} in antiphase in both dimensions and the passive coupling J_{13} in-phase.

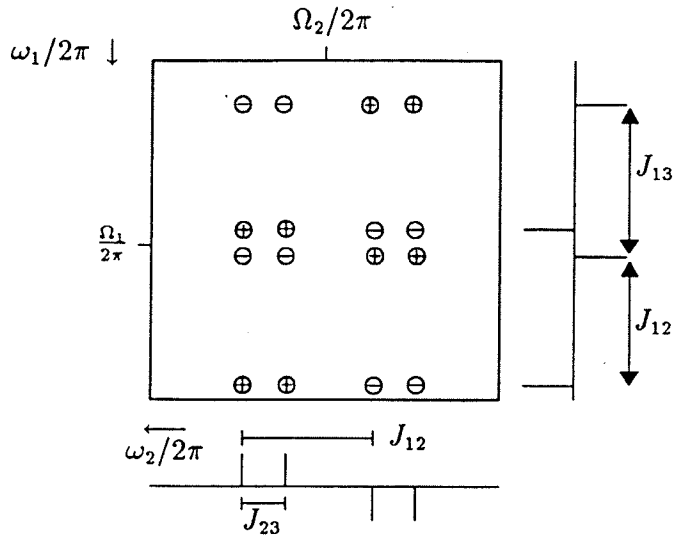

3.5.2 P. COSY:

The diagonal peak in the COSY experiment is dispersive in both dimensions when the cross peaks are in absorption. The dispersive tails of the diagonal peaks therefore often overlap with the cross peaks close to the diagonal and deteriorate the spectral quality. Therefore it is highly desirable to suppress this signal. This can be achieved in the following way.
If we consider the transfer pathway that leads to the diagonal peak in the COSY we have:

$$I_{1z} \xrightarrow{90_x} I_{1x} \xrightarrow{t_1} I_{1y} \xrightarrow{90_y} I_{1y} \xrightarrow{t_2} I_{1x}$$

This is transfer is effective independent of the flip angle of the mixing pulse. Therefore we can suppress the dispersive diagonal peak by subtracting a second experiment, in which the flip angle of the mixing pulse is 0.

$$I_{1z} \xrightarrow{90_x} I_{1x} \xrightarrow{t_1} I_{1y} \xrightarrow{0_y} I_{1y} \xrightarrow{t_2} I_{1x}$$

The latter transfer does not create any cross peaks so that the signal to noise for the cross peaks decreases by a factor $\sqrt{2}$. The experiment with the 0 degree mixing pulse allows also for the following transfer leading to a diagonal peak:

$$I_{1z} \xrightarrow{90_x} I_{1x} \xrightarrow{t_1} I_{1x} \xrightarrow{0_y} I_{1x} \xrightarrow{t_2} I_{1x}$$

This transfer yields however an absorptive in phase signal which can be more easily tolerated.

3.6. Basic heteronuclear experiments

Correlation experiments between heteronuclei make use of the coupling constants between these nuclei; values for some heteronuclear coupling constants are summarized in Table 3-2.

Table 3-2: Some Heteronuclear Coupling Constants

Nuclei	H,C	H,N	H,P
^1J	125-250	90	700
^2J	0-20	0-10	
^3J	0-10	0-5	0-20

Heteronuclear ^1J couplings are at least an order of magnitude larger than the homonuclear $^2J(H,H)$ and $^3J(H,H)$ couplings. The ^2J and ^3J couplings tend to be smaller and of the order of proton-proton coupling constants. Since the time required to transfer magnetization from one nucleus to another nucleus is of the order of J^{-1}, the use of large couplings is advantageous for molecules with short T_2 times. This concept is important in the studies of completely ^{13}C labeled proteins.
Consider a correlation experiment between two protons separated by three bonds. In a homonuclear experiment the time required to transfer magnetization between two protons in a H-C-C-H moiety, with the protons sharing a rather large ^3J coupling of 10 Hz, is 1/J = 100ms. The double heteronuclear relayed transfer, however, H->^{13}C->^{13}C->H requires only 42ms for $^1J_{HC}$ = 140 Hz and $^1J_{CC}$ = 35 Hz (Fig. 3-4). In addition, the $^3J(H,H)$ coupling is strongly conformation dependent whereas the $^1J(C,C)$ and $^1J(C,H)$ couplings are not. Furthermore, every relay step involving a carbon atom can be directly transformed to an evolution period, leading to multidimensional NMR-experiments that spread out overlapping proton resonances from large molecules.

Heteronuclear sequences are constructed almost exclusively from 90° and 180° pulses and delays. The essential building blocks are:
1) Simultaneous application of 90° pulses to both nuclei. Assume that we have transverse magnetization of a spin at a given time during the course of a pulse sequence. After a suitable delay Δ, there will be antiphase magnetization of spin I present, of the form $2I_yS_z$. Two 90° pulses perform coherence transfer to $-2I_zS_y$ which represents antiphase magnetization of spin S. This transfer was already described for COSY (5,6) and applies to the heteronuclear analog INEPT (7-9) (Fig. 3-5a,b). Thus transverse magnetization of spin I ($-I_y$ at the beginning of Ω) can be transferred to transverse antiphase coherence of spin S: $-2I_zS_y$ (a) or vice versa (b). This method of transfer forms the basis for so called transfer experiments via scalar coupling in the majority of pulse sequences. Chemical shift of spin I evolves before the transfer and chemical shift of spin S evolves after the transfer. Longitudinal two spin order (represented by the product operator $2I_zS_z$) is obtained between the two 90° pulses when they are applied consecutively rather than

simultaneously. The longitudinal two-spin order $2I_zS_z$ is not detectable, but it is oriented along z and therefore invariant under rotations about the z-axis. Therefore B_o gradients (vide infra) can be inserted in coherence transfer segments between the 90°(I) pulse and the 90°(S) pulse without affecting the coherence transfer from I-coherence to S-coherence.

2) Selective application of a 90°(S) pulse: this turns antiphase magnetization of spin I: $2I_yS_z$ into two spin coherence which is transverse on both spins: $2I_yS_y$ (Fig. 3-5c and d). Two spin coherence evolves according to the chemical shift of both spins I and S. The coupling J(I,S) between the two spins is, however, switched off. Subsequent insertion of 180° pulses can refocus chemical shift evolution of either I or S.

3) Application of 180° pulses in the middle of a delay to refocus chemical shift and/or heteronuclear couplings. Four different situations must be distinguished (Fig. 3-6a-d):
A 180° pulse applied to a spin I in the middle of a delay 2Δ refocusses its chemical shift at the end of the delay 2Δ. The heteronuclear coupling between I and S is refocussed after 2Δ if either a 180°(I) or a 180°(S) pulse is applied in the middle of the delay.
Another way to think about the action of 180° pulses is the following (10): Each individual 180° pulse inverts the evolution of chemical shift of the nucleus to which it is applied (jumping from the Ω line to the $-\Omega$ line or the reverse, figure 3.6). Each 180° pulse also inverts evolution of all heteronuclear couplings of the spin to which the pulse is applied (jumping from the J_{HC} line to the $-J_{HC}$ line or the reverse). The evolution of heteronuclear coupling and chemical shifts in arbitrary sequences of 180° pulses can thus be visualized as shown in Fig. 3-6.
As an example, the more complicated sequence in Fig. 3-7a behaves as follows. The duration of the proton pulses is assumed to be negligible:

- Evolution of heteronuclear J(I,S) coupling (Fig. 3-7b) during $\Delta_1 - \Delta_2 + \Delta_3 - \Delta_4$
- Evolution of the chemical shift of I (Fig. 3-7c) during $\Delta_1 - \Delta_2 - \tau(180°_S) - \Delta_3 + \Delta D_4$
- Evolution of the chemical shift of S (Fig. 3-7d) during $\Delta_1 + \Delta_2 - \Delta_3 - \Delta_4$

With this graphical representation of the evolution of interactions, sequences that achieve a certain desired behaviour with respect to evolution of all three possible interactions can easily be designed. If, for example, the coherence at the beginning of Δ_1 contains only longitudinal proton-operators, proton chemical shift evolution need not be taken into account. The two 180°(I) pulses can then be concatenated to one 180°(I) pulse at $\Delta_1+2\Delta_2+\Delta_4$ provided $\Delta_3>\Delta_2$ (Fig. 3-7e). Net evolution of J_{CH} and Ω_C is the same as for the original sequence. If on the other hand the coherence at the beginning of Δ_1 contains only longitudinal carbon operators, carbon chemical shift evolution need not be taken into account. The two 180°(I) pulses can then be concatenated at the position $\Delta_1+\Delta_4$ and the 180°(S) pulse is located at $\Delta_1 - \Delta_2$ (Fig. 3-7f).

As a rule of thumb, 180° pulses can be concatenated if the number of 180° pulses is larger than the number of interactions one has to consider..

We now discuss some basic sequences.

3.6.1. HMQC (Heteronuclear Multiple Quantum Correlation), HMBC (Heteronuclear Multiple Bond Correlation)

HMQC (11-14) is one of the oldest sequences employed (Fig. 3-8a). Disregarding for the moment the decoupling with the GARP sequence during t_2 it is also a very simple sequence, consisting of only four pulses. Transverse proton magnetization is excited by the first pulse and is present during the whole sequence. Without the heteronuclear pulses a 2D J spectrum (15) would result. The 90°(S) pulse turns the carbon "operator" also into the transverse plane. Heteronuclear double- and zero-quantum coherences ($2I_{x,y}S_y$) evolve during t_1. Proton chemical shift is refocussed by the 180° proton pulse during t_1. Therefore it evolves during t_2-Δ+Δ'. Homonuclear J(H,H) couplings evolve during the whole sequence t_1+t_2+Δ+Δ', carbon chemical shift and homonuclear carbon-carbon couplings evolve during t_1 and the heteronuclear coupling evolves during Δ and again during Δ'+t_2. The transfer amplitude of this pulse sequence for a H,C cross peak in a H,C,H_j,C_k spin system (where j indicates the number of passive proton spins and k the number of passive carbon spins on the carbon of interest) is therefore:

$$\sin(\pi J_{HC}\Delta)\quad \sin(\pi J_{HC}(\Delta'+t_2))\quad \Pi_j\cos(\pi J_{H,Hj}(t_1+t_2+\Delta+\Delta')\quad \Pi_k\cos(\pi J_{C,Ck}t_1)\quad \exp(i\Omega_H(t_2-\Delta+\Delta')\quad \cos(\Omega_C t_1)$$

The heteronuclear zero- and double quantum coherence evolving during t_1 is selected by the phase cycle ϕ= 0,180, ψ= 0,0,180,180; receiver phase = 0, 180, 180, 0

Note that suppression of protons not bound to ^{13}C is achieved only after two experiments by subtraction of unwanted coherences. Without decoupling in t_2, the signal that is cancelled by the phase cycle is at least 200 times stronger than the desired signal given the 1% natural abundance of ^{13}C and the doublet character of the carbon-bound proton. Therefore the dynamic range of the digitizer must be high for proton detected heteronuclear spectroscopy of natural abundance samples. If the desired signal is a factor of 200 smaller than the undesired signal, almost half the number of bits of a 16 bit digitizer are used for signal that is cancelled away by the phase cycling procedure (8 bits correspond to a factor of 256). To obtain good subtraction the phases of the proton pulses are <u>not</u> changed during the sequence. Change of proton phases generally leads to poorer cancellation of undesired signals because a new equilibrium state is established between scans.

As we have done in this example we will throughout this chapter represent the state of the spin system by product operators at crucial points. Phase cycles should be applied in such a way as to

select the specified transformations. We will denote the phases to be incremented according to the TPPI or States-Haberkorn-Ruben procedure by ϕ.

In the HMQC experiment, heteronuclear decoupling can be applied during t_2 to gain sensitivity due to the reduction of the multiplet structure from a doublet to a singlet. The transfer amplitude is simplified:

$$\sin(\pi J_{HC}\Delta)\,\sin(\pi J_{HC}\Delta')\,\Pi_j\cos(\pi J_{H,Hj}(t_1+t_2+\Delta+\Delta'))\,\exp(i\Omega_H(t_2-\Delta+\Delta'))\,\Pi_k\cos(\pi J_{C,Ck}t_1)\,\cos(\Omega_C t_1)$$

Fourier transformation of the decoupled experiment yields a multiplet as shown schematically in Fig. 3-9a (echo part). The antiecho multiplet structure is obtained by reflection at the line $\omega_1 = \Omega_C$. In natural abundance samples, the number of multiplet lines is minimal, namely, just the number of lines in the proton multiplet, irrespective of the size of the heteronuclear coupling. Pure phases can only approximately be achieved, because the echo and the antiecho part do not exactly match after folding at ω_1=0 (Fig. 3-9a). The deviation from amplitude modulation in t_1 is small if the resolution is of the order of, or less than, the width of the proton multiplets. Then one can Fourier transform an HMQC in the standard way. If the resolution in ω_1 approaches the width of the proton multiplets, this recipe is no longer applicable.

The HMQC sequence can be used for transfer via long range heteronuclear couplings. In this so called HMBC experiment (16) the second refocussing period is normally omitted and no decoupling is applied. This approach turns out to have a higher signal to noise than the refocused and ω_2 decoupled HMBC as has been investigated in ref. 17. The HMBC sequence is shown in Fig. 3-8b. The transfer amplitude is identical to the transfer amplitude of the fully coupled HMQC-experiment with $\Delta' = 0$. (The evolution of homonuclear couplings of the heterospin is not considered further here because in fully labeled molecules the transfer via ^1J couplings is much faster than via heteronuclear long range couplings, making other experimental approaches more attractive.):

$$\sin(\pi J_{HC}\Delta)\,\sin(\pi J_{HC}t_2)\,\Pi_j\cos(\pi J_{H,Hj}(t_1+t_2+\Delta))\,\exp(i\Omega_H(t_2-\Delta))\,\cos(\Omega_C t_1).$$

This gives rise to a schematic multiplet in the echo part as shown in Fig. 3-9b. The difference between the carbon decoupled HMQC and the HMBC multiplet is the additional convolution of the 2D multiplet by the heteronuclear antiphase splitting J_{HC} in ω_2, due to the modulation of the two-dimensional signal with $\sin(\pi J_{HC}t_2)$. Like in the HMQC experiment, the signal is phase modulated in t_1. In addition, in the non-refocussed HMBC there is a large phase gradient in ω_2 due to the evolution of chemical shift during Δ. However, if t_1^{max} is short such that the resolution achieved in ω_1 is lower than the multiplet width the signal is approximately amplitude modulated in t_1. Therefore the spectrum is usually recorded in the standard way, e.g. with TPPI, and Fourier transformed in such a way as to obtain pure phases. The ω_1 dimension is then phased to pure absorption. Since the phasing in ω_2 is impossible due to the evolution of homonuclear coupling

(during Δ in the non-decoupled and during 2Δ in the decoupled variant) and chemical shift in Δ (in the non-decoupled variant), the absolute value of the signal in ω_2 is taken. This is obtained by combining the R_1R_2 and the R_1I_2 parts according to: $[(R_1R_2)^2+(R_1I_2)^2]^{1/2}$ (18). The resulting spectrum has pure absorption phase in ω_1 (X-nucleus) but shows the absolute value of the signal in ω_2 (^{1}H). The abbreviations R_1R_2 and R_1I_2 refer to real (R) and imaginary (I) parts of the spectrum in ω_1 (index 1) and ω_2 (index 2), respectively.

An experimental spectrum of cyclo-(D-Pro^6-Phe^{11}-Thr^{10}-Ala^9-Trp^8-Phe^7-) is shown in Fig. 3-10. The HMBC experiment can be used to connnect proton spin systems that are interrupted by non-protonated atoms. In peptides for example, the carbonyl groups constitute such an interruption of the proton spin system. The detection of cross peaks between the NH_{i+1},C' and $H_{\alpha i}$,C' permits the sequential assignment of a sequence of amino acids. This type of sequential assignment method does not produce non-sequential cross peaks, in contrast to NOE based sequential assignment. However, the size of the ^{2}J(H,C') coupling constants depends on the conformation (ϕ and ψ angles) (19).

The HMBC spectrum shown in Fig. 3-10 was aquired with a selective pulse (Gaussian 90° pulse (20) see also chapter 2 in this volume) in the carbonyl region to avoid folding problems in ω_1 and to achieve high resolution in the indirectly sampled frequency domain. A 270° Gaussian pulse (21) or a G4 Gaussian pulse cascade (22) would be more up to date. In Fig. 3-10 only the echo part of the spectrum is shown. The sequential assignment of the cyclic hexapeptide is indicated in the figure (23).

Due to the $\exp(i\Omega_H(t_2-\Delta))$ factor in the transfer amplitude of the HMBC experiment a large first order phase correction would be required in ω_2. Magnitude calculation of the spectrum in ω_2 is therefore usually performed as described above. However, when a quantitative evaluation of heteronuclear coupling constants is required, the distorted phases are retained (vide infra).

The abundance of connectivity information available in HMBC spectra is demonstrated (Fig. 3-11) with another variation of the HMBC experiment applied to a protected dissacharide, Ethyl-6-*O*-(2,3,4-tri-*O*-benzyl-a-L-fucopyranosyl)-(1,6)-3-*O*-acetyl-4-*O*-(p-methoxybenzyl)-2-desoxy-2-phthalimido-1-thio-β-D-glucopyranoside. Non-selective carbon pulses were used. Folding (see **Folding**) was applied to obtain sufficient resolution. The spectrum shows non-protonated carbon resonances (e.g. the carbonyl carbon of the acetyl group) as well as resonances of protonated carbons that are detected also in the HSQC-spectrum (Fig. 3-23). Due to the intensity modulation of the cross peaks in HMBC spectra with $\sin\pi J_{HC}\Delta$ some connectivities via $^1J_{CH}$ couplings are missing if $^1J_{HC}\Delta$ is close to a multiple of 1. For example the direct connectivity of the $\underline{CH}_2$ of S-CH_2-CH_3 (ω_1 = 66.3 ppm, ω_2 = 2.4 ppm) is missing in the spectrum.

The HMBC spectrum shows the sugar linkage via the glucose-C(6) (ω_1 = 65.8 ppm), fucose-H(1) (ω_2 = 4.9 ppm) cross peak. The assignment of the benzyl groups can be derived from the Φ-$\underline{C}H_2$-O-C$\underline{H}$ as well as from the Φ-C$\underline{H}_2$-O-$\underline{C}$H cross peaks. The assignment of the benzyl protons and carbons can be derived from the $\underline{C}_o$,C$\underline{H}_2$ as well as from the $\underline{C}_i$,C$\underline{H}_2$ cross peak (C_i, C_o, C_m and C_p for ipso, ortho, meta and para position in the aromatic ring). These cross peaks are indicated in the

spectrum for the MOBO group. The connectivities within the aromatic ring are derived from the C_m and C_p resonances in ω_1, observing that cross peaks due to $^3J(C,H)$ couplings are much stronger than those due to $^2J(C,H)$ couplings in aromatic systems. Note the direct $^1J(C,H)$ as well as remote $^3J(C,H)$ connectivities between ortho protons and ortho carbons, which lead to an apparent triplet structure of these cross peaks (e.g. at ω_1 = 61 ppm, ω_2 = 7.1 ppm for the direct C_o,H_o (doublet) and the remote C_o,$H_{o'}$ peak (singlet)).

In HMQC and in HMBC, the resolution in ω_1 is limited by the proton multiplet width because the cross peaks are modulated with the homonuclear proton couplings in t_1. In addition, for macromolecules, the heteronuclear zero- and double-quantum coherence containing transverse proton magnetization relaxes quickly due to the rather short T_2 of proton (24,25). Both these problems are solved in the next basic experiment.

3.6.2 HSQC (Heteronuclear Single Quantum Correlation)

The HSQC (26) sequence can be derived from the HMQC sequence by rotating the transverse proton magnetization to the longitudinal plane at the beginning of t_1 and then rotating it back to the transverse plane again after t_1. To refocus chemical shift modulation during Δ, a 180°(I,S) pulse is introduced in the middle of the each of the two delays Δ. Because the proton magnetization is longitudinal during t_1 no homonuclear J(H,H) couplings evolve during t_1. The evolution of heteronuclear couplings is refocussed by the 180(I) pulse in the middle of t_1. The pulse sequence is shown in Fig. 3-8c).

The transfer amplitude for the desired coherence transfer (proton magnetisation longitudinal during t_1) is:

$$\sin^2(\pi J_{HC}\Delta)\ \Pi_j\cos(\pi J_{H,Hj}\Delta)\ \exp(i\Omega_H t_2)\ \Pi_j\cos[\pi J_{H,Hj}(\Delta+t_2)]\ \ \Pi_k\cos(\pi J_{C,Ck}t_1)\ \cos(\Omega_C t_1)$$

This formula is only true for a very large difference between J(X,H) and J(H,H), which is the situation for transfer via $^1J(X,H)$ couplings. If the heteronuclear coupling used for the polarization transfer is about the same size as the homonuclear coupling, the transfer becomes inefficient due to the excitation of proton multiple quantum coherences after the second 90°(I) pulse. Therefore, in contrast to HMQC, HSQC is used only for transfer via $^1J(H,C)$ couplings.

The schematic multiplet structure of an HSQC correlation peak is shown in Fig. 3-9b) for a HCH_1H_2 spin system. The sensitivity of the experiment is comparable to HMQC for transfer via $^1J(H,X)$ couplings. The resolution in ω_1 is no longer limited by the homonuclear proton couplings. For biomolecules HSQC has a higher signal to noise ratio than HMQC because the fast decay due to proton transverse relaxation during t_1 is absent (24,25).

So far we have seen that chemical shift information about a heteronuclear spin can be obtained by evolution of two types of operators:

Experiment	Initial operator	Couplings	Relaxation rate
HMQC	I_xS_x	homonuclear couplings of I and S	$1/T_{2I}+1/T_{2S}$
HSQC	I_zS_x, S_x	homonuclear couplings of S	$1/2T_{1I}+1/T_{2S}$

In the HSQC experiment the heteronuclear chemical shift evolution is obtained from operators of the type: $2I_zS_x$ and S_x. The $2I_zS_x$ antiphase operator relaxes faster than the in phase operator S_y since the former also decays due to proton longitudinal relaxation. This effect is especially strong in larger molecules. To circumvent this problem, one may refocus the heteronuclear antiphase operator prior to t_1. This leads to the next experiment, the Double INEPT sequence. Here in-phase heteronuclear single quantum coherence S_x evolves under decoupling of protons during t_1:

3.6.3 DOUBLE INEPT

The double INEPT sequence (24,25,28) introduces refocussing and defocussing periods for the heteronuclear coupling before and after t_1. Therefore pure in phase heteronuclear magnetization S_x, S_y encodes heteronuclear chemical shifts during t_1 (Fig. 3-8d). The sequence is applied exclusively for transfer via ^1J couplings for the same reasons cited for the HSQC experiment.
The transfer amplitude of this sequence is:

$$\sin^2(\pi J_{HC}\Delta)\quad \sin^2(\pi J_{HC}\Delta')\quad \cos^{2(n-1)}(\pi J_{C,H}\Delta')\quad \cos(\Omega_C t_1)\quad \exp(i\Omega_H t_2)\quad \Pi_j\cos(\pi J_{H,Hj}\Delta)\quad \Pi_j\cos(\pi J_{H,Hj}\Delta+t_2)$$

n is the number of protons bound to the heteronucleus. The optimal delays to refocus heteronuclear antiphase coherence I_zS_y before t_1 and to defocus heteronuclear in-phase coherence after t_1 depend on the multiplicity of the heteronucleus. Maximum transfer is obtained with 1/2J, 1/4J and 1/6J for IS, I_2S and I_3S moieties, respectively. Consequently the sequence has a signal to noise ratio identical to HMQC or HSQC only for IS moieties. For low natural abundance nuclei, however, the transfer efficiency can be improved by incorporating composite bilinear rotations (2).
Since the heteronuclear coherence relaxes during t_1 only with the heteronuclear transverse relaxation time T_{2S} Double INEPT is optimal for macromolecules, where proton self relaxation is fast. Double INEPT is therefore used with advantage for H,N correlations, where NH groups are of main interest. Figure 3.12 shows the comparison of HMQC (a), HSQC (b) and Double INEPT (c) cross sections through the $^{15}N,^1H$ cross peak of Gln^{74}-NH in ^{15}N labeled ribonuclease A.

3.7. Amplitude and Phase Modulation

We want to introduce some additional notions that are frequently used throughout this course: Consider a spin I_1 with its characteristic chemical shift Ω_1. Assuming that this spin has an

interaction with another spin I_2, with its characteristic chemical shift Ω_2, such that we can transfer magnetization of spin I_1 to I_2. Now let us consider a pulse sequence that first excites spin I_1 and then allows for evolution of chemical shift during t_1:

$$I_{1x} \quad -> \quad I_{1x}\cos(\Omega_1 t_1) + I_{1y}\sin(\Omega_1 t_1)$$

Now we apply the specific mixing scheme that transfers magnetization from I_1 to I_2. There are two possibilities. Either magnetization is transferred from both magnetization components of I_1 to I_2 or only from one. We first consider transfer from both components:

$$I_{1x} \quad -> \quad I_{2x} \quad \text{and}$$
$$I_{1y} \quad -> \quad I_{2y}$$

In this case, the following two dimensional FID is obtained after evolution of chemical shift during t_2:

$$\begin{array}{lcccl} & t_1 & & \text{magnetization transfer} & t_2 \\ I_{1x} & -> & I_{1x}\cos(\Omega_1 t_1) + I_{1y}\sin(\Omega_1 t_1) & -> & I_{2x}\cos(\Omega_1 t_1) + I_{2y}\sin(\Omega_1 t_1) \; -> \\ & & I_{2x}[\cos(\Omega_1 t_1)\cos(\Omega_2 t_2) - \sin(\Omega_1 t_1)\sin(\Omega_2 t_2)] + I_{2y}[\sin(\Omega_1 t_1)\cos(\Omega_2 t_2) + \cos(\Omega_1 t_1)\sin(\Omega_2 t_2)] & & \end{array}$$

The 2D FID that the phase sensitive receiver records by complex addition of x magnetization plus i times y-magnetization is therefore given by: $\exp(i\Omega_1 t_1)\exp(i\Omega_2 t_2)$. Such a 2D FID is said to be phase modulated in t_1, because t_1 enters the FID in t_2 solely by a phase factor. It yields after complex Fourier transformation so called mixed phases (a mixture of absorptive and dispersive signals) in the 2D spectrum. The phase modulated FID cannot be Fourier transformed such that pure phases result in ω_1 and ω_2 and at the same time the sign of the chemical shift is recognized. This is undesirable because purely absorptive peaks have minimum linewidth. It is obvious that the phase modulated signal allows the differentiation of the sign of frequencies in t_1. This is always the case if the phase modulation is due to the chemical shift. The above mentioned FID $\exp(i\Omega_1 t_1)\exp(i\Omega_2 t_2)$ gives rise to the antiecho part of a spectrum (see Chapter 2 in this volume). Antiecho pathways are characterized by the fact that the sign of the chemical shift is the same for t_1 ($+\Omega_1$) and t_2 ($+\Omega_1$). The echo part of the signal is characterized by the fact that the sign of the chemical shift is opposite in t_1 ($-\Omega_1$) and in t_2 ($+\Omega_2$): $\exp(-i\Omega_1 t_1)\exp(i\Omega_1 t_2)$. The echo part of the spectrum could be obtained in the above sequence by introducing a 180^o_x pulse before the transfer of magnetization from I_1 to I_2. The echo part of the signal derives its name from the fact that B_0 inhomogeneities behave like chemical shift and are refocussed after $\gamma(I_1)t_1 = \gamma(I_2)t_2$, where $\gamma(I_n)$ is the gyromagnetic ratio of I_n. Refocussing of B_0 inhomogeneities gives rise to the formation of an echo. There is a product operator basis set that allows to describe echo and antiecho signals in a

simple way. Using the equations for the evolution of chemical shift for I_x and I_y it is easily found that the two new operators: $I_+ = I_x + iI_y$ and $I_- = I_x - iI_y$ evolve chemical shift in the following way:

$I_+ \rightarrow I_+ \exp(-i\Omega t)$ and $I_- \rightarrow I_- \exp(i\Omega t)$.

The antiecho transfer therefore comes about from $I_{1-} \rightarrow I_{2-}$, whereas the echo transfer originates from $I_{1+} \rightarrow I_{2-}$.

If magnetization is transferred only from either of the two components: I_{1x} to I_{2x} or I_{1y} to I_{2y}, then the signal that is obtained in the hypothetical experiment described above is given by:

$$\begin{array}{lccccc} & t_1 & & \text{magnetization transfer} & & t_2 \\ I_{1x} & \rightarrow & I_{1x}\cos(\Omega_1 t_1) + I_{1y}\sin(\Omega_1 t_1) & \rightarrow & I_{2x}\cos(\Omega_1 t_1) & \rightarrow \\ & I_{2x}\cos(\Omega_1 t_1)\cos(\Omega_2 t_2) + I_{2y}\cos(\Omega_1 t_1)\sin(\Omega_2 t_2) & & & & \end{array}$$

The signal the phase sensitive receiver records is now given by $\cos(\Omega_1 t_1)\exp(i\Omega_2 t_2)$. Now the amplitude of the FID in t_2 is modulated by $\cos(\Omega_1 t_1)$. The signal is amplitude modulated in t_1. Sign discrimination is no longer possible since cosine is an even function. Therefore a second experiment is recorded that modulates the t_2 FID with $\sin(\Omega_1 t_1)$. This can easily be done by starting with I_{1y} magnetization instead of I_{1x} at the beginning of t_1, hence by a phase shift by 90° of the pulses that preceed the evolution time. The Fourier transformation of these two amplitude modulated signals yields pure phases in the spectrum.
The reader should note that the two amplitude modulated parts of the spectrum:

$\cos(\Omega_1 t_1)\exp(i\Omega_2 t_2)$ and $\sin(\Omega_1 t_1)\exp(i\Omega_2 t_2)$

can be obtained from the echo and from the antiecho by linear combination and vice versa:

$\cos(\Omega_1 t_1)\exp(i\Omega_2 t_2) = (1/2)[\exp(i\Omega_1 t_1)\exp(i\Omega_2 t_2)+\exp(-i\Omega_1 t_1)\exp(i\Omega_2 t_2)]$ and
$\sin(\Omega_1 t_1)\exp(i\Omega_2 t_2) = (1/2i)[\exp(i\Omega_1 t_1)\exp(i\Omega_2 t_2)-\exp(-i\Omega_1 t_1)\exp(i\Omega_2 t_2)]$

We will in the following discuss sequences that record FIDs that can be phased to pure absorption after Fourier transformation by recording separately the echo and the antiecho part.

Figure Legends

Fig. 3-1: Representation of the evolution of chemical shift in a vector diagram. a) x-magnetization evolves under the influence of chemical shift by rotation with frequency Ω in the rotating frame. After a time t, the phase of the magnetization is given by Ωt. The magnetization is composed of the two orthogonal components M_x and M_y. b) Rotation of a magnetization vector under the action of a pulse. The pulse induces a rotation of the magnetization about its direction with the frequency γB_1. The flip angle β is given by the duration of the pulse t and the strength of the field: $\beta = \gamma B_1 t$

Fig. 3-2: Vector diagram representation of the evolution of coupling of spin I_1 to spin I_2 in the rotating frame. The chemical shift is assumed to be zero. The two lines in the spectrum, one for the spin isomer with I_2 in the α state and one for I_2 in the β state, correspond to two vectors that rotate in the rotating frame with identical frequency πJ but in opposite directions. At time zero the two vector components are parallel resulting in full observable magnetization. At time t they have acquired a phase shift of πJt and $-\pi Jt$, respectively. The two parallel vector components $I_{1x}I_{2\alpha}$ and $I_{1x}I_{2\beta}$ are combined to yield the magnetization I_{1x}. The two vectors that lie antiparallel $I_{1y}I_{2\alpha}$ and $I_{1y}I_{2\beta}$ are combined to $2I_{1y}I_{2z}$. This product operator is modulated with $\sin(\pi Jt)$.

Fig. 3-3: Evolution of coupling during a time t starting from antiphase coherence of spin I_1. This state of the spin system contains no observable magnetization at time t=0. Evolution of coupling according to Fig. 3-2 leads to a refocussing of the two antiphase components and detectable magnetization again appears. Since the state of the spin system in the vector diagram at time t=0 is indistinguishable from two magnetization vectors originating from two spins with a difference in chemical shift of $2\pi J$ that lie in opposite directions a spectrum results in which the two lines have opposite sign (one line in emission, the other in absorption).

Fig. 3-4: HXXH spin system: a) Double relayed transfer from H to H via the HX, XX and HX coupling. Since each transfer takes about 1/J the relay transfer: H->C->C->H takes takes $[2(140\ \text{Hz})^{-1} + (35\ \text{Hz})^{-1}]^{-1} = 42$ ms. b) Transfer via the homonuclear coupling of 10 Hz takes $(10\text{Hz})^{-1} = 100$ ms.

Fig. 3-5: Building blocks in heteronuclear spectroscopy:

a) Coherence transfer from antiphase I ($2I_yS_z$) to antiphase S coherence ($2I_zS_y$) is effected by two 90° pulses on I and S. Sequential application of the pulses creates intermediate longitudinal two-spin order $2I_zS_z$. b) Reverse coherence transfer from antiphase S coherence ($2I_zS_y$) to antiphase I coherence ($2I_yS_z$) which is refocussed to in-phase I coherence (I_y) at the end of Δ. c) Creation of heteronuclear multi quantum coherence ($2I_yS_y$) by application of an S pulse to antiphase I magnetization. d) Reverse of c)

Fig. 3-6: 180° pulses in the middle of a delay 2Δ. The evolution of coupling, chemical shift of H and chemical shift of C is graphically represented in the manner often used for coherence

orders. a) with no 180° pulse all three interactions evolve. b) application of a 180°(I) pulse refocusses chemical shift of I and heteronuclear J(I,S) coupling. c) application of a 180°(S) pulse refocusses heteronuclear J(I,S) and chemical shift of S, d) application of 180°(I,S) pulses refocusses chemical shift of I and S but not J(I,S) coupling.

Fig. 3-7: a) Pulse sequence containing two 180°(I) pulses and a 180°(S) pulse. The evolution of interactions is given below: b) for the heteronuclear I,S coupling, c) for the I chemical shift and d) for the S chemical shift. e) If all I spins are longitudinal the I chemical shift need not be taken into account. Then the two I pulses can be concatenated. f) If the chemical shift of S need not be taken into account, the two proton pulses are concatenated in a different way.

Fig. 3-8: a) Pulse sequence of the HMQC experiment with refocussing of the proton chemical shift in t_1 and decoupling in t_2. In absense of the carbon pulses a 2D J resolved experiment results. The phases ϕ and ψ are cycled according to 0,180 and 0,0,180,180, respectively. The receiver phase is cycled accordingly. TPPI, RSH or States-TPPI is performed on ϕ. b) Pulse sequence of the HMBC experiment. Only the refocussing period is missing compared to the HMQC. Consequently, proton decoupling must be avoided and the active heteronuclear coupling is in antiphase. c) Pulse sequence of the HSQC experiment. Defocussing of the heteronuclear J(I,S) coupling occurs during Δ. The S-spin antiphase coherence evolves during t_1. The 180° pulse refocusses heteronuclear coupling in t_1. The efficiency of the sequence is independent of the multiplicity. d) Double INEPT sequence with refocussing during Δ'. In phase heteronuclear magnetization at the beginning of t_1 evolves under proton decoupling. Since spin polarization is lost during the I_n->S and S->I_n transfer the sequence leads to lower signal to noise than HSQC/HMQC for multiplicities n>1.

Fig. 3-9: a) Schematic multiplet structure in a HMQC experiment. Modulation by the homonuclear coupling in t_1 and t_2 leads to the tilted multiplet structure in the echo and antiecho spectra. The two spectra do not match upon folding at $\omega_1 = 0$, which leads to mixed phases in HMQC. b) HMBC multiplet pattern. In contrast to the HMQC pattern, the HMBC pattern is convoluted with an antiphase splitting in ω_2 due to the active heteronuclear coupling. c) Multiplet pattern in HSQC and Double INEPT: Modulation with the homonuclear coupling in ω_1 is removed. Because the echo and antiecho part superimpose exactly upon folding at $\omega_1 = 0$, spectra with pure phases can be obtained.

Fig. 3-10: HMBC spectrum with a 90° Gaussian carbon pulse of the cyclic hexapeptide cyclo-(D-Pro^6-Phe^{11}-Thr^{10}-Ala^9-Trp^8-Phe^7-). The connectivities between the neighboring amino acids are visible from the H^N_{i+1},C'_i cross peaks. Δ = 70 ms, 128 t_1 experiments, the Gaussian pulse had a duration of 3.5 ms. The inserts show the tilted multiplet structure of the $W^8(H_\alpha,C')$ and $F^{11}(H_\alpha,C')$ cross peaks.

Fig. 3-11: HMBC experiment on Ethyl-6-*O*-(2,3,4-tri-*O*-benzyl-α-L-fucopyranosyl)-(1,6)-3-*O*-acetyl-4-*O*-(p-methoxybenzyl)-2-desoxy-2-phthalimido-1-thio-β-D-glucopyranoside 1. Δ = 50 ms; non selective pulses were used. The spectral width in ω_1 was limited to 50 ppm. Peaks with F refer to the fucosyl resonances, MOBO refers to the (p-methoxybenzyl) protecting

group. The carbons assigned C_i, C_o, C_m, C_p refer to the aromatic carbons of this group. The protons are refered to as o, o', m, m'. 2, 3, and MOBO are the methylene carbons of the benzyl/methoxybenzyl protection groups at positions 2 and 3 of the fucose and 4 of glucose. Et-CH_3 and Et-CH_2 refer to the 1-thioethyl group of the glucose. The direct CH_2-peak of the ethyl group is missing.

Fig. 3-12: Comparison of a) HMQC, b) HSQC, and c) Double INEPT at Gln^{74} of ^{15}N labeled ribonuclease A by taking Ω_2 traces through the respective spectra. The intensity loss of the HMQC due to the H_α,H^N coupling is clearly visible. No relaxation effect is visible at this molecular weight as an intensity difference between HSQC and Double INEPT.

Fig. 3-13: Four spectra obtained from the pulse sequence of Fig. 3-22 for Ethyl-6-*O*-(2,3,4-tri-*O*-benzyl-α-L-fucopyranosyl)-(1,6)-3-*O*-acetyl-4-*O*-(p-methoxybenzyl)-2-desoxy-2-phthalimido-1-thio-β-D-glucopyranoside 1. ϕ = x,-x; ψ = y,y,-y,-y ensures that the signals that are folded an odd number of times have inverted sign. a) CH/CH_3 "even-folded": positive peaks in the difference of Fig. 3-22a and Fig. 3-22b. b) CH_2 "even folded": positive peaks in the sum of Fig. 3-22a and Fig. 3-22b. c) CH/CH_3 "odd-folded": negative peaks in the difference of Fig. 3-22a and Fig. 3-22b. d) CH_2 "odd folded": negative peaks in the sum of Fig. 3-22a and Fig. 3-22b.

Literature:

Introducing text books:

H. Friebolin: "One and twodimensional NMR Spectroscopy", VCH Verlagsgesellschaft, Weinheim, 1988

R.K. Harris, "Magnetic Resonance Spectroscopy", Longman, New York, 1983

^{1}H-NMR

H.Günther: NMR-Spectroscopy, Thieme Verlag, Stuttgart, 1983

^{13}C-NMR

H.O.Kalinowski: S.Berger, S.Braun, ^{13}C-NMR-Spectroscopy, Thieme Verlag, Stuttgart, 1984

Multinuclear NMR:

J. Mason, "Multinuclear NMR", Plenum Press, New York, 1987

NMR including modern Techniques:

A.E.Derome: "Modern NMR Techniques for Chemistry Research", Pergamon Press, Oxford, 1987

R.Benn, H.Günther: Angew.Chem.95 ,(1983) 381-411; Angew.Chem.Int. Ed. Engl.,22 (1983) 350-380

N. Chandrakumar, S.Subramanian: "Modern Techniques in High Resolution FT-NMR", Springer, New York 1987

J.K.M.Sanders, B.K.Hunter: "Modern NMR Spectroscopy", University Press, Oxford 1987

Attar-ur-Rahman, "One and Two Dimensional NMR Spectroscopy, Elsevier, Amsterdam, 1989

Applications:

K.Wüthrich: NMR of Proteins and Nucleic Acids, Wiley, New York 1986

Review Articles:

Benn, Günther: Angew. Chemie 95, 381-411 (1983)

Bax, Lerner: Science 232, 960-67 (1986)

N. Chandrakumar, S. Subramanian, "Modern Techniques in High Resolution FT NMR", Springer Verlag, New York, 1978

H.Kessler, M.Gehrke, C.Griesinger: Angew.Chem. 100, 507 (1988)

Theory of NMR Spectroscopy:

W.P. Aue, E. Bartholdi, R.R. Ernst, J. Chem. Phys. 64, 2229-2246 (1976)

A. Abragam, "The Principles of Nuclear Magentism, Clarendon Press, Oxford, 1978

R.R. Ernst, G. Bodenhausen, A. Wokaun, "Principles of Nuclear Magnetic Resonance in One and Two Dimensions, Oxford Science Publications, Clarendon Press, 1987

C.P. Slichter, "Principles of Magnetic Resonance" Springer, Berlin, 1978

D. Neuhaus, Williamson, "The Nuclear Overhauser Effect"

J.H. Noggle, R.E. Shirmer, "The Nuclear Overhauser Effect, Chemical Applications", Academic Press, New York, 1971

Literature

(1) O.W. Sørensen, G.W. Eich, M.H. Levitt, G. Bodenhausen, and R.R. Ernst, Prog. Nucl. Magn. Reson. Spectr. **16**, 163 (1983)

(2) O.W. Sørensen, Prog. Nucl. Magn. Reson. Spectr. **21**, 503 (1989)

(3) R.R. Ernst, G. Bodenhausen, A. Wokaun "Principles of Nuclear Magnetic Resonance in One and Two Dimensions", Clarendon, Oxford, 1987

(4) H. Kessler, M. Gehrke und C. Griesinger, Angew. Chem. **100**, 507 (1988)

(5) W.P. Aue, E. Bartholdi, and R.R. Ernst, J. Chem. Phys. **64**, 2229 (1976)

(6) A. Bax and R. Freeman, J. Magn. Reson. **44**, 542 (1981)

(7) G.A. Morris and R. Freeman, J. Am. Chem. Soc. **101**, 760 (1979)

(8) D.P. Burum and R.R. Ernst, J. Magn. Reson. **39**, 163 (1980)

(9) P.H. Bolton, J. Magn. Reson. **41**, 287 (1980)

(10) H. Kessler, C. Griesinger, and G. Zimmermann, Magn. Reson. Chem. **25**, 579 (1987)

(11) L. Müller, J. Am. Chem. Soc. **101**, 4481 (1979)

(12) M.R. Bendall, D.T. Pegg, and D.M. Doddrell, J. Magn. Reson. **52**, 81 (1983)

(13) A. Bax. R.H. Griffey, and B.L. Hawkins, J. Am. Chem. Soc. **105**, 7188 (1983)

(14) A. Bax. R.H. Griffey, and B.L. Hawkins, J. Magn. Reson. **55**, 301 (1983)

(15) W.P. Aue, J. Karhan, R.R. Ernst, J. Chem. Phys. **64**, 4226 (1976)

(16) A. Bax, and M.F. Summers, J. Am. Chem. Soc. **108**, 2093 (1986)

(17) W. Bermel, K. Wagner, and C. Griesinger, J. Magn. Reson. **83**, 223 (1989)

(18) A. Bax and D. Marion, J. Magn. Reson. **78**, 186 (1988)

(19) V.F. Bystrov, Prog. NMR Spectrosc. **10**, 44 (1976)

(20) C.J. Bauer, R. Freeman, T. Frenkiel, J. Keeler, and A.J. Shaka, J. Magn. Reson. **58**, 442 (1984)

(21) L. Emsley and G. Bodenhausen, J. Magn. Reson. **82**, 211 (1989)

(22) L. Emsley and G. Bodenhausen, Chem. Phys. Lett. **165**, 469 (1990)

(23) W. Bermel, C. Griesinger, H. Kessler, and K. Wagner, Magn. Reson. Chem. **25**, 325 (1987)

(24) A. Bax, M. Ikura, L.E. Kay, D.A. Torchia, and R. Tschudin, J. Magn. Reson. **86**, 304 (1990)

(25) T.J. Norwood, H. Boyd, H.E. Heritage, N. Soffe, and I.D. Campbell, J. Magn. Reson. **87**, 488 (1990)

(26) G. Bodenhausen and D.J. Ruben, Chem. Phys. Lett. **69**, 185 (1980)

(27) D. Brüschwiler and G. Wagner, J. Magn. Reson. **69**, 546 (1986)

(28) D.G. Davis, J. Magn. Reson. **90**, 589 (1990)

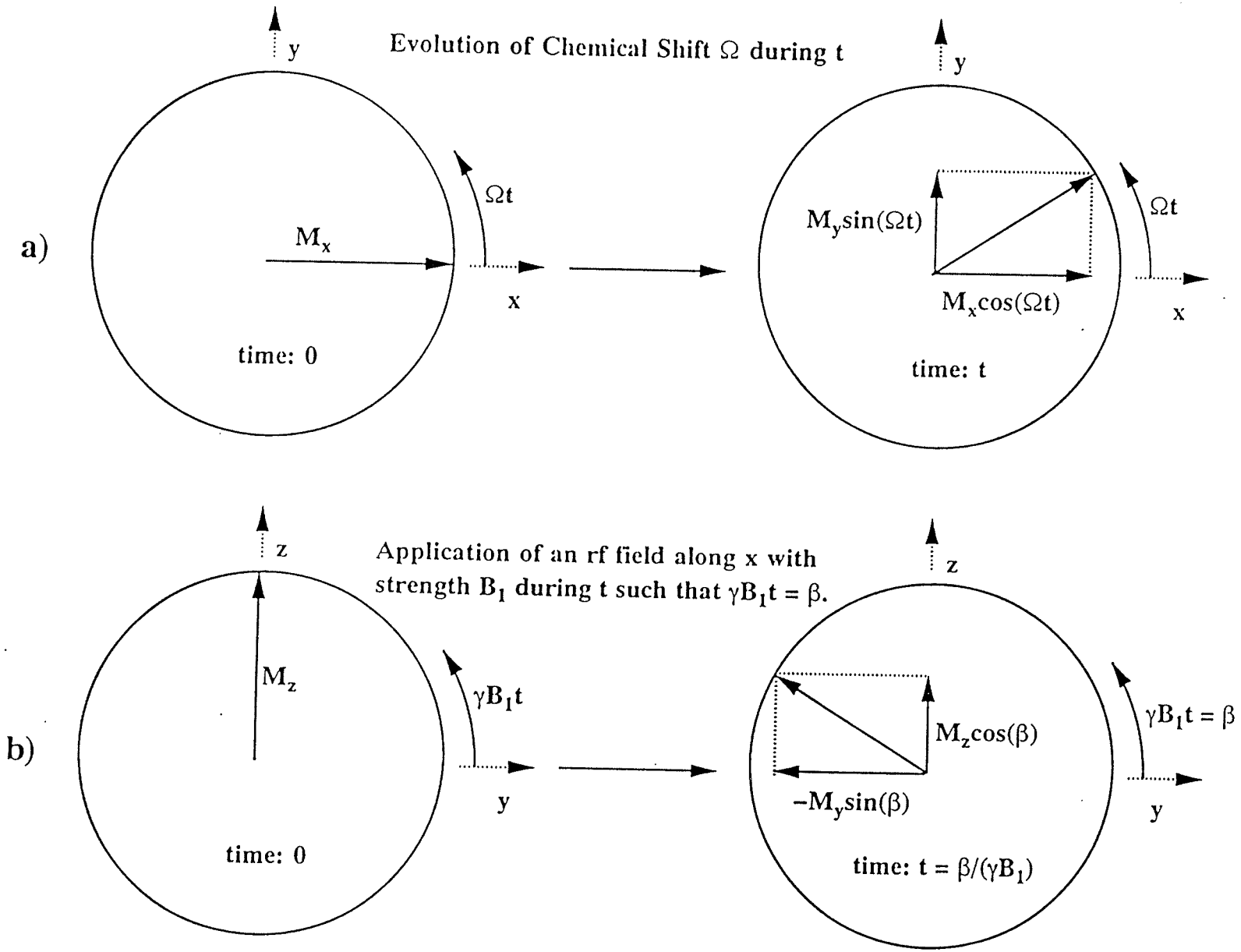
a)
y
Evolution of Chemical Shift Ω during t
M_x
Ωt
x
time: 0
y
$M_y\sin(\Omega t)$
$M_x\cos(\Omega t)$
Ωt
x
time: t
b)
z
Application of an rf field along x with
strength B_1 during t such that $\gamma B_1 t = \beta$.
M_z
$\gamma B_1 t$
y
time: 0
z
$M_z\cos(\beta)$
$-M_y\sin(\beta)$
$\gamma B_1 t = \beta$
y
time: $t = \beta/(\gamma B_1)$

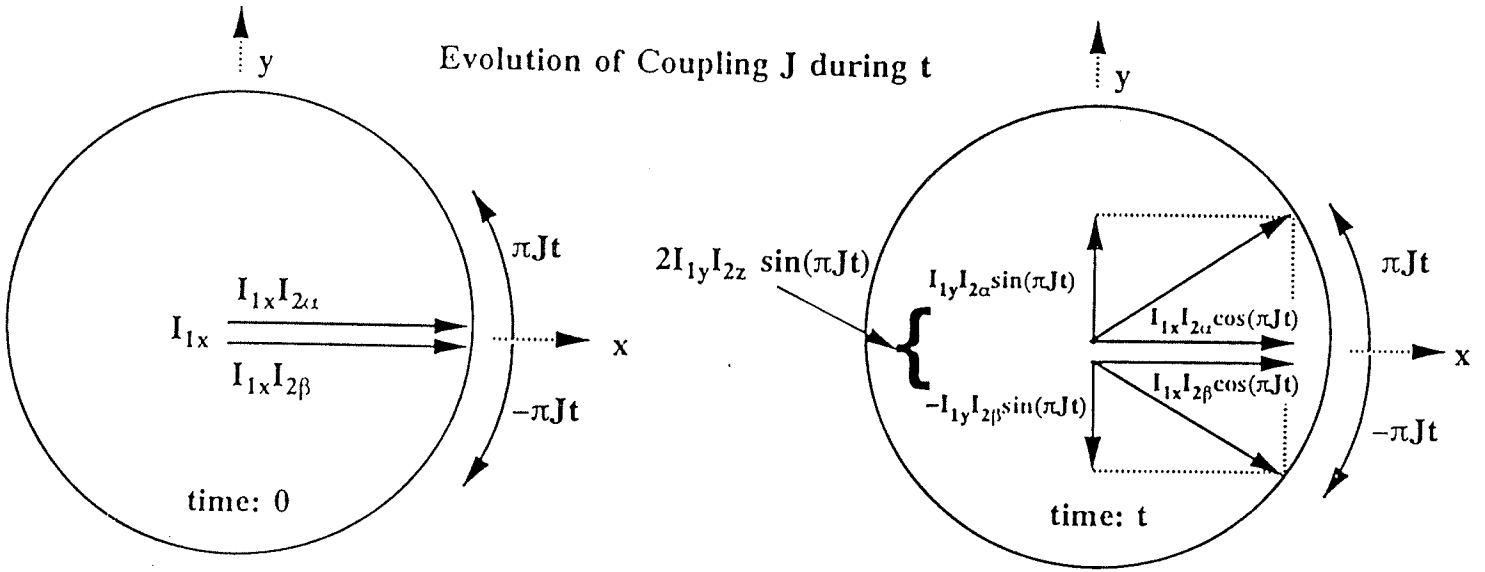

$I_{1x} \longrightarrow I_{1x}\cos(\pi Jt) + 2I_{1y}I_{1z}\sin(\pi Jt)$

In-Phase Operator

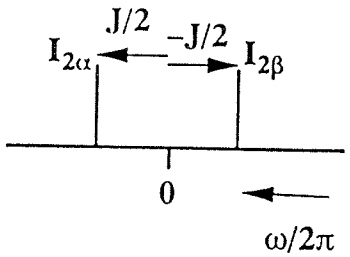

Spectrum of I_1

In-Phase Doublet

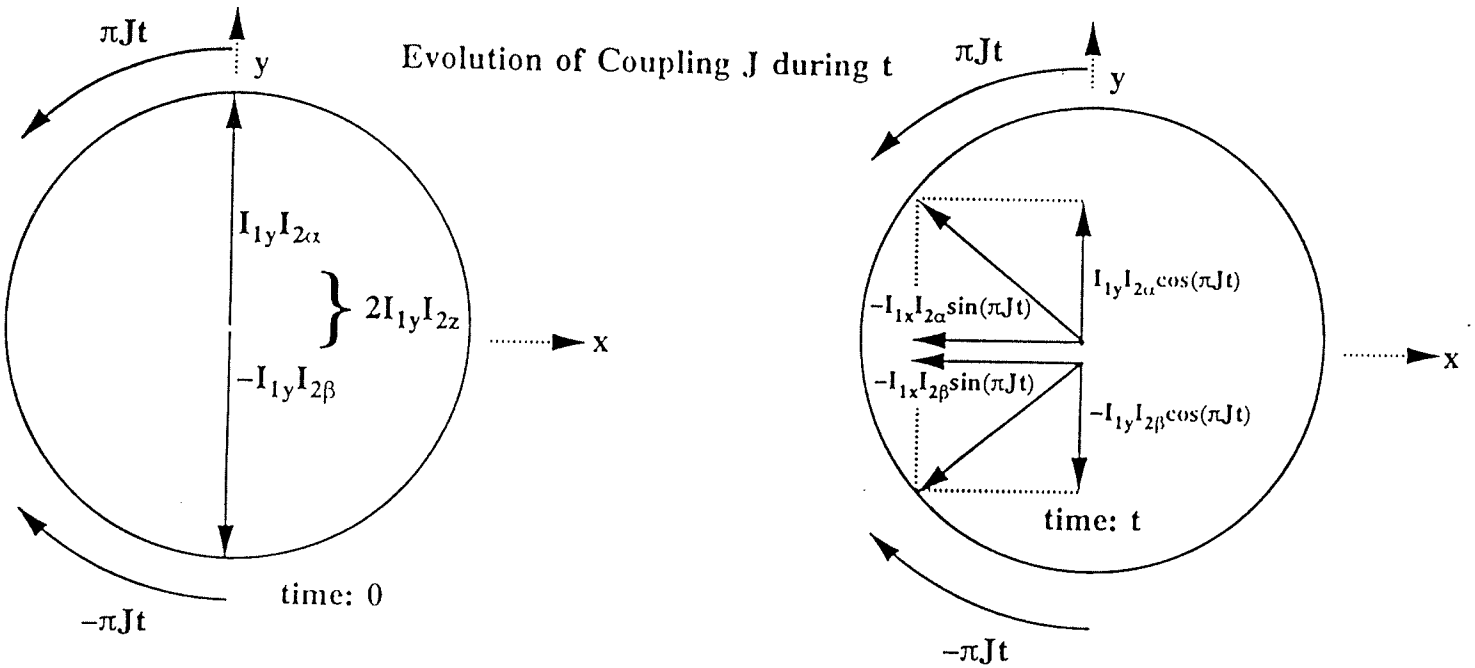

$2I_{1y}I_{2z} \longrightarrow 2I_{1y}I_{2z}\cos(\pi Jt) - I_{1x}\sin(\pi Jt)$

Antiphase Operator

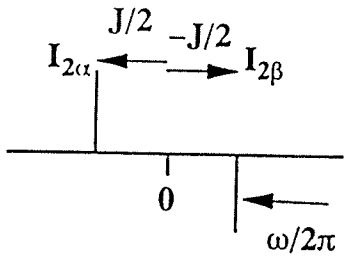

Spectrum of I_1

Antiphase Doublet

Double heteronuclear Relay Transfer

a)

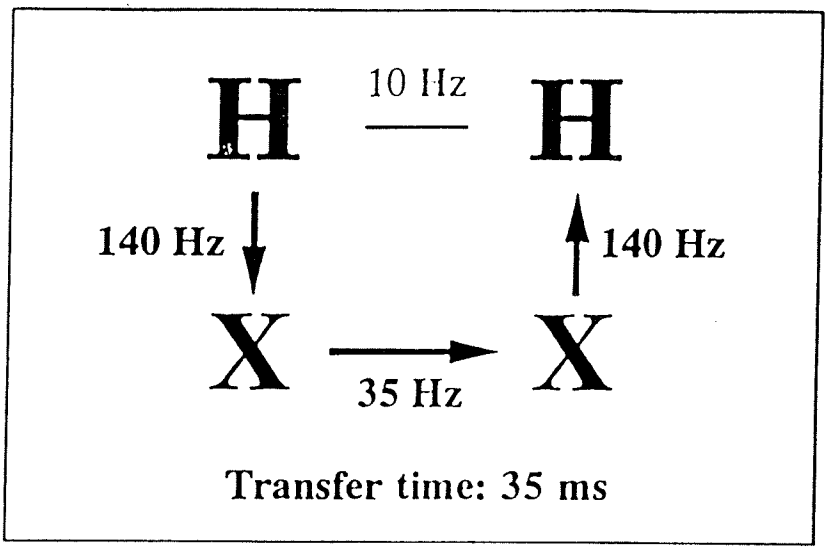

Direct homonuclear Transfer

b)

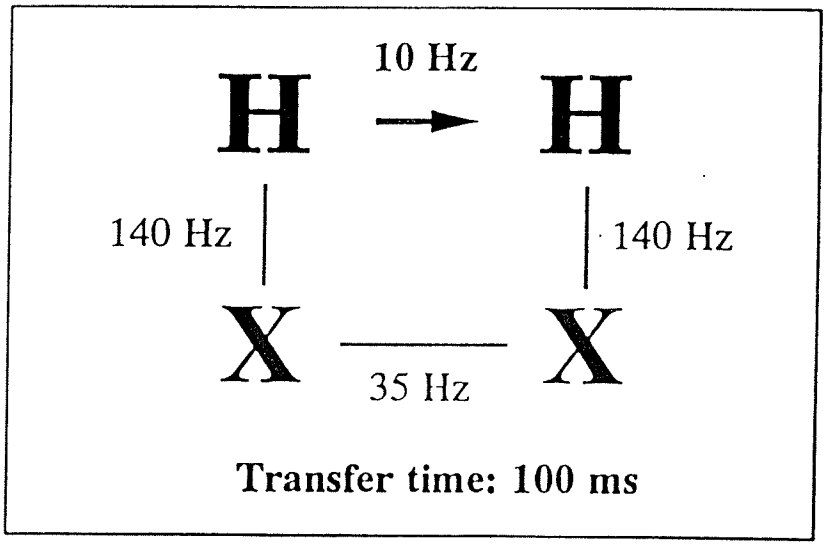

a) Polarisation Transfer

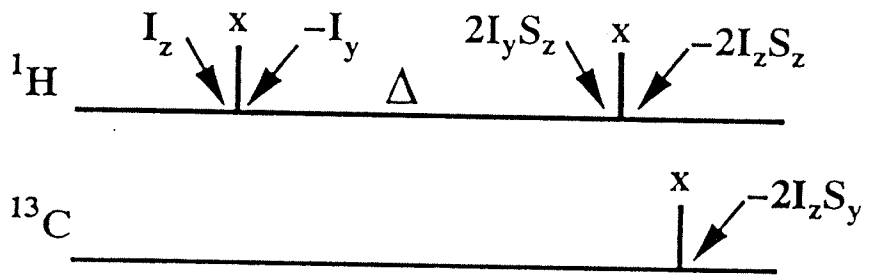

b) Reverse Polarisation Transfer

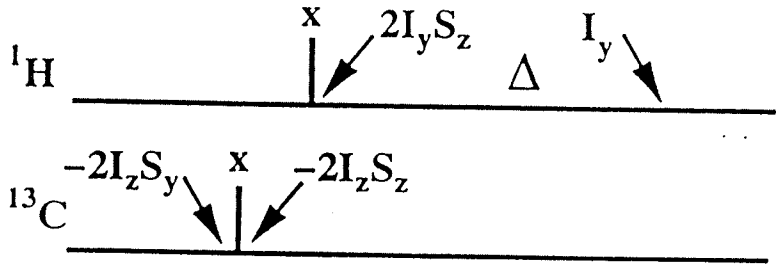

c) Creation of heteronuclear multiquantum coherence

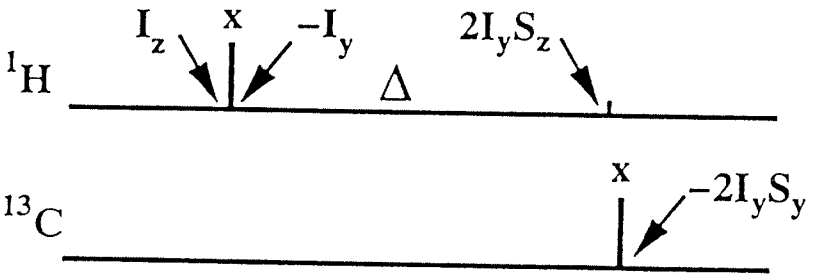

d) Creation of single quantum coherence out of heteronuclear multiquantum coherence

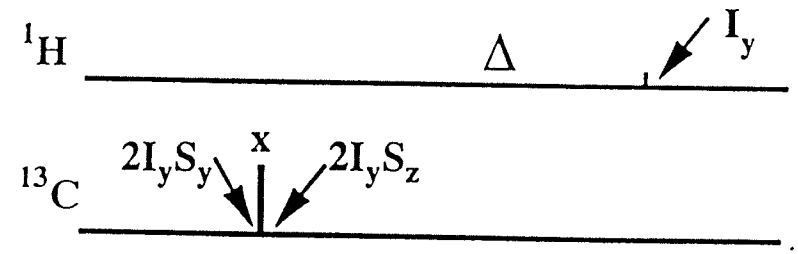

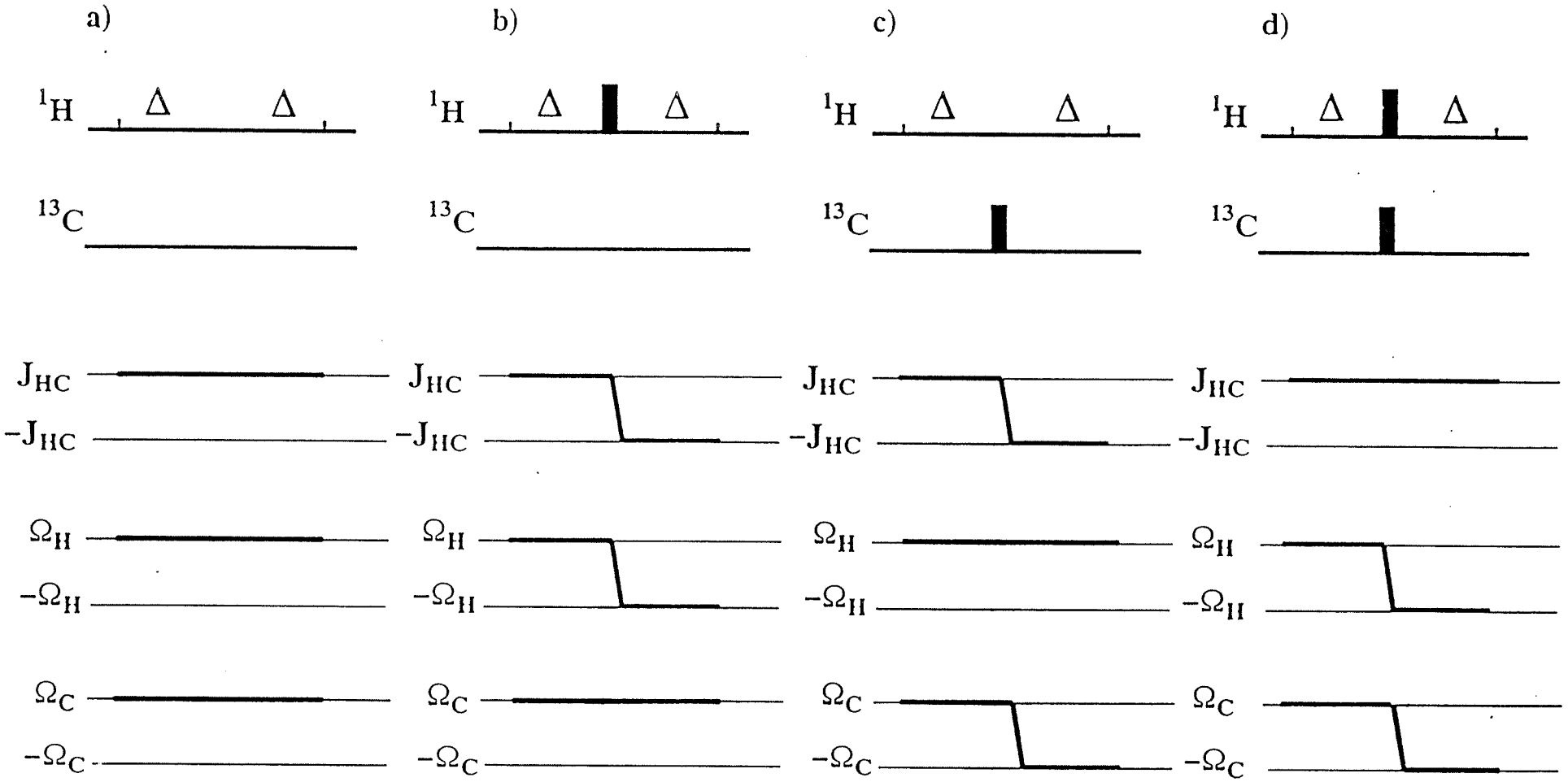
a)
b)
c)
d)
^{1}H
^{13}C
Δ
J_{HC}
$-J_{HC}$
Ω_H
$-\Omega_H$
Ω_C
$-\Omega_C$

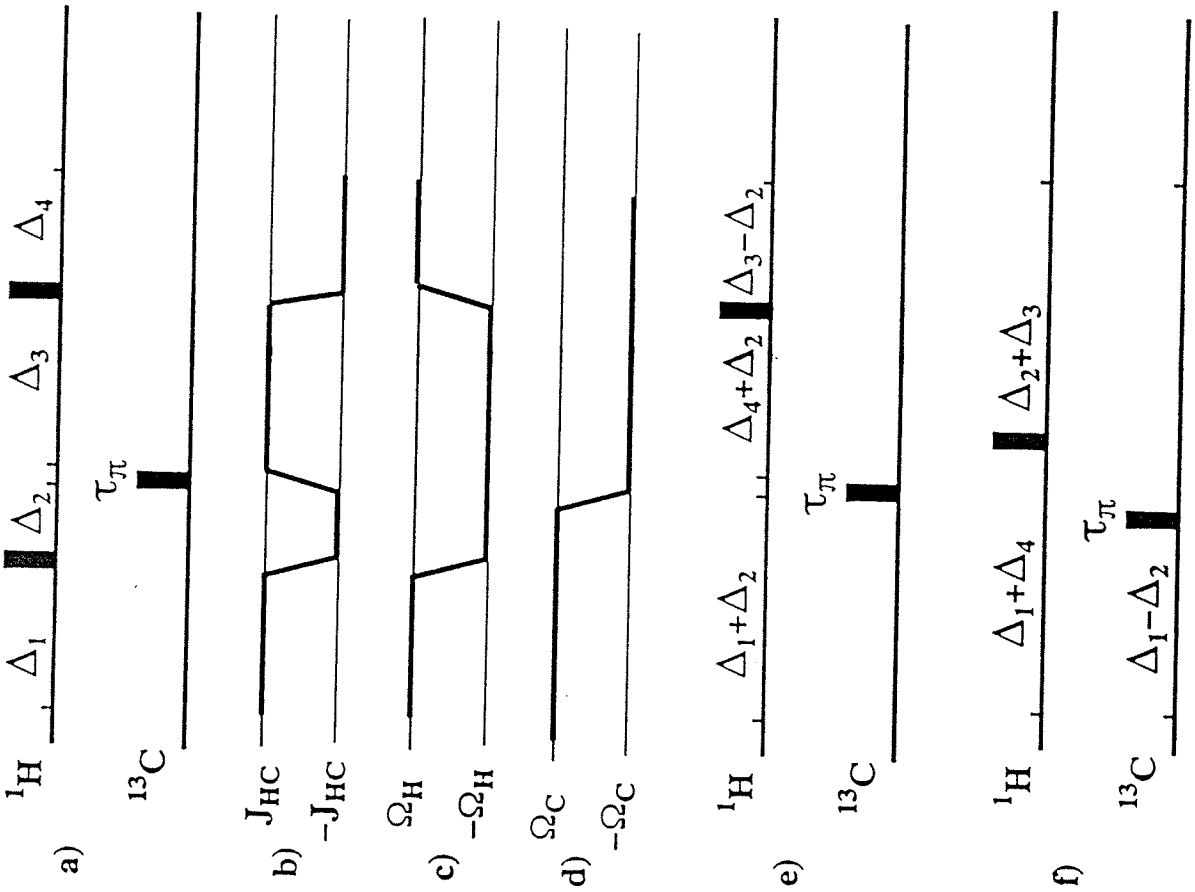
a)
^1H
Δ_1
Δ_2
Δ_3
Δ_4
τ_π
^{13}C
b)
J_{HC}
$-J_{HC}$
J_{HC} $(\Delta_1-\Delta_2+\Delta_3-\Delta_4)$
c)
Ω_H
$-\Omega_H$
Ω_H $(\Delta_1-\Delta_2-\tau_\pi-\Delta_3+\Delta_4)$
d)
Ω_C
$-\Omega_C$
Ω_C $(\Delta_1+\Delta_2-\Delta_3-\Delta_4)$
e)
^1H
$\Delta_1+\Delta_2$
$\Delta_4+\Delta_2$
$\Delta_3-\Delta_2$
τ_π
^{13}C
J_{HC} $(\Delta_1-\Delta_2+\Delta_3-\Delta_4)$
Ω_C $(\Delta_1+\Delta_2-\Delta_3-\Delta_4)$
f)
^1H
$\Delta_1+\Delta_4$
$\Delta_2+\Delta_3$
τ_π
^{13}C
$\Delta_1-\Delta_2$
J_{HC} $(\Delta_1-\Delta_2+\Delta_3-\Delta_4)$
Ω_H $(\Delta_1-\Delta_2-\Delta_3+\Delta_4)$

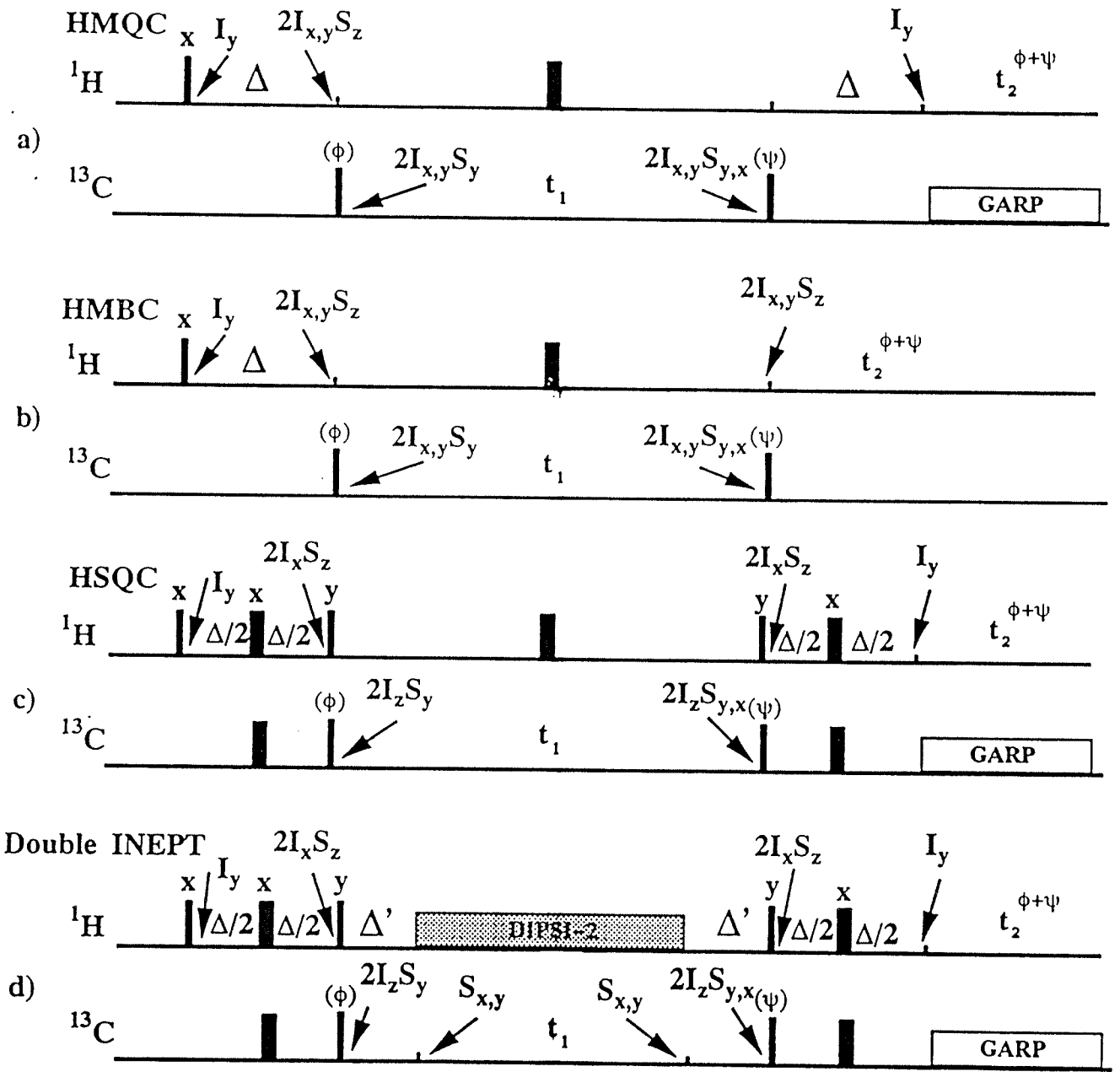
HMQC
x
I_y
$2I_{x,y}S_z$
I_y
^1H
Δ
Δ
t_2
$\phi+\psi$
a)
^{13}C
(ϕ)
$2I_{x,y}S_y$
t_1
$2I_{x,y}S_{y,x}(\psi)$
GARP
HMBC
x
I_y
$2I_{x,y}S_z$
$2I_{x,y}S_z$
^1H
Δ
t_2
$\phi+\psi$
b)
^{13}C
(ϕ)
$2I_{x,y}S_y$
t_1
$2I_{x,y}S_{y,x}(\psi)$
HSQC
x
I_y
x
$2I_xS_z$
y
$2I_xS_z$
y
x
I_y
^1H
Δ/2
Δ/2
Δ/2
Δ/2
t_2
$\phi+\psi$
c)
^{13}C
(ϕ)
$2I_zS_y$
t_1
$2I_zS_{y,x(\psi)}$
GARP
Double INEPT
$2I_xS_z$
$2I_xS_z$
I_y
x
I_y
x
y
y
x
^1H
Δ/2
Δ/2
Δ'
DIPSI-2
Δ'
Δ/2
Δ/2
t_2
$\phi+\psi$
d)
^{13}C
(ϕ)
$2I_zS_y$
$S_{x,y}$
t_1
$S_{x,y}$
$2I_zS_{y,x(\psi)}$
GARP

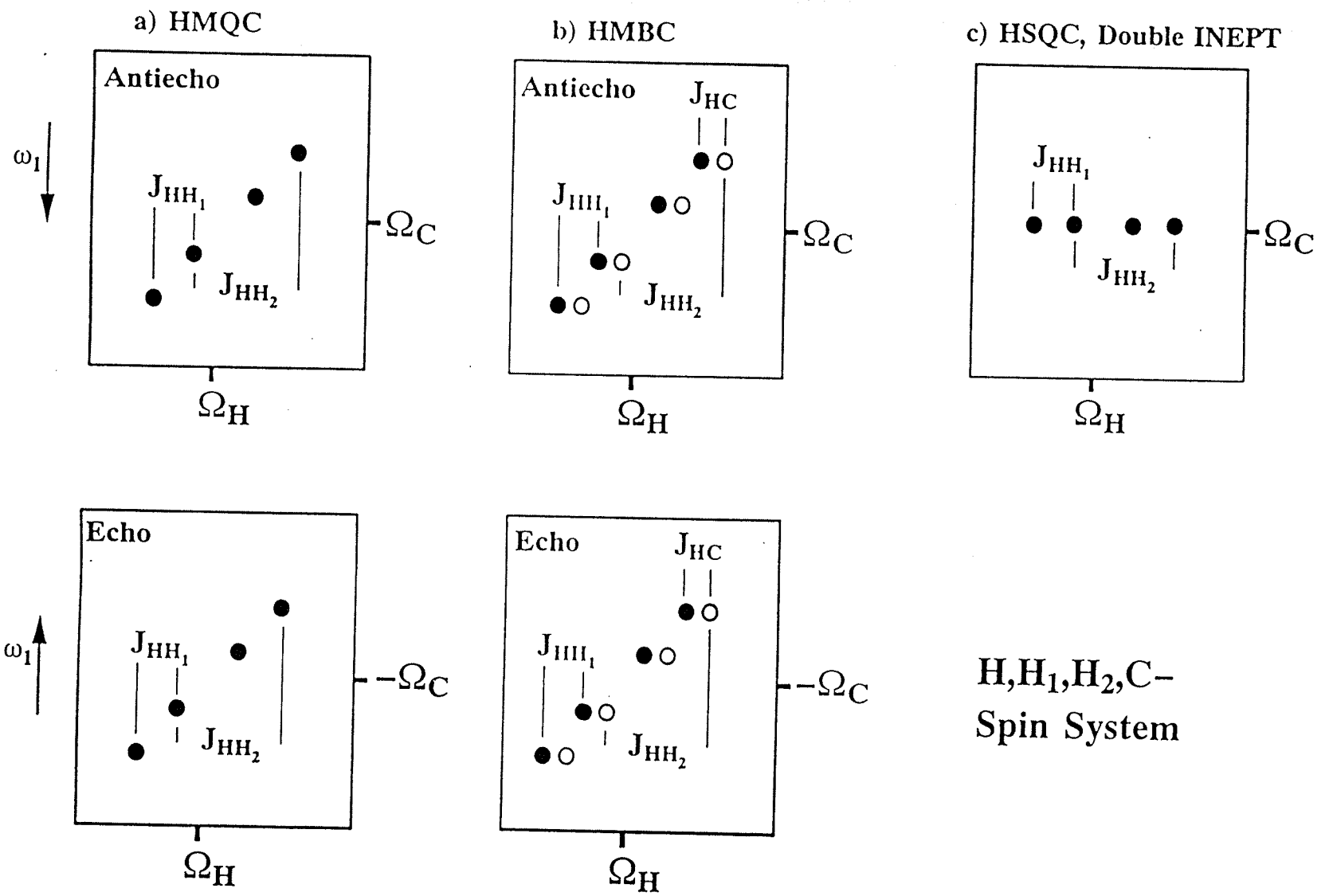

H,H_1,H_2,C–Spin System

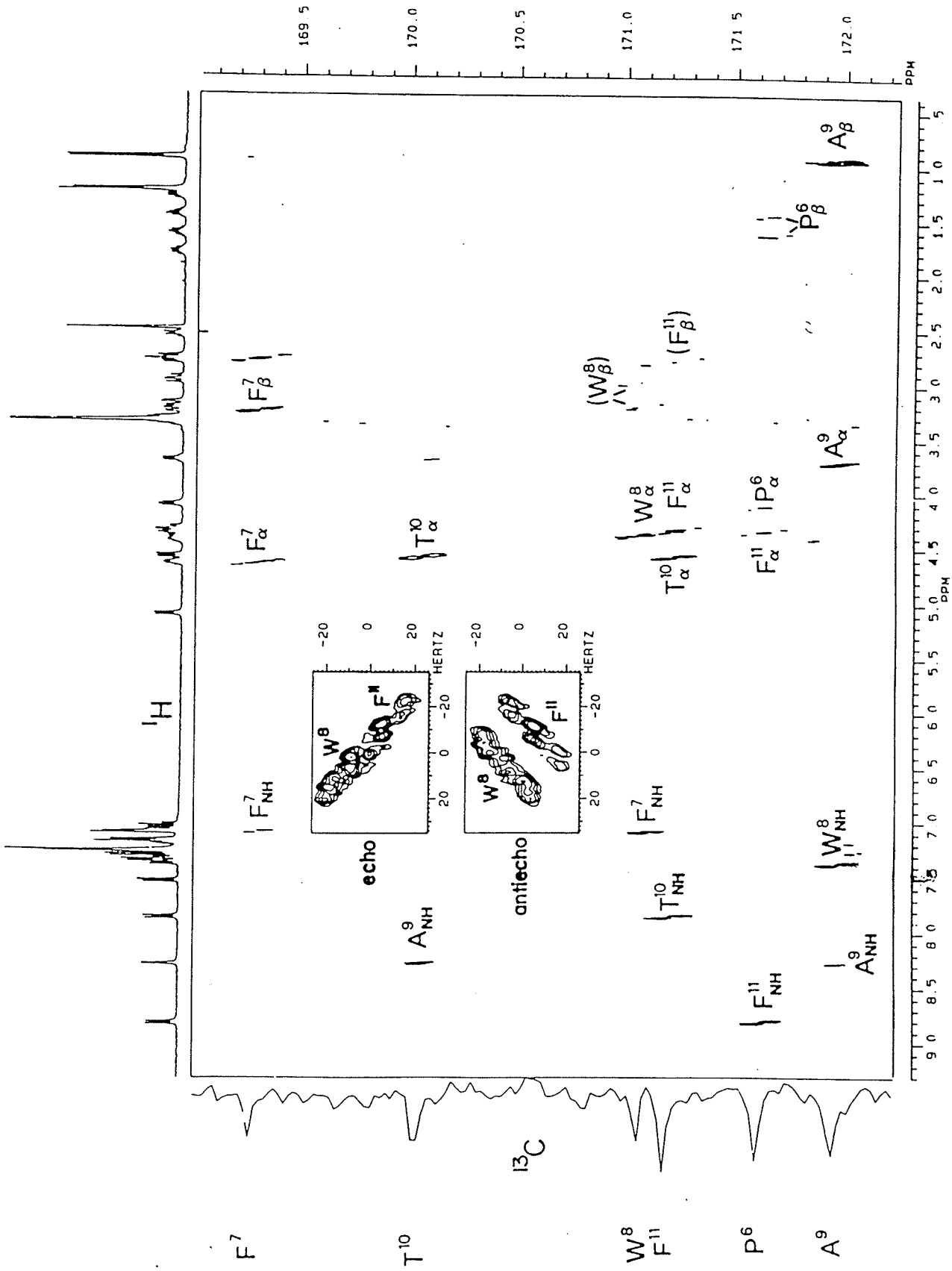
169.5
170.0
170.5
171.0
171.5
172.0
PPM
^{1}H
^{13}C
F^7
T^{10}
W^8 F^{11}
P^6
A^9
F^7_{NH}
F^7_α
F^7_β
T^{10}_α
A^9_{NH}
(W^8_β)
(F^{11}_β)
W^8_α
F^{11}_α
T^{10}_α
iP^6_α
P^6_β
A^9_α
A^9_β
F^7_{NH}
T^{10}_{NH}
W^8_{NH}
F^{11}_{NH}
A^9_{NH}
echo
antiecho
W^8
F^M
F^{11}
-20
0
20
HERTZ
9.0
8.5
8.0
7.5
7.0
6.5
6.0
5.5
5.0
4.5
4.0
3.5
3.0
2.5
2.0
1.5
1.0
.5
PPM

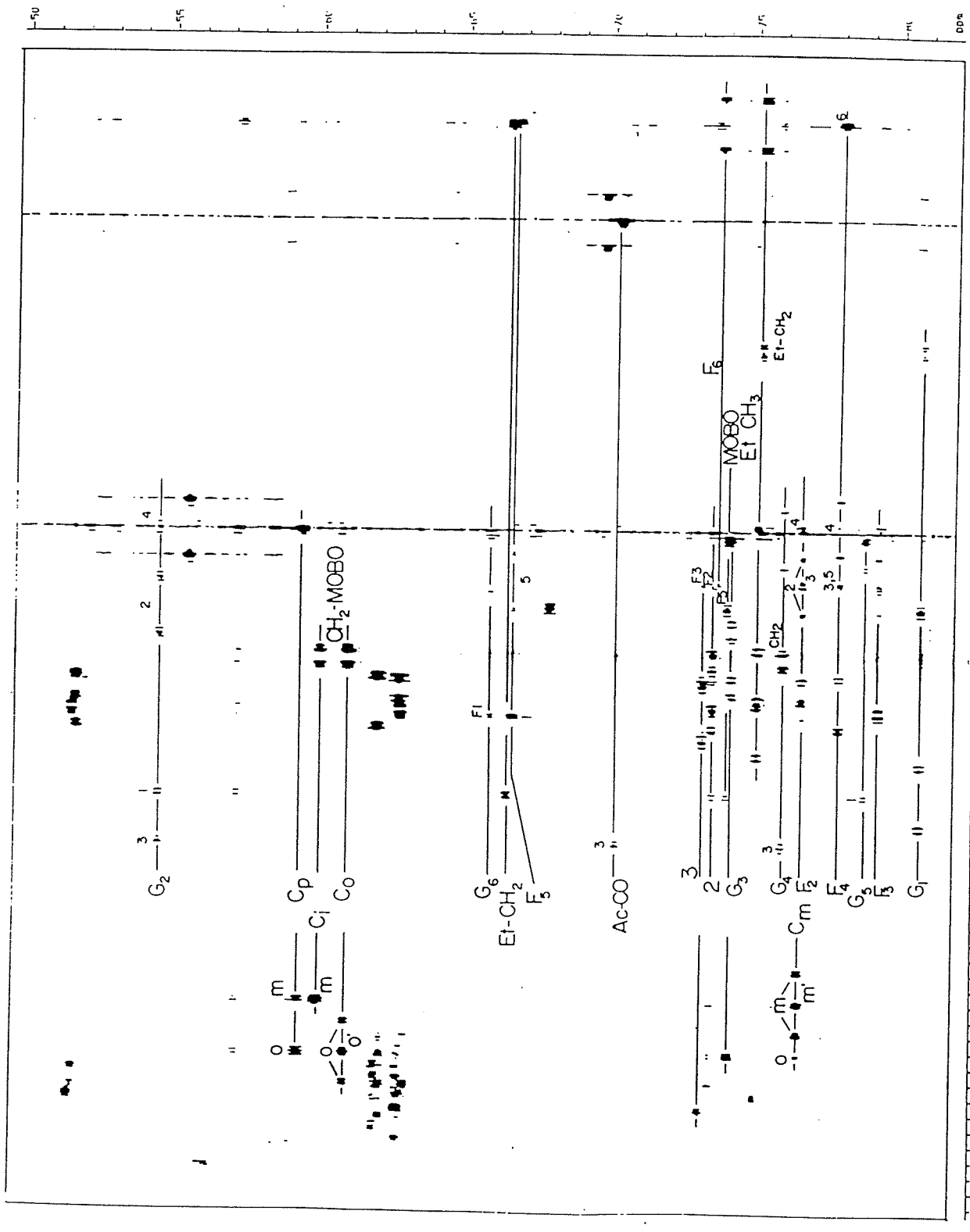
G2
Cp
Ci
Co
CH2-MOBO
G6
Et-CH2
F5
F1
Ac-CO
F6
MOBO
Et CH3
Et-CH2
G3
G4
F2
Cm
F4
G5
F3
G1
CH2
F3
F2
3,5
6

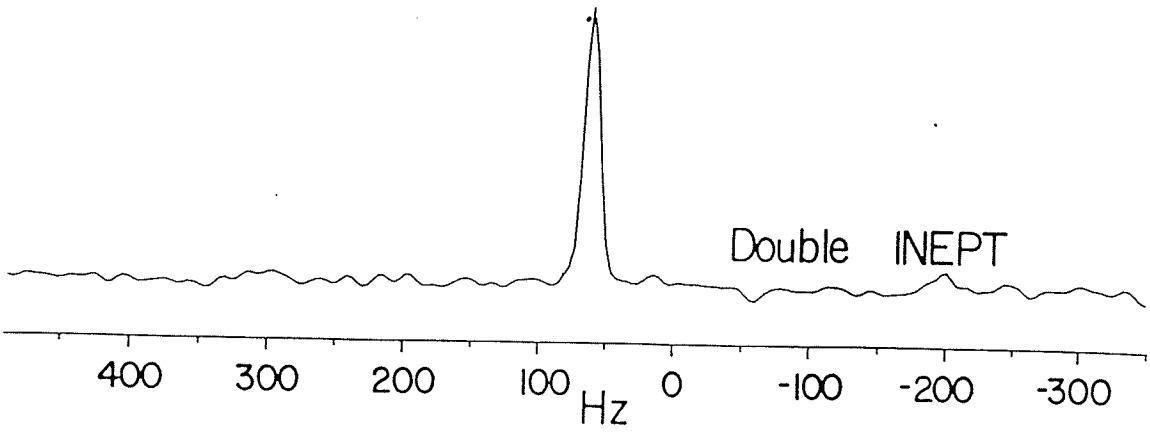
Double INEPT
400
300
200
100
Hz
0
-100
-200
-300

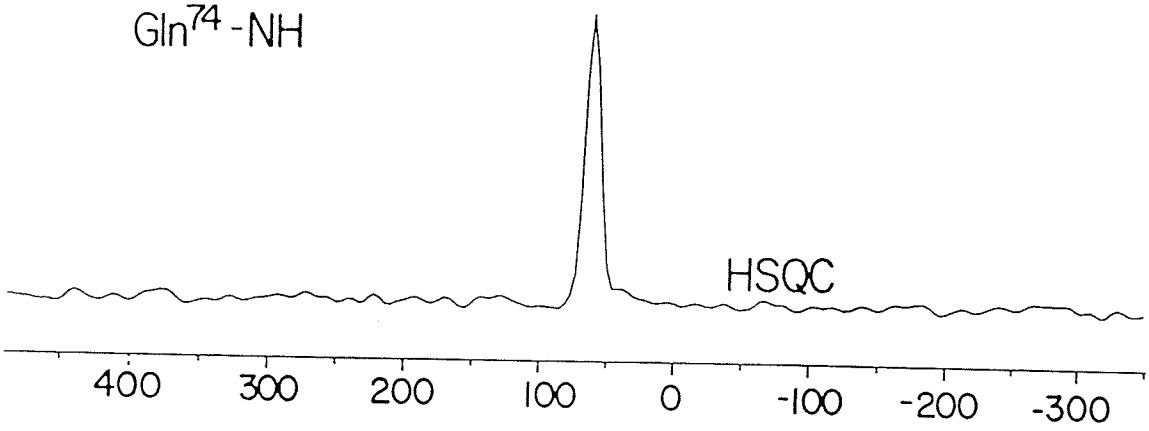
Gln74-NH
HSQC
400
300
200
100
0
-100
-200
-300

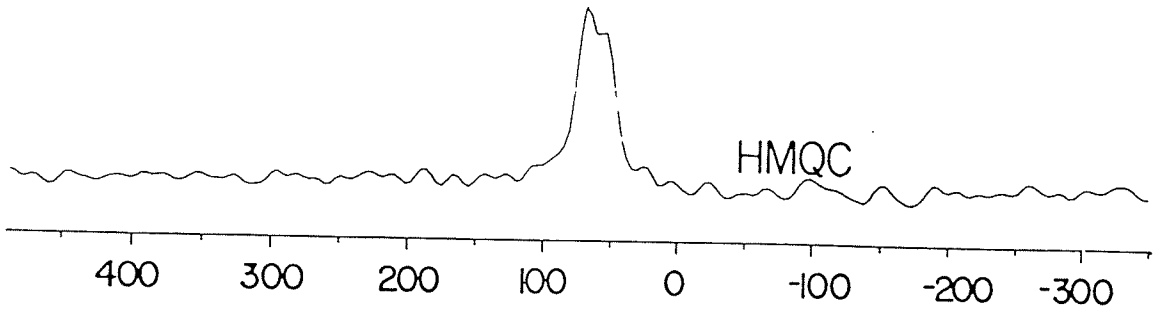
HMQC
400
300
200
100
0
-100
-200
-300

A 3-13a

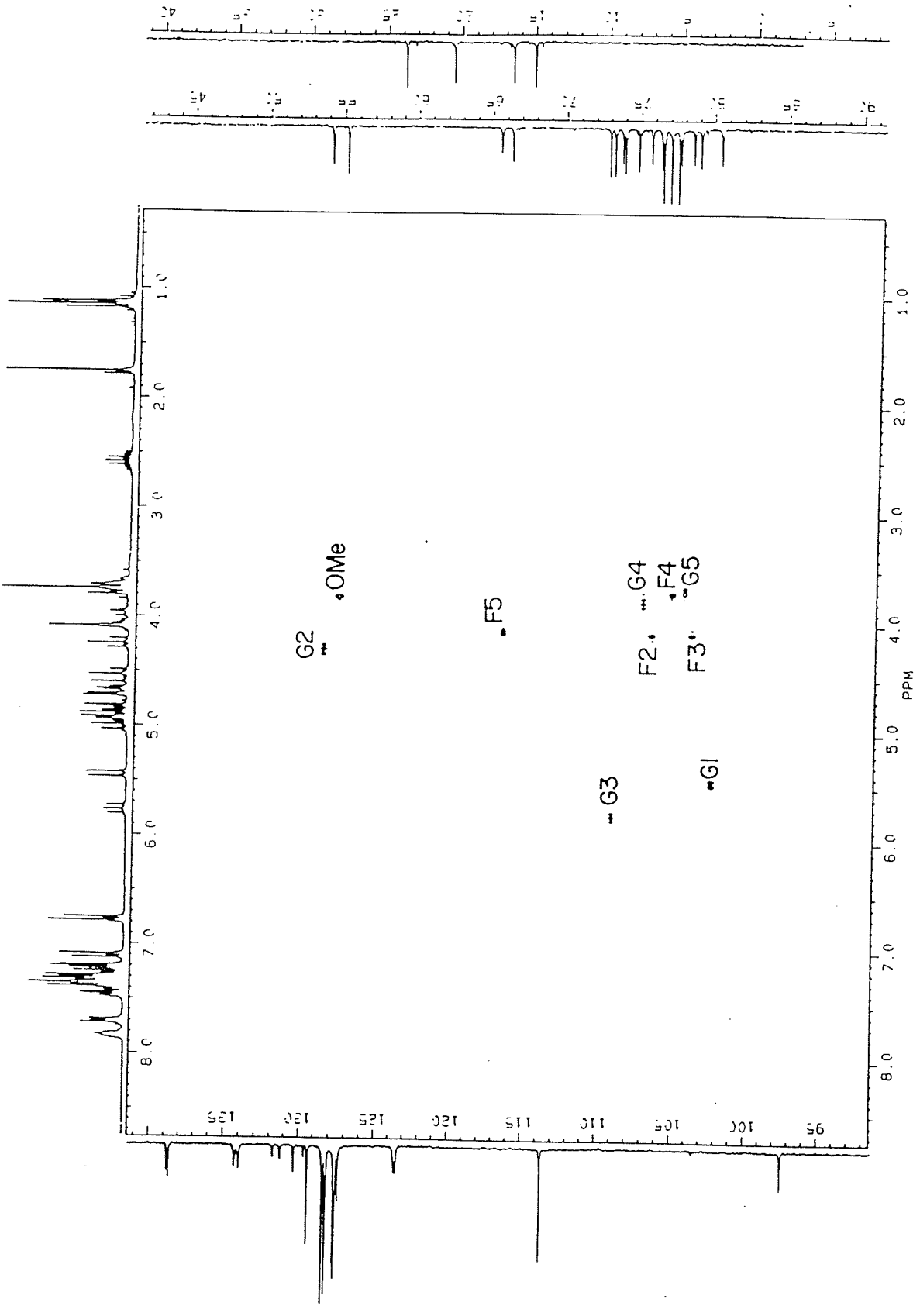

A 3-13b

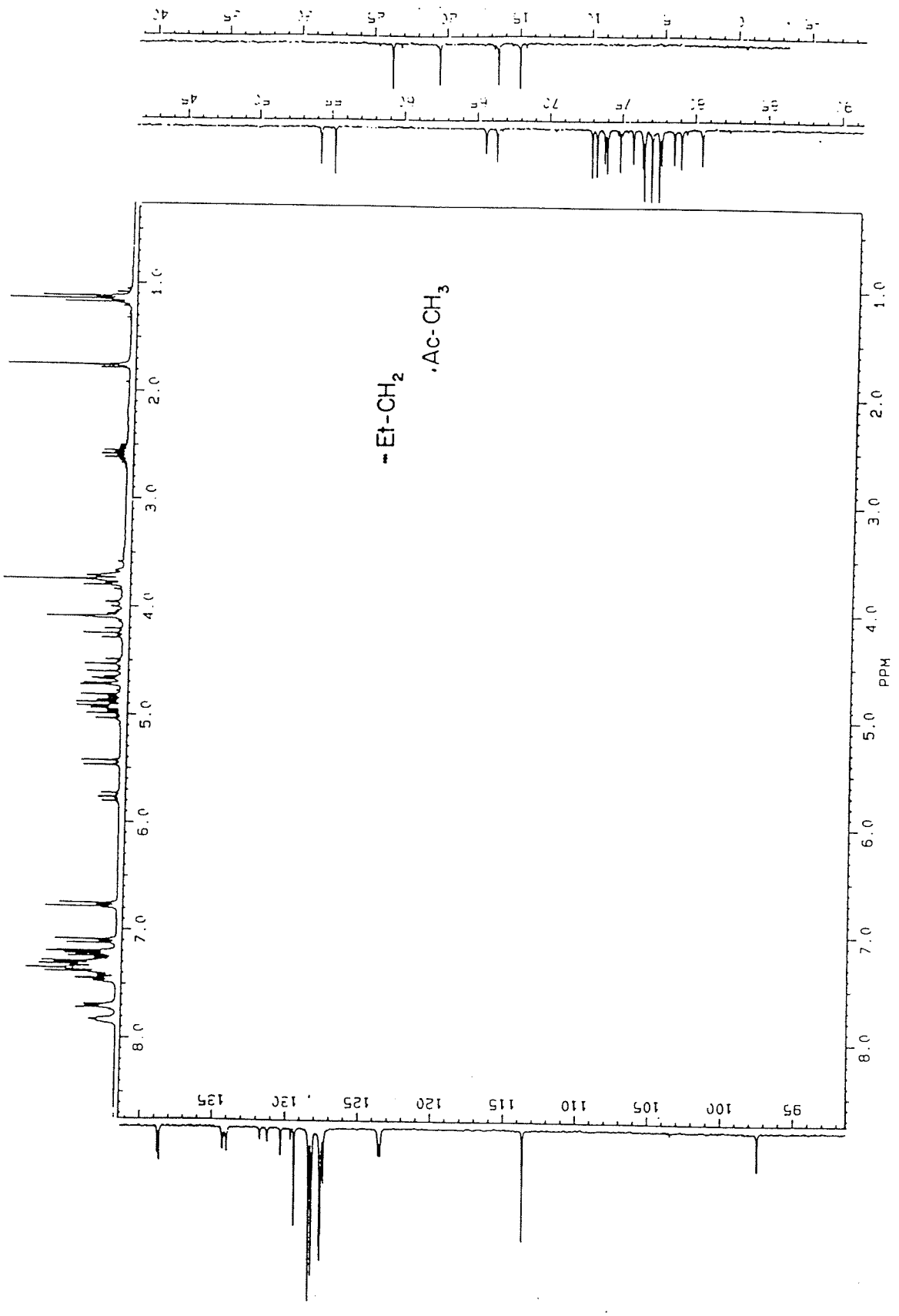

A 3-13c

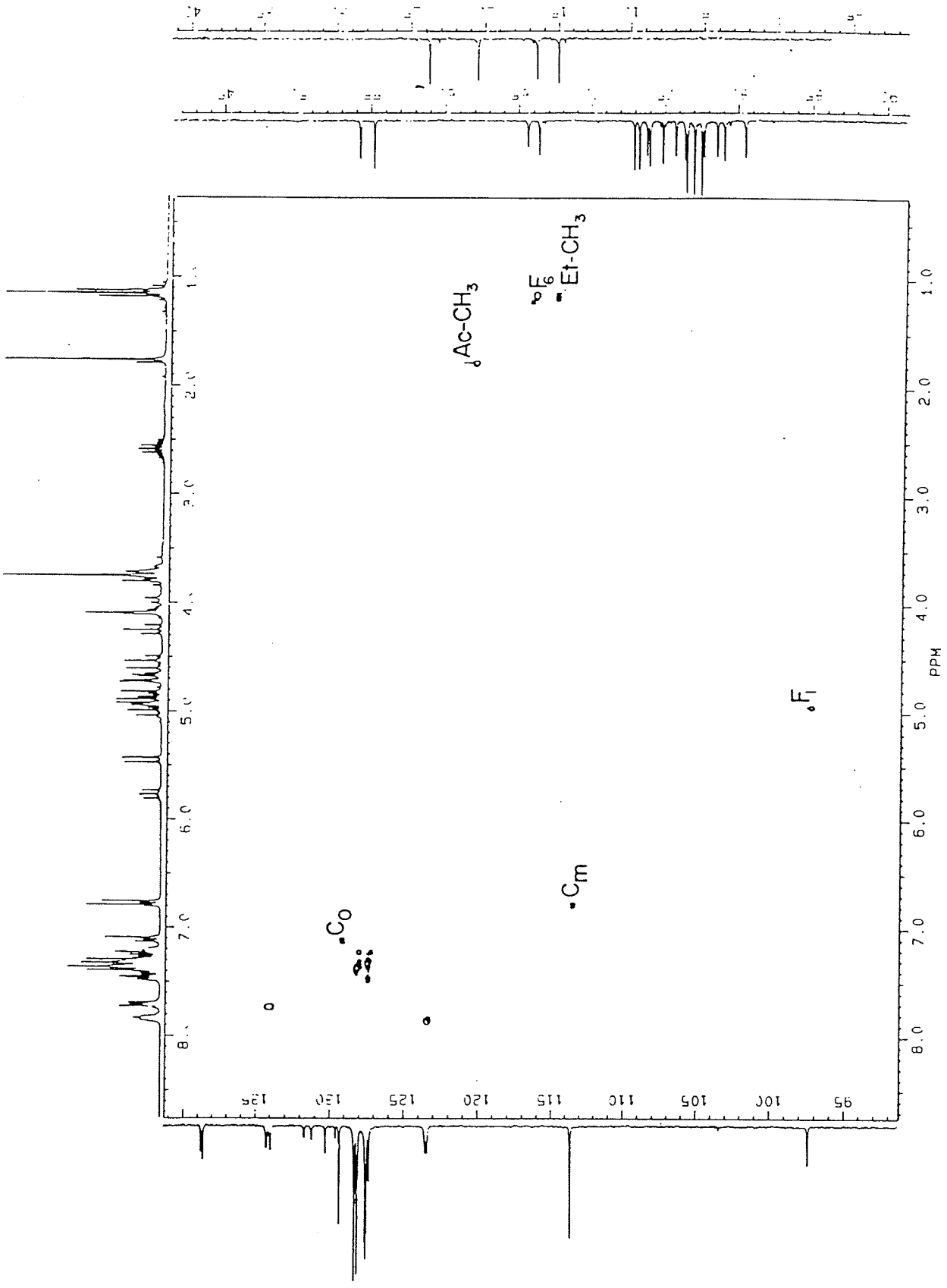
Ac-CH3
E
Et-CH3
F1
Cm
Co
PPM
1.0
2.0
3.0
4.0
5.0
6.0
7.0
8.0
95
100
105
110
115
120
125
130
135

Density Matrices:

We have two levels of description for the status of a spin system, the density matrix expressed as cartesian operators, or single element operators or the energy level diagram.

Cartesian Basis **Single element basis**

$r : 1, I_x; I_y; I_z;$ $r : I_a, I_b; I_+; I_-;$

Energy level diagram

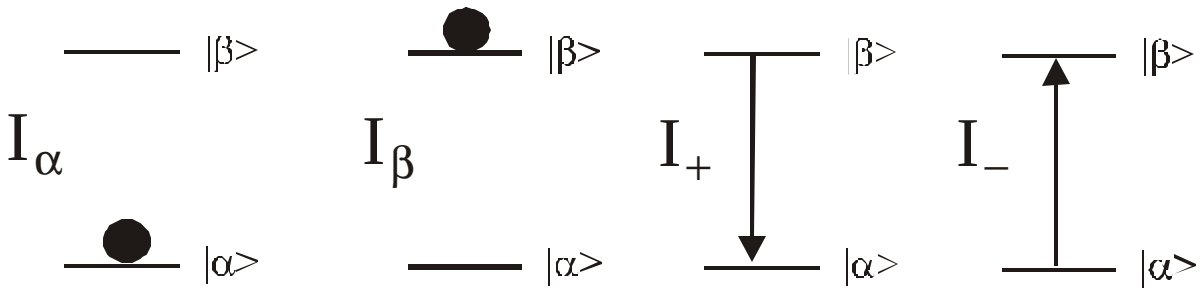

Time evolution of Density Matrices:

The density matrix transforms under the Liouville von Neumann equation in the following form:

$$i\dot{r} = [H, r]$$

Hamiltonian Operators under which the density matrix transforms are:

Chemical Shift: $H^{CS} = \Omega_I I_z + \Omega_S S_z$

Pulses: $H^{pulse} = g_I B_1 I_x = w_I I_x$. After time τ the pulse has aquired the phase: $w_I t = b$. A pulse with the Hamiltonian: $H^{pulse} = g_I B_1 I_x = w_I I_x$ of duration τ is therefore called a $b_x(I)$ pulse.

Scalar Coupling between spin I and S: $H^J = 2pJ_{IS} I_z S_z$

Transformation of Density Matrices under pulses, chemical shift and coupling for a two spin system of I and S in the cartesian operator basis:

Chemical Shift:

$$I_x \xrightarrow{H^{CS}} I_x \cos\Omega_I t + I_y \sin\Omega_I t\,;\; I_y \xrightarrow{H^{CS}} I_y \cos\Omega_I t - I_x \sin\Omega_I t\,;\; I_z \xrightarrow{H^{CS}} I_z$$
$$S_x \xrightarrow{H^{CS}} S_x \cos\Omega_S t + S_y \sin\Omega_S t\,;\; S_y \xrightarrow{H^{CS}} I_y \cos\Omega_S t - S_x \sin\Omega_S t\,;\; S_z \xrightarrow{H^{CS}} S_z$$

Pulses:

$$I_x \xrightarrow{b_x(I)} I_x\,;\; I_y \xrightarrow{b_x(I)} I_y \cos b + I_z \sin b\,;\; I_z \xrightarrow{b_x(I)} I_z \cos b - I_z \sin b$$
$$S_x \xrightarrow{b_x(S)} S_x\,;\; S_y \xrightarrow{b_x(S)} S_y \cos b + S_z \sin b\,;\; S_z \xrightarrow{b_x(S)} S_z \cos b - S_z \sin b$$

Scalar Coupling:

$$I_x \xrightarrow{H^J} I_x \cos pJ_{IS}t + 2I_yS_z \sin pJ_{IS}t\,;\; I_y \xrightarrow{H^J} I_y \cos pJ_{IS}t - 2I_xS_z \sin pJ_{IS}t\,;\; I_z \xrightarrow{H^J} I_z$$
$$2I_yS_z \xrightarrow{H^J} 2I_yS_z \cos pJ_{IS}t - I_x \sin pJ_{IS}t\,;\; 2I_xS_z \xrightarrow{H^J} 2I_xS_z \cos pJ_{IS}t + I_y \sin pJ_{IS}t$$

Transformation of Density Matrices under pulses, chemical shift and coupling for a two spin system of I and S in the single element operator basis:

Chemical Shift:

$$I_+ \xrightarrow{H^{CS}} I_+ e^{-i\Omega_I t}\,;\; I_- \xrightarrow{H^{CS}} I_- e^{+i\Omega_I t}\,;\; I_a \xrightarrow{H^{CS}} I_a\,;\; I_b \xrightarrow{H^{CS}} I_b$$
$$S_+ \xrightarrow{H^{CS}} S_+ e^{-i\Omega_S t}\,;\; S_- \xrightarrow{H^{CS}} S_- e^{+i\Omega_S t}\,;\; S_a \xrightarrow{H^{CS}} S_a\,;\; S_b \xrightarrow{H^{CS}} S_b$$

Pulses:

$$I_a \xrightarrow{b_f(I)} I_a \cos^2\frac{b}{2} + I_b \sin^2\frac{b}{2} + \frac{i}{2}\left(I_+ e^{-if} + I_- e^{if}\right)\sin b$$
$$I_b \xrightarrow{b_f(I)} I_b \cos^2\frac{b}{2} + I_a \sin^2\frac{b}{2} - \frac{i}{2}\left(I_+ e^{-if} + I_- e^{if}\right)\sin b$$
$$I_+ \xrightarrow{b_f(I)} I_+ \cos^2\frac{b}{2} + I_- e^{i2f} \sin^2\frac{b}{2} + \frac{i}{2}\left(I_a e^{if} + I_b e^{-if}\right)\sin b$$
$$I_- \xrightarrow{b_f(I)} I_- \cos^2\frac{b}{2} + I_+ e^{-i2f} \sin^2\frac{b}{2} - \frac{i}{2}\left(I_a e^{-if} + I_b e^{if}\right)\sin b$$

Scalar Coupling:

$$I_+S_a \xrightarrow{H^J} I_+S_a e^{-ipJ_{SI}t}\,;\; I_-S_a \xrightarrow{H^J} I_-S_a e^{ipJ_{SI}t}\,;\; I_a \xrightarrow{H^J} I_a\,;\; I_b \xrightarrow{H^J} I_b$$
$$I_+S_b \xrightarrow{H^J} I_+S_b e^{+ipJ_{SI}t}\,;\; I_-S_b \xrightarrow{H^J} I_-S_b e^{-ipJ_{SI}t}$$

Transformation of Density Matrices under pulses, chemical shift and coupling for a two spin system of I and S in the energy level picture:

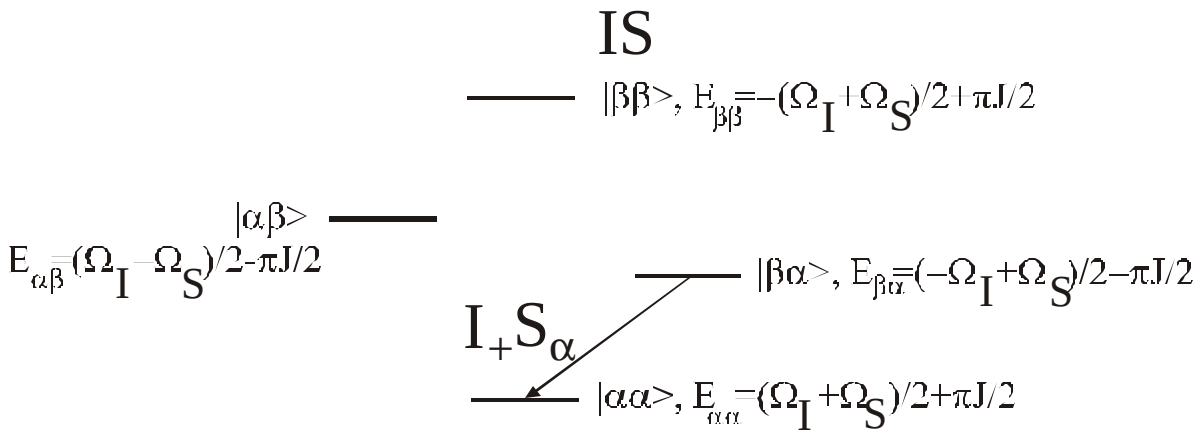

The evolution of coherences between the levels is given by the energy difference of the levels connected. The evolution goes like: $e^{-i\Delta Et}$: E.g.

$$I_+S_a \xrightarrow{H^J+H^{CS}} I_+S_a e^{-i(\Omega_I+pJ_{SI})t}$$

Populations have no energy difference, therefore they are invariant under time evolution.
Pulses can be calculated by looking at the action of a pulse on each of the functions involved in a coherence. For that we need the transformation of the functions under pulses:

$$|a> \xrightarrow{b_x} |a>\cos\frac{b}{2}+i|b>\sin\frac{b}{2}$$
$$|b> \xrightarrow{b_x} |b>\cos\frac{b}{2}+i|a>\sin\frac{b}{2}$$

Thus a $b_x(I)$ pulse onto the operator $I_+S_a = |aa><ba|$ effects the following transformation:

$$e^{iI_xb}I_+S_ae^{-iI_xb} =$$
$$e^{i(b/2)(|aa><ba|+|ba><aa|+|ab><bb|+|bb><ab|)}\,|aa><ba|\,e^{-i(b/2)(|aa><ba|+|ba><aa|+|ab><bb|+|bb><ab|)}$$

In order to simplify this expression, we first notice that the the two pairs of operators contained in each of the exponentials commute:

$$[|aa><ba|+|ba><aa|,|ab><bb|+|bb><ab|]=0$$

Due to this fact, they can be applied sequentially:

$$e^{i(b/2)(|aa><ba|+|ba><aa|+|ab><bb|+|bb><ab|)} =$$

$$e^{i(b/2)(|aa><ba|+|ba><aa|)} e^{i(b/2)(|ab><bb|+|bb><ab|)}$$

We calculate now one of the two expressions:

$$e^{i(b/2)(|aa><ba|+|ba><aa|)} =$$

$$\sum_n \frac{[i(b/2)(|aa><ba|+|ba><aa|)]^n}{n!} =$$

$$\cos(b/2)(|aa><aa|+|ba><ba|) + i\sin(b/2)(|aa><ba|+|ba><aa|)$$

or in matrix form:

$$\cos(b/2)(|aa><aa|+|ba><ba|) + i\sin(b/2)(|aa><ba|+|ba><aa|) =$$

$$\begin{pmatrix} \cos(b/2) & i\sin(b/2) & & \\ i\sin(b/2) & \cos(b/2) & & \\ & & 1 & \\ & & & 1 \end{pmatrix}$$

The ordering of the basis functions is: $\alpha\alpha$, $\beta\alpha$, $\alpha\beta$, $\beta\beta$.

The second rotation matrix can be constructed in the same way and we find:

$$\cos(b/2)(|ab><ab|+|bb><bb|) + i\sin(b/2)(|ab><bb|+|bb><ab|) =$$

$$\begin{pmatrix} 1 & & & \\ & 1 & & \\ & & \cos(b/2) & i\sin(b/2) \\ & & i\sin(b/2) & \cos(b/2) \end{pmatrix}$$

Application to $I_+S_a = |aa><ba|$ can be obtained now in the following way:

$$e^{iI_x b} I_+ S_a e^{-iI_x b} =$$

$$e^{i(b/2)(|aa><ba|+|ba><aa|+|ab><bb|+|bb><ab|)} \; |aa><ba| \; e^{-i(b/2)(|aa><ba|+|ba><aa|+|ab><bb|+|bb><ab|)}$$

$$= \{c_b(|ab><ab|+|bb><bb|) + is_b(|ab><bb|+|bb><ab|)\}\{c_b(|aa><aa|+|ba><ba|) + is_b(|aa><ba|+|ba><aa|)\}$$

$$|aa><ba|$$

$$\{c_b(|ab><ab|+|bb><bb|) - is_b(|ab><bb|+|bb><ab|)\}\{c_b(|aa><aa|+|ba><ba|) - is_b(|aa><ba|+|ba><aa|)\}$$

Of all the indicated transitions, only the ones that carry |αα> as „ket“ and <βα| as „bra“ Calculation of the transformation leads to:

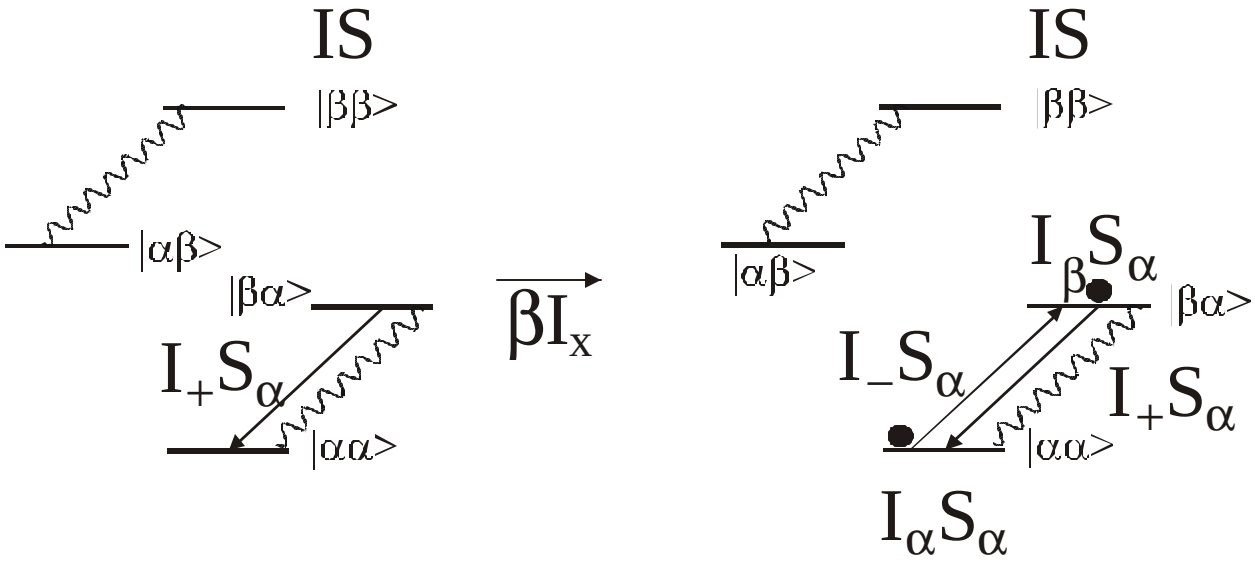

Fictitious Two Level Operators:

How do we transfer population on the αβ state into the βα state? We can look how we do this in the simplest spin system, namely a single spin system and we ask the question, how do we transfer population on the α state into population on the β state. This can be done by a π pulse as we know. A π_x pulse is given by: $p_x = e^{ipI_x} = e^{i(p/2)(|a><b|+|b><a|)}$. Thus if we want to apply a pulse across a certain transition rs, we simply apply a $q_x^{rs} = e^{iqI_x^{rs}} = e^{i(q/2)(|r><s|+|s><r|)}$ pulse. Here the flip angle is θ. The effect of this pulse will be as known for the single spin operator transformations:

$$I_z^{rs} \xrightarrow{qI_x^{rs}} I_z^{rs}\cos q - I_y^{rs}\sin q; I_z^{rs} \xrightarrow{qI_y^{rs}} I_z^{rs}\cos q + I_x^{rs}\sin q; I_z^{rs} \xrightarrow{qI_z^{rs}} I_z^{rs}$$

$$I_x^{rs} \xrightarrow{qI_x^{rs}} I_x^{rs}; I_x^{rs} \xrightarrow{qI_y^{rs}} I_x^{rs}\cos q - I_z^{rs}\sin q; I_x^{rs} \xrightarrow{qI_z^{rs}} I_x^{rs}\cos q + I_y^{rs}\sin q \qquad \text{Eq. [5]}$$

$$I_y^{rs} \xrightarrow{qI_x^{rs}} I_y^{rs}\cos q + I_z^{rs}\sin q; I_y^{rs} \xrightarrow{qI_y^{rs}} I_y^{rs}; I_y^{rs} \xrightarrow{qI_z^{rs}} I_y^{rs}\cos q - I_x^{rs}\sin q$$

Optimization of Pulse Sequences:

When optimizing pulse sequences one has to distinguish the following levels:

a) Optimal experimental implementation of the pulse sequence? This addresses the question whether the pulse sequence does what it is supposed to do. E.g. off-resonance effects of pulses or polarization transfer segements, decoupling bandwidth etc. There is a vast body of literature addressing this problem: e.g. broad band decoupling (WALTZ, GARP, WURST), TOCSY transfer: (CW, MLEV, DIPSI, FLOPSY etc.). Inversion pulses (normal, composite, shaped). This shall be mentioned only shortly in this lecture.

b) Optimal pulse sequence?
Every pulse sequence consists of one or several transfers of coherences. The question addresses the problem whether the coherence transfers are optimal with respect to sensitivity. This question can be answered by analysing the bounds of coherence transfer ignoring relaxation. These bounds will be introduced and examples will be given. It will also be discussed on several examples how to find the optimal pulse sequence.

c) Optimal coherences?
This is perhaps the most fundamental question out of those a)-c). It addresses the question whether the right coherences are chosen to create the spectrum. There are several coherences that provide the same spectroscopic information but they may give rise to considerably varying quality of spectra even after optimization according to b) and a).

Bounds and optimal pulse sequences for Hermitian A and C:

The optimization of a desired coherence transfer ignoring relaxation requires to find the unitary transformation U that maximizes a transfer that goes from a coherence A to a coherence C:

$$A \xrightarrow{U} aC + B \qquad \text{Eq. [1]}$$

a is given by: $$a = \frac{Tr\{UAU^{-1}C^{\dagger}\}}{Tr\{C^{\dagger}C\}} \qquad \text{Eq. [2]}$$

Let's assume that A and C are both hermitian matrices and that we have chosen the eigenbasis of C with the eigenvalues in descending order. Then the trace is maximized if A is also diagonalized and the eigenvalues of A are also sorted in descending order.

$$Tr\begin{pmatrix} A_{11} & 0 & 0 & 0 \\ 0 & A_{22} & 0 & 0 \\ 0 & 0 & A_{33} & 0 \\ 0 & 0 & 0 & A_{44} \end{pmatrix}\begin{pmatrix} C_{11} & 0 & 0 & 0 \\ 0 & C_{22} & 0 & 0 \\ 0 & 0 & C_{33} & 0 \\ 0 & 0 & 0 & C_{44} \end{pmatrix} = \max. \qquad \text{Eq. [3]}$$

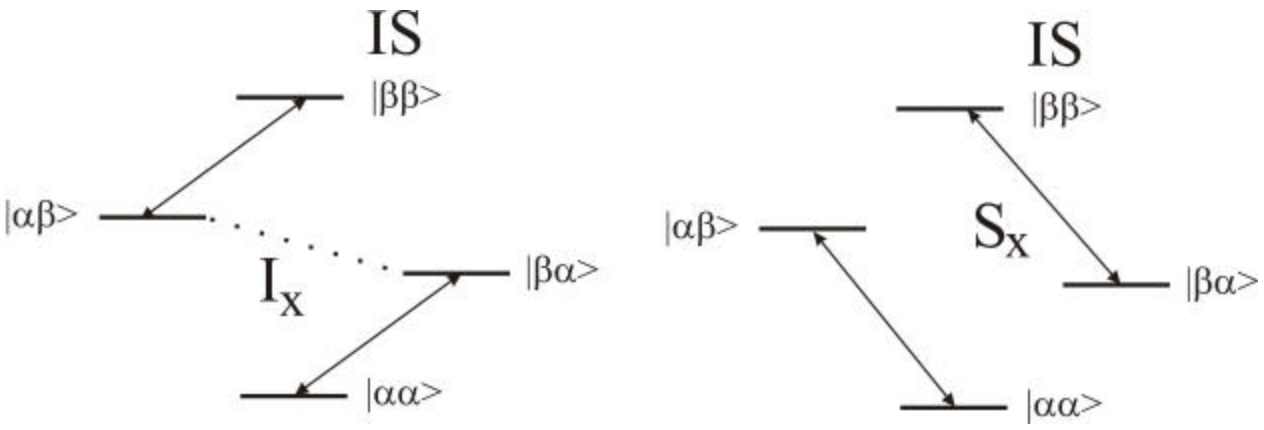

Example: INEPT transfer in IS system:

For the INEPT transfer it is possible to transfer completely I_x -> S_x in an IS spin system, however, this is not possible for a I_2S spin system where one can achieve $I_{1x} + I_{2x}$ -> S_x. The question is, whether this is a fundamental limitation or whether the INEPT is not optimal.

The matrices for I_x and S_x in an IS spin system are both diagonalized by a 90_y pulse. We look therefore for I_z and S_z:

$$A = I_z = \begin{pmatrix} 0.5 & 0 & 0 & 0 \\ 0 & 0.5 & 0 & 0 \\ 0 & 0 & -0.5 & 0 \\ 0 & 0 & 0 & -0.5 \end{pmatrix}; C = S_z = \begin{pmatrix} 0.5 & 0 & 0 & 0 \\ 0 & -0.5 & 0 & 0 \\ 0 & 0 & 0.5 & 0 \\ 0 & 0 & 0 & -0.5 \end{pmatrix} \qquad \text{Eq. [4]}$$

The eigenvalues are still not yet ordered correctly for S_z. If we do this by exchanging the $\alpha\beta$ and the $\beta\alpha$ populations we obtain:

$$I_z = \begin{pmatrix} 0.5 & 0 & 0 & 0 \\ 0 & 0.5 & 0 & 0 \\ 0 & 0 & -0.5 & 0 \\ 0 & 0 & 0 & -0.5 \end{pmatrix}; S_z' = \begin{pmatrix} 0.5 & 0 & 0 & 0 \\ 0 & 0.5 & 0 & 0 \\ 0 & 0 & -0.5 & 0 \\ 0 & 0 & 0 & -0.5 \end{pmatrix} \qquad \text{Eq. [5]}$$

Obviously I_z and S'_z are the same. Therefore the transfer from I_z to S_z is possible with an a=1, thus full transfer.

Fictitious Two Level Operators:

How do we transfer population on the $\alpha\beta$ state into the $\beta\alpha$ state? We can look how we do this in the simplest spin system, namely a single spin system and we ask the question, how do we transfer population on the α state into population on the β state. This can be done by a π pulse as we know. A π_x pulse is given by: $p_x = e^{ipI_x} = e^{i(p/2)(|a><b|+|b><a|)}$. Thus if we want to apply a pulse across a certain transition rs, we simply apply a $q_x^{rs} = e^{iqI_x^{rs}} = e^{i(q/2)(|r><s|+|s><r|)}$ pulse. Here the flip angle is θ. The effect of this pulse will be as known for the single spin operator transformations:

$$I_z^{rs} \xrightarrow{qI_x^{rs}} I_z^{rs}\cos q - I_y^{rs}\sin q; I_z^{rs} \xrightarrow{qI_y^{rs}} I_z^{rs}\cos q + I_x^{rs}\sin q; I_z^{rs} \xrightarrow{qI_z^{rs}} I_z^{rs}$$

$$I_x^{rs} \xrightarrow{qI_x^{rs}} I_x^{rs}; I_x^{rs} \xrightarrow{qI_y^{rs}} I_x^{rs}\cos q - I_z^{rs}\sin q; I_x^{rs} \xrightarrow{qI_z^{rs}} I_x^{rs}\cos q + I_y^{rs}\sin q \quad \text{Eq. [5]}$$

$$I_y^{rs} \xrightarrow{qI_x^{rs}} I_y^{rs}\cos q + I_z^{rs}\sin q; I_y^{rs} \xrightarrow{qI_y^{rs}} I_y^{rs}; I_y^{rs} \xrightarrow{qI_z^{rs}} I_y^{rs}\cos q - I_x^{rs}\sin q$$

With this information, we can now directly write down the pulse sequence for this transfer I_z -> S_z. Application of a $p_x^{|ab>|ba>}$ pulse will effect the desired transfer. The popagator that represents this pulse is: $e^{i(p/2)(|ab><ba|+|ba><ab|)}$. We now have to translate $(|ab><ba|+|ba><ab|)$ into the cartesian product operators. This yields:

$$(|ab><ba|+|ba><ab|) = \begin{pmatrix} 0 & 0 & 0 & 0 \\ 0 & 0 & 1 & 0 \\ 0 & 1 & 0 & 0 \\ 0 & 0 & 0 & 0 \end{pmatrix} = 2(I_x S_x + I_y S_y) \quad \text{Eq. [6]}$$

Thus we have to apply the following propagator:

$$p_x^{|ab>|ba>} = e^{i(p/2)(|ab><ba|+|ba><ab|)} = \quad \text{Eq. [7a]}$$

$$e^{i(p/2)(2I_x S_x + 2I_y S_y)} = \quad \text{Eq. [7a]}$$

$$e^{i(p/2)(2I_x S_x)} e^{i(p/2)2I_y S_y)} \quad \text{Eq. [7c]}$$

The first transformation Eq. 7a is a planar coupling Hamiltonian $pJ(I_xS_x + I_yS_y)(1/J)$ applied during duration (1/J). This is indeed an implementation of the heteronuclear polarization transfer. The planar Hamiltonian $pJ(I_xS_x + I_yS_y)$ is generated from the weak coupling Hamiltonian $2pJI_zS_z$ by a multipulse sequence that applies pulses only along x (e.g. DIPSI-2) and flanking 90_y pulses on I and S. The multipulse sequence generates: $pJ(I_zS_z + I_yS_y)$ and the flanking 90_y pulses on I and S rotate this to $pJ(I_xS_x + I_yS_y)$:

$$e^{i(p/2)(2I_xS_x+2I_yS_y)} =$$
$$e^{i(p/2)e^{-i(p/2)I_y}e^{-i(p/2)S_y}(2I_zS_z+2I_yS_y)e^{i(p/2)I_y}e^{i(p/2)S_y}}$$
$$= e^{-i(p/2)I_y}e^{-i(p/2)S_y}e^{i(p/2)(2I_zS_z+2I_yS_y)}e^{i(p/2)I_y}e^{i(p/2)S_y}$$

Eq. [8]

This yields the implementation given in Fig. 2a).

a)

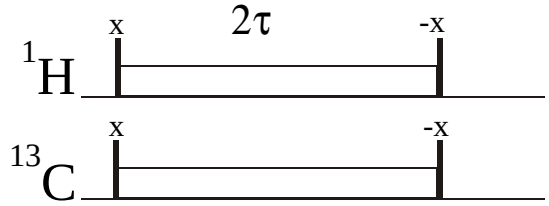

b)

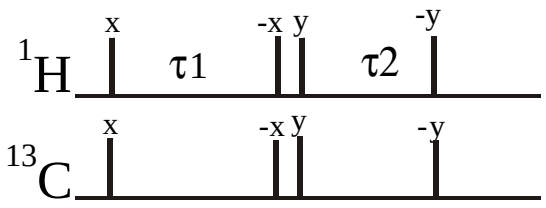

c)

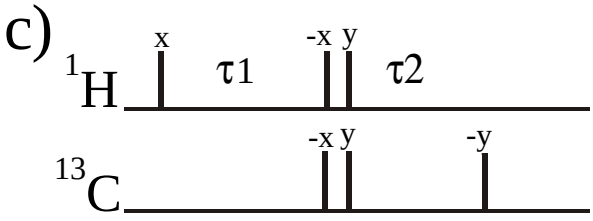

d)

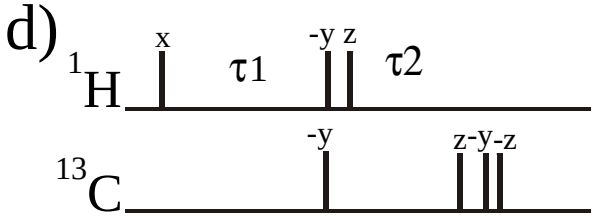

e)

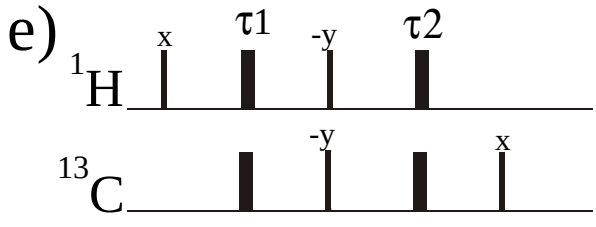

The second (Eq. 7c) consists of two terms. Looking at the first of the two we find the transformation of Eq. 8:

$$e^{i(p/2)(2I_xS_x)} = e^{i(p/2)}e^{-i(p/2)I_y}e^{-i(p/2)S_y}(2I_zS_z)e^{i(p/2)I_y}e^{i(p/2)S_y}$$
$$e^{i(p/2)I_y}e^{i(p/2)S_y}$$
$$= e^{-i(p/2)I_y}e^{-i(p/2)S_y}e^{i(p/2)(2I_zS_z)}e^{i(p/2)I_y}e^{i(p/2)S_y} =$$
$$90_y(I,S)e^{i(p/2)(2I_zS_z)}90_{-y}(I,S) \qquad \text{Eq. [9]}$$

The middle term is free evolution of heteronuclear coupling during a delay $(2J)^{-1}$: $2pJ(I_zS_z)(1/2J)$. Thus the pulse sequence that implements the propagator of Eq. 7c is given by:

$$90_y(I,S)(1/2J)90_{-y}(I,S)90_x(I,S)(1/2J)90_{-x}(I,S)$$

This can be transformed from Fig. 2b) to e) by using the fact that e.g. $90_y = 90_{-z}\,90_x\,90_z$. Furthermore, z rotations that are before or after the pulse sequence can be introduced and skipped as well.

Example: INEPT transfer in I_2S system:

Let's now look at the I_2S case:
Here the matrices are a twice as big:

$$I_{1z}+I_{2z} = \begin{pmatrix} 1 & & & & & & & \\ & 0 & & & & & & \\ & & 0 & & & & & \\ & & & -1 & & & & \\ & & & & 1 & & & \\ & & & & & 0 & & \\ & & & & & & 0 & \\ & & & & & & & -1 \end{pmatrix}; S_z = \begin{pmatrix} 0.5 & & & & & & & \\ & 0.5 & & & & & & \\ & & 0.5 & & & & & \\ & & & 0.5 & & & & \\ & & & & -0.5 & & & \\ & & & & & -0.5 & & \\ & & & & & & -0.5 & \\ & & & & & & & -0.5 \end{pmatrix}$$

Application of Eq. [2] to this transfer yields after reordering of the matrix elements: a=1. The problem contains symmetry and we can use this symmetry to achieve a simpler notation. The composite spin of I_1 and I_2 is called F. There is a spin 1 and a spin 0 multiplicity. The corresponding matrices then become:

$$I_{1z}+I_{2z}=\begin{pmatrix}1&&&&&&&\\&0&&&&&&\\&&-1&&&&&\\&&&0&&&&\\&&&&1&&&\\&&&&&0&&\\&&&&&&-1&\\&&&&&&&0\end{pmatrix};\ S_z=\begin{pmatrix}0.5&&&&&&&\\&0.5&&&&&&\\&&0.5&&&&&\\&&&0.5&&&&\\&&&&-0.5&&&\\&&&&&-0.5&&\\&&&&&&-0.5&\\&&&&&&&-0.5\end{pmatrix}$$

The ordering of the levels is: (1,1)α, (1,0)α, (1,-1)α, (0,0)α, (1,1)β, (1,0)β, (1,-1)β, (0,0)β, where (1,1) is the m=1 state of the spin 1 combination of the two spins I_1 and I_2. The (0,0) means the m=0 state of the spin 0 combination of the two spins. The second polarization state refers to S. The states of the composite I spin = 0 can be ignored since they have no population in the initial operator. Also except for the application of selective pulses, the I spins will always be affected in the same way. This however means that throghout the whole pulse sequence the total I spin does not change. We then are left with two 6x6 matrices:

$$I_{1z}+I_{2z}=\begin{pmatrix}1&&&&&\\&0&&&&\\&&-1&&&\\&&&1&&\\&&&&0&\\&&&&&-1\end{pmatrix};\ S_z=\begin{pmatrix}0.5&&&&&\\&0.5&&&&\\&&0.5&&&\\&&&-0.5&&\\&&&&-0.5&\\&&&&&-0.5\end{pmatrix}$$

We can obtain now total transfer if we apply the following π pulses: $p_x^{|0a>|1b>}p_x^{|-1a>|0b>}$. Thus we have to rotate by: $(p/2)\{|0a><1b|+|1b><0a|\}$ and $(p/2)\{|-1a><0b|+|0b><-1a|\}$. The two rotations affect different levels, therefore they commute. We note that for a spin 1 the operator F_x looks in the following way:

$$F_x=\begin{pmatrix}0&\sqrt{2}/2&0\\\sqrt{2}/2&0&\sqrt{2}/2\\0&\sqrt{2}/2&0\end{pmatrix}$$

Thus it connects the 0 and -1 levels as well as the 1 and 0 levels. Therefore from analogy with the previous IS spin system, we arrive at the operator expression that implements the desired pulses:

$$(p/2)\sqrt{2}(F_xS_x + F_yS_y) = \begin{pmatrix} 0 & 0 & 0 & 0 & 0 & 0 \\ 0 & 0 & 0 & \sqrt{2}/2 & 0 & 0 \\ 0 & 0 & 0 & 0 & \sqrt{2}/2 & 0 \\ 0 & \sqrt{2}/2 & 0 & 0 & 0 & 0 \\ 0 & 0 & \sqrt{2}/2 & 0 & 0 & 0 \\ 0 & 0 & 0 & 0 & 0 & 0 \end{pmatrix};$$

This Hamiltonian is again a planar heteronuclear mixing operator. It can be implemented by two flanking 90(IS) pulses and a pulse sequence that generates the Hamiltonian $pJ(F_xS_x + F_yS_y)$ during a time $\left(\sqrt{2}J\right)^{-1}$. This is the same sequence as for the IS spin system, however, the delay $\tau = \left(\sqrt{2}J\right)^{-1}$ instead of $\tau = J^{-1}$ as in the case of the IS spin system. It should also be noted that this pulse sequence is a little bit shorter than the familiar implementation of the INEPT with delays $\tau_1 = (2J)^{-1}$ and $\tau_2 = (4J)^{-1}$.

Bounds and optimal pulse sequences for non-Hermitian A and C:

In the hermitian case we have obtained the bounds by calculating the eigenvalues of the involved matrices A and C. These eigenvalues are, however, always 0 for transfers that interchange operators that would be selected by echo gradient selection. Therefore another bound, the so called gradient bound was developed. So far there are no analytical expressions for this bound. We just give their values and then try to find implementations of pulse sequences that achieve a certain transfer. Let's look at the antiphase transfer in a two spin system: $2S^-I_z$ shall be transfered to I^-. The gradient bound tells that this transformation should be possible with an a of 1. Indeed, it is possible to accomplish the following transfer:

$2S_xI_z$ -> I_y by a $(\pi/2)S_xI_x$ rotation and
$2S_yI_z$ -> $-I_x$ by a $(\pi/2)S_yI_y$ rotation.

The two operators commute and therefore one can either apply them consecutively or simultaneously. You can see that the required transfers are exactly the same as for the INEPT in the IS spin system. Therefore the implementation is the same as in Fig. 2b. However, now, only the last 90(S) pulse can be ommitted yielding the pulse sequences in Fig. 2f or g.

Now, let us consider the I_2S spin system. The maximum achievable transfer is like in the case of the hermitian operators given by: a = 1. We can again look at the necessary matrices:

$$2F_zS^- = \begin{pmatrix} 0 & 0 & 0 & 2 & 0 & 0 \\ 0 & 0 & 0 & 0 & 0 & 0 \\ 0 & 0 & 0 & 0 & 0 & -2 \\ 0 & 0 & 0 & 0 & 0 & 0 \\ 0 & 0 & 0 & 0 & 0 & 0 \\ 0 & 0 & 0 & 0 & 0 & 0 \end{pmatrix}; F^- = \begin{pmatrix} 0 & \sqrt{2} & 0 & 0 & 0 & 0 \\ 0 & 0 & \sqrt{2} & 0 & 0 & 0 \\ 0 & 0 & 0 & 0 & 0 & 0 \\ 0 & 0 & 0 & 0 & \sqrt{2} & 0 \\ 0 & 0 & 0 & 0 & 0 & \sqrt{2} \\ 0 & 0 & 0 & 0 & 0 & 0 \end{pmatrix}$$

Now, let us consider the I_2S spin system. We recognize that by a rotation about the transitions: 2,4 and 3,5 we accomplish the desired transfer. This rotation can again be expressed as:

$$(p/2)\sqrt{2}(F_xS_x + F_yS_y) = \begin{pmatrix} 0 & 0 & 0 & 0 & 0 & 0 \\ 0 & 0 & 0 & \sqrt{2}/2 & 0 & 0 \\ 0 & 0 & 0 & 0 & \sqrt{2}/2 & 0 \\ 0 & \sqrt{2}/2 & 0 & 0 & 0 & 0 \\ 0 & 0 & \sqrt{2}/2 & 0 & 0 & 0 \\ 0 & 0 & 0 & 0 & 0 & 0 \end{pmatrix};$$

Thus we find that the heteronuclear Hartmann Hahn transfer indeed achieves in a two spin system the desired optimal transfer.

Optimal coherences?

We shall now discuss the question of choosing optimal coherences for pulse sequences. This question has become very interesting for large molecules where certain coherences relax much slower than other coherences. There are essentially two examples of this approach.

a) The use of heteronuclear multiple quantum coherences that relax slower than single quantum coherences.

b) The use of single multiplet components that relax much slower than other multiplet components.

Multiple Quantum Coherences:

We consider only molecules that are in the slow tumbling regime. Then we can neglect all spectral densities to the relaxation except for J(0). For the dipolar relaxation double commutator, we find:

$$d\rho/dt = -\left(\frac{\mu_0 g_S g I\hbar}{4\pi r_{IS}^3}\right)^2 [2S_zI_z,[2S_zI_z,\rho]\ J(0) = 0 \text{ if } [2S_zI_z,\rho]=0.$$

It is obvious that the only coherences that commute with this double commutator are also those that do not evolve heteronuclear coupling. Thus, z-magnetization or zero or double quantum coherences. This approach has been successfully used for proteins, especially with partial deuteration and RNA. A selection of respective papers can be found in the papers accompanying this lecture.

Differential Line Widths in Submultiplets (TROSY):

The concept that a multiplet has the same linewidth is no longer true as soon as molecules become larger. Let's look again at an IS spins system. There will be relaxation due to the dipolar interaction and there will be relaxation due to the anisotropy of the transverse spin. Thus there will be autocorrelated relaxation due to the dipolar interaction: $(-m_0)\frac{g_S g I \hbar}{4\pi r_{IS}^3} S_z I_z = b_D S_z I_z$ and due to the anisotropy of the S spin: $\frac{1}{3}(s_{\|} - s_{\perp}) g_S B_0 S_z = b_a S_z$. In addition there will be the cross term due to the cross correlation of the two interactions. If we look at the individual multiplet components: S^-I^a and S^-I^b we find the following expressions:

$$\begin{aligned}
\left(S^- I^a\right)^{\bullet} &= \left[b_D I_z S_z, \left[b_D I_z S_z, S^- I^a\right]\right] + \left[b_a S_z, \left[b_a S_z, S^- I^a\right]\right] \frac{2t_c}{5} \\
&\quad (+\left[b_D I_z S_z, \left[b_a S_z, S^- I^a\right]\right] + \left[b_a S_z, \left[b_D I_z S_z, S^- I^a\right]\right]) \frac{1}{5}\left(3\cos^2\theta - 1\right) 2t_c \\
&= S^- I^a \left(b_D^2/4 + b_a^2 + b_D b_a (3\cos^2\theta - 1)/2\right)\frac{2t_c}{5} \\
\left(S^- I^b\right)^{\bullet} &= \left[b_D I_z S_z, \left[b_D I_z S_z, S^- I^b\right]\right] + \left[b_a S_z, \left[b_a S_z, S^- I^b\right]\right] \frac{2t_c}{5} \\
&\quad (+\left[b_D I_z S_z, \left[b_a S_z, S^- I^b\right]\right] + \left[b_a S_z, \left[b_D I_z S_z, S^- I^b\right]\right]) \frac{1}{5}\left(3\cos^2\theta - 1\right) 2t_c \\
&= S^- I^b \left(b_D^2/4 + b_a^2 - b_D b_a (3\cos^2\theta - 1)/2\right)\frac{2t_c}{5}
\end{aligned}$$

Obviously, if $\left(b_D^2/4 + b_a^2 \pm b_D b_a (3\cos^2\theta - 1)/2\right)$ is 0, the linewidth can be very small. For a NH bond, the nitrogen as well as the hydrogen CSA tensor are almost exactly aligned along the NH bond. Therefore $(3\cos^2\theta - 1)/2$ is close to 1. This means that $\left(b_D^2/4 + b_a^2 - b_D b_a (3\cos^2\theta - 1)/2\right) = 0$.

Thus the optimal coherences are: $S^- I^b$ and $I^- S^b$. Therefore transfer sequences that transfer between those coherences in an optimal way are desirable.

There are two implementations that can achieve this transfer so far published in the literature. The first is again the planar heteronuclear Hartmann Hahn mixing: It implements a rotation about the 2,3 transition. This rotation achieves the following transfer:

$$S^{-}I^{b} \longrightarrow I^{-}S^{b}\,;\; S^{-}I^{a} \longrightarrow I^{-}S^{a}$$
$$S^{+}I^{b} \longrightarrow I^{+}S^{b}\,;\; S^{+}I^{a} \longrightarrow I^{+}S^{a}$$

These transformations will create a spectrum that contains in the antiecho and echo part the following peaks:

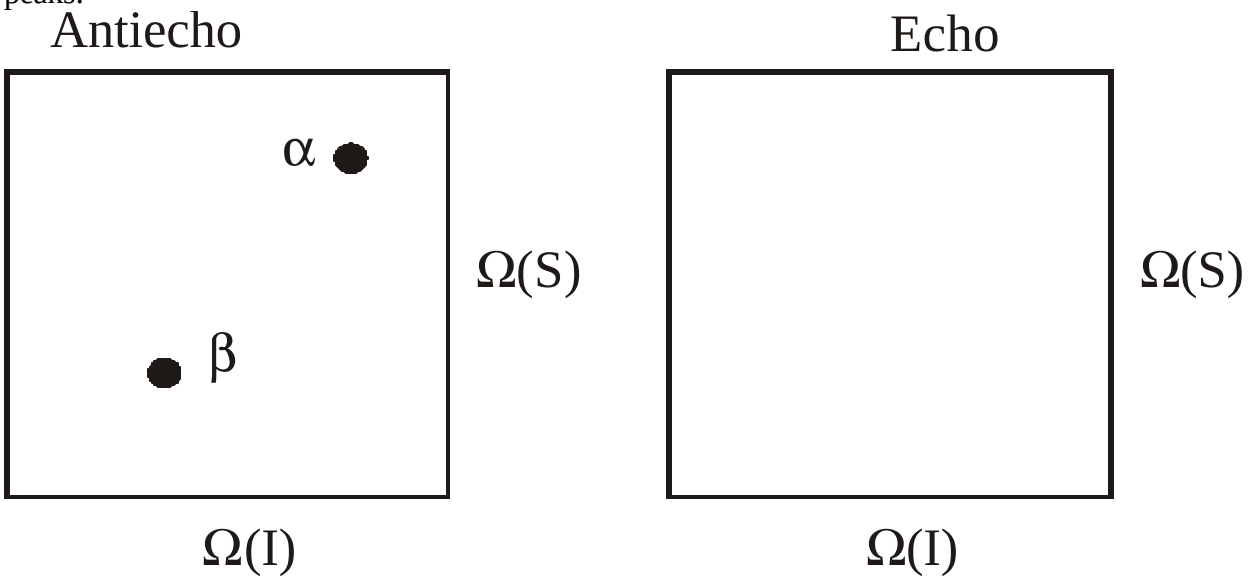

Of course either one of the peaks will be broad and it is not optimal to have it in the spectrum.
This problem is solved in the TROSY sequence. Here one can show that the following transformations are achieved:

$$S^{-}I^{b} \longrightarrow I^{-}S^{b}\,;\; S^{-}I^{a} \longrightarrow I^{+}S^{a}$$
$$S^{+}I^{b} \longrightarrow I^{+}S^{b}\,;\; S^{+}I^{a} \longrightarrow I^{-}S^{a}$$

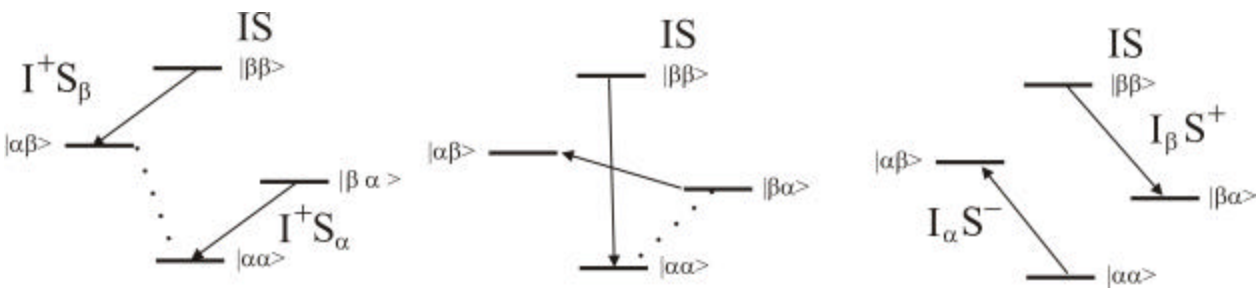

This produces the following spectrum:

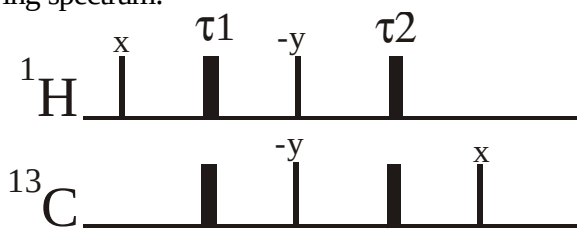

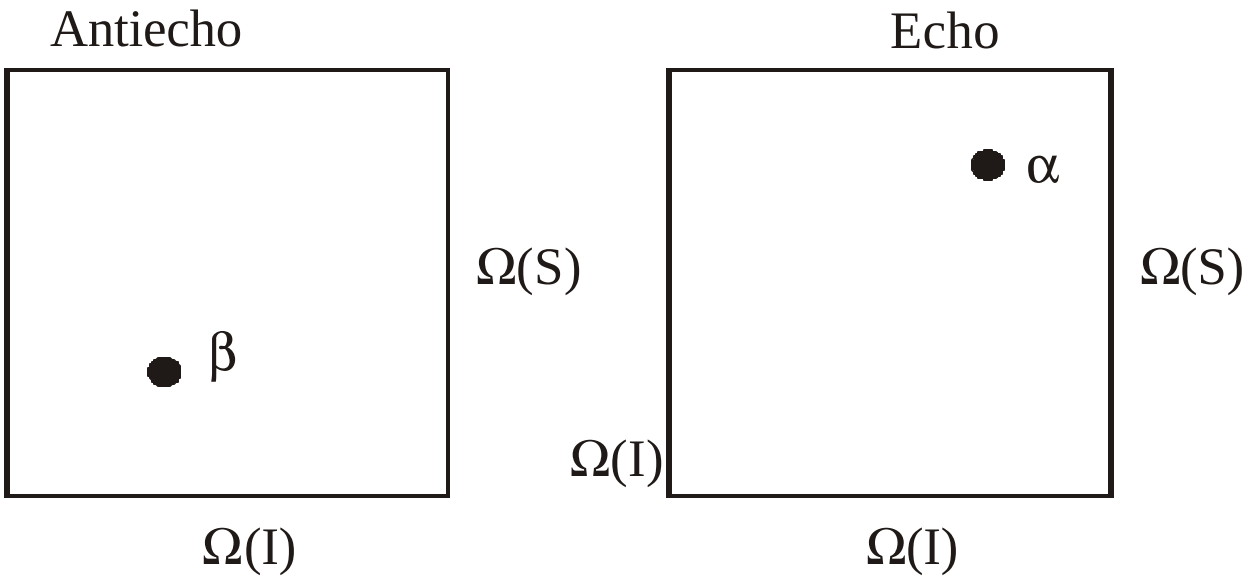

This is optimal in combination with gradients to select exactly one line only.